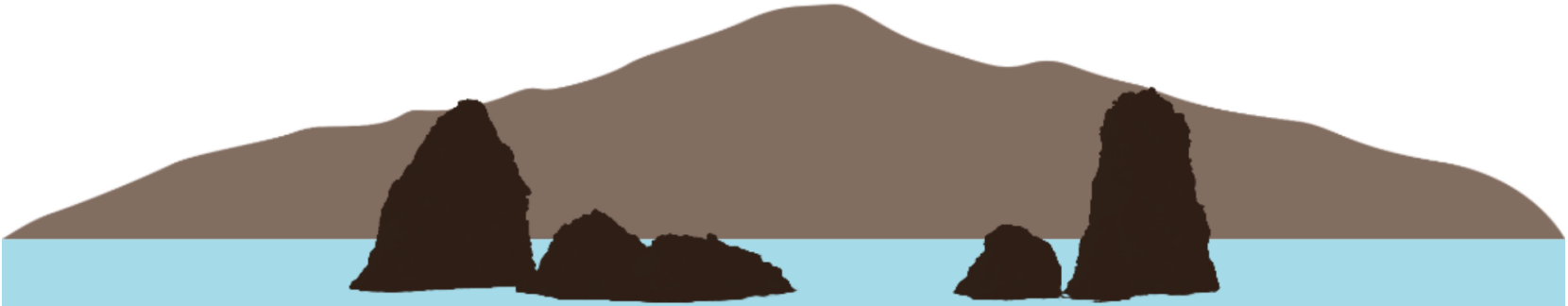


Indirect Methods in Nuclear Astrophysics

C.A. Bertulani



**THE 12TH EUROPEAN SUMMER
SCHOOL ON EXPERIMENTAL
NUCLEAR ASTROPHYSICS**

Aci Trezza, 16-22 June 2024

Nuclear reactions in astrophysics

decay

Abundance changes

$$\frac{dY_i}{dt} = \sum_j N_j^i \lambda_j Y_j + \sum_{jk} N_{jk}^i \rho N_A \langle \sigma v \rangle Y_j Y_k + \sum_{jkm} N_{jkm}^i \rho^2 N_A^2 \langle \sigma v \rangle Y_j Y_k Y_m + \dots$$

Input:

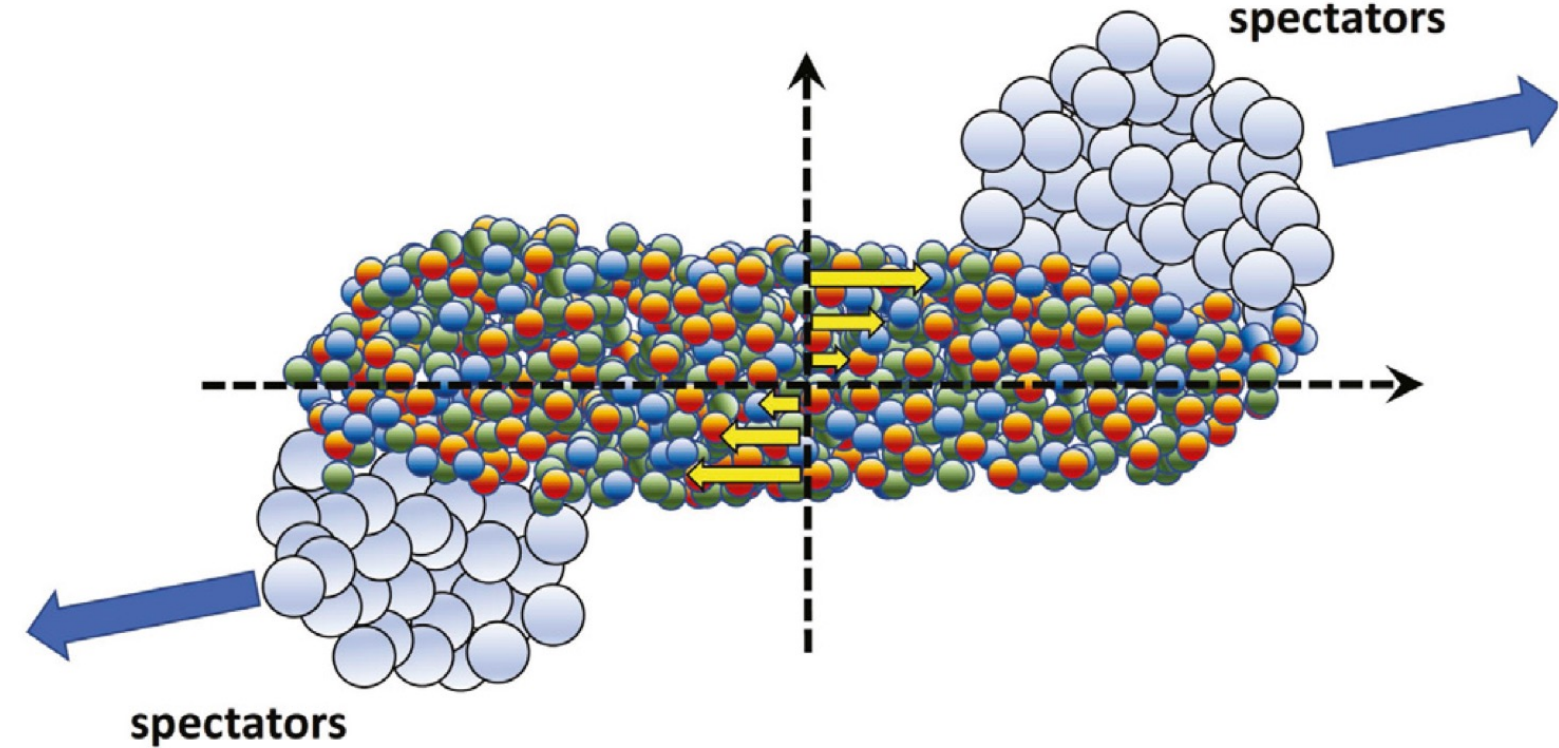
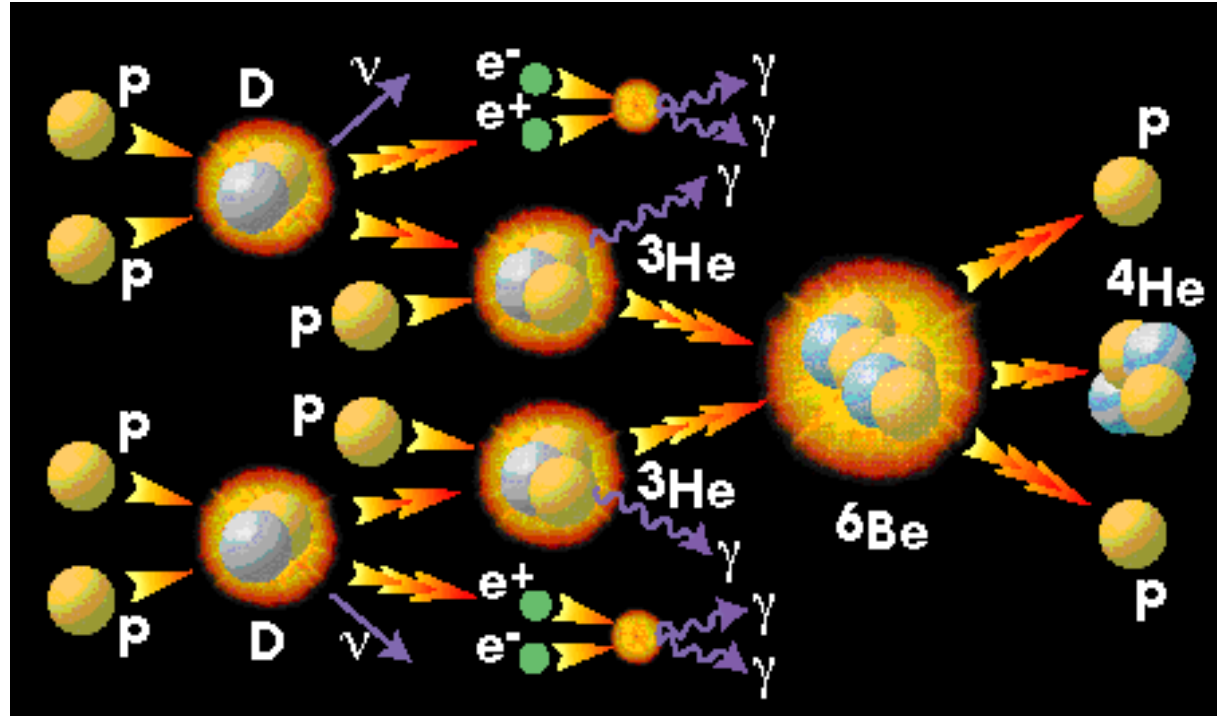
- density
- temperature
- composition
- nuclear masses
- decay constants
- reaction rates
- . . .

formation

Output:

- nucleosynthesis
- stellar evolution
- bursts, explosions
- neutron stars
- black holes
- . . .

Nuclear reactions



keV
???

Stellar evolution

Elemental
abundance

Nuclear many-body problem:

the hardest problem

of all physics!

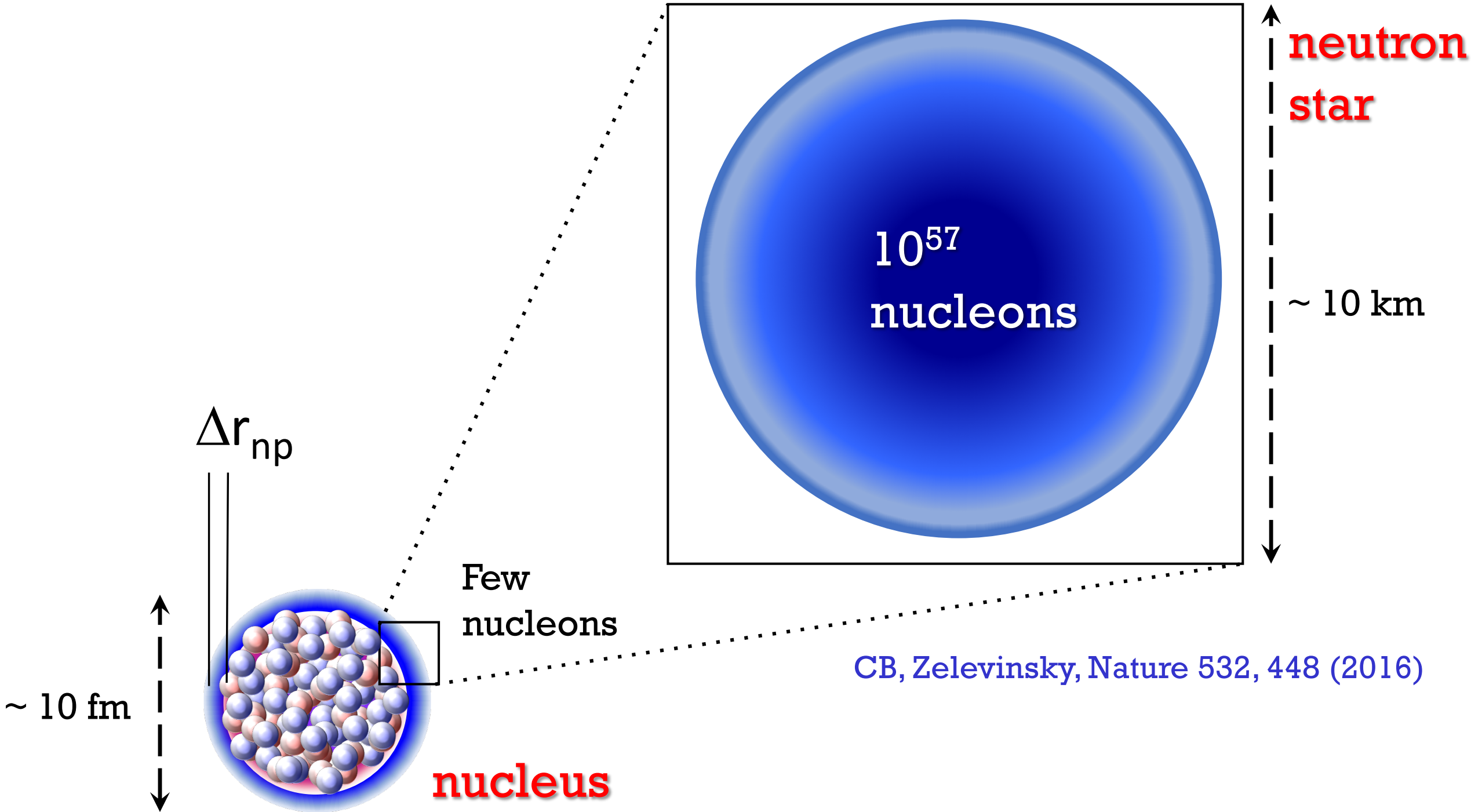
- Interactions are complicated
- Nucleons = composite particles

TeV
???

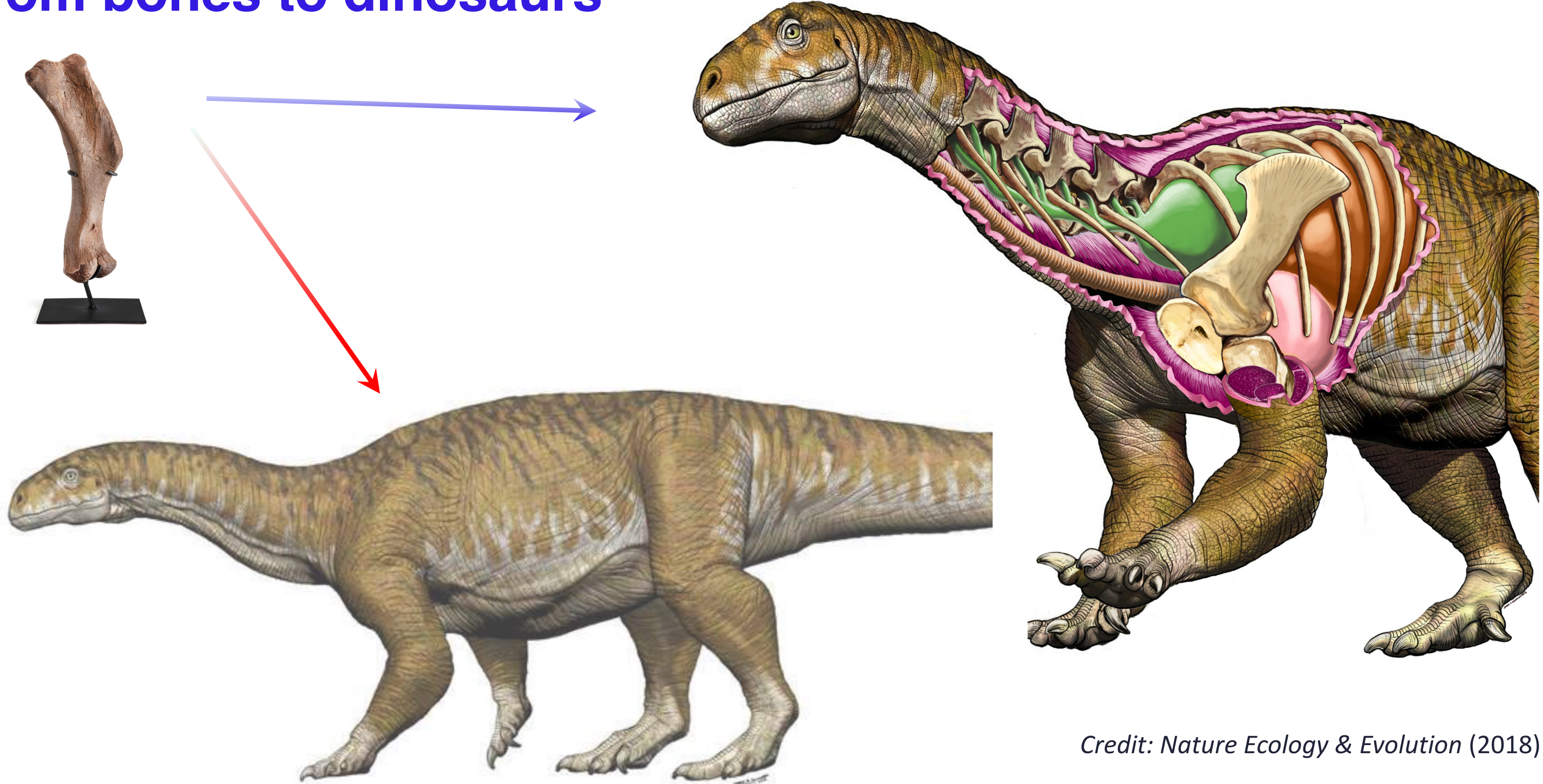
Big bang

neutron
star

From laboratory experiments to neutron stars



From bones to dinosaurs



Credit: Nature Ecology & Evolution (2018)

Neutron stars

EOS

$$p[\rho] = \rho^2 \frac{d}{d\rho} \left(\frac{E}{A}[\rho] \right)$$

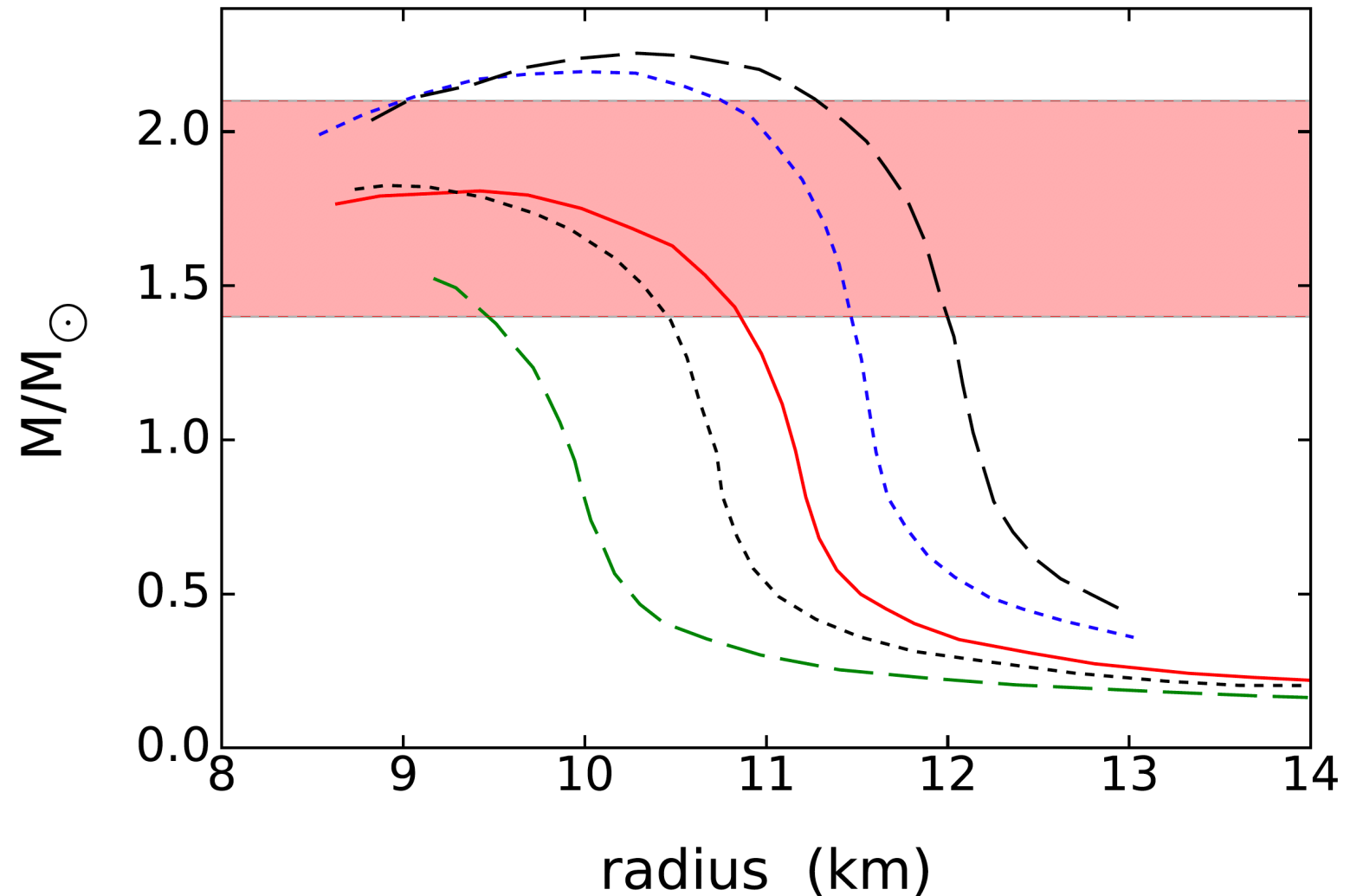
$$\frac{E}{A}[\rho] = \frac{E}{A}[\rho_0] + \frac{1}{18} K_\infty \left(\frac{\rho - \rho_0}{\rho_0} \right)^2 + \dots$$

$$K_\infty = 9\rho^2 \left. \frac{d^2 [E/A]}{d\rho^2} \right|_{\rho_0}$$

$$\frac{dP}{dr} = - \frac{G\rho(r)M(r)}{r^2} \left[1 + \frac{P(r)}{\rho(r)} \right] \left[1 + \frac{4\pi r^3 P(r)}{M(r)} \right] \left[1 - \frac{2GM(r)}{r} \right]^{-1}$$

$$\frac{dM}{dr} = 4\pi r^2 \rho(r)$$

Tolman-Oppenheimer-Volkoff



EOS + symmetry energy

$$\frac{E}{A}[\rho] = \frac{E}{A}[\rho_0] + \frac{1}{18} K_\infty \left(\frac{\rho - \rho_0}{\rho_0} \right)^2 + S \left(\frac{\rho_n - \rho_p}{\rho} \right)^2 + \dots$$

$$S = \frac{1}{2} \frac{\partial^2 (E/A)}{\partial \delta^2} \Big|_{\delta=0} = J + Lx + \frac{1}{2} K_{\text{sym}} x^2 + O(x^3),$$

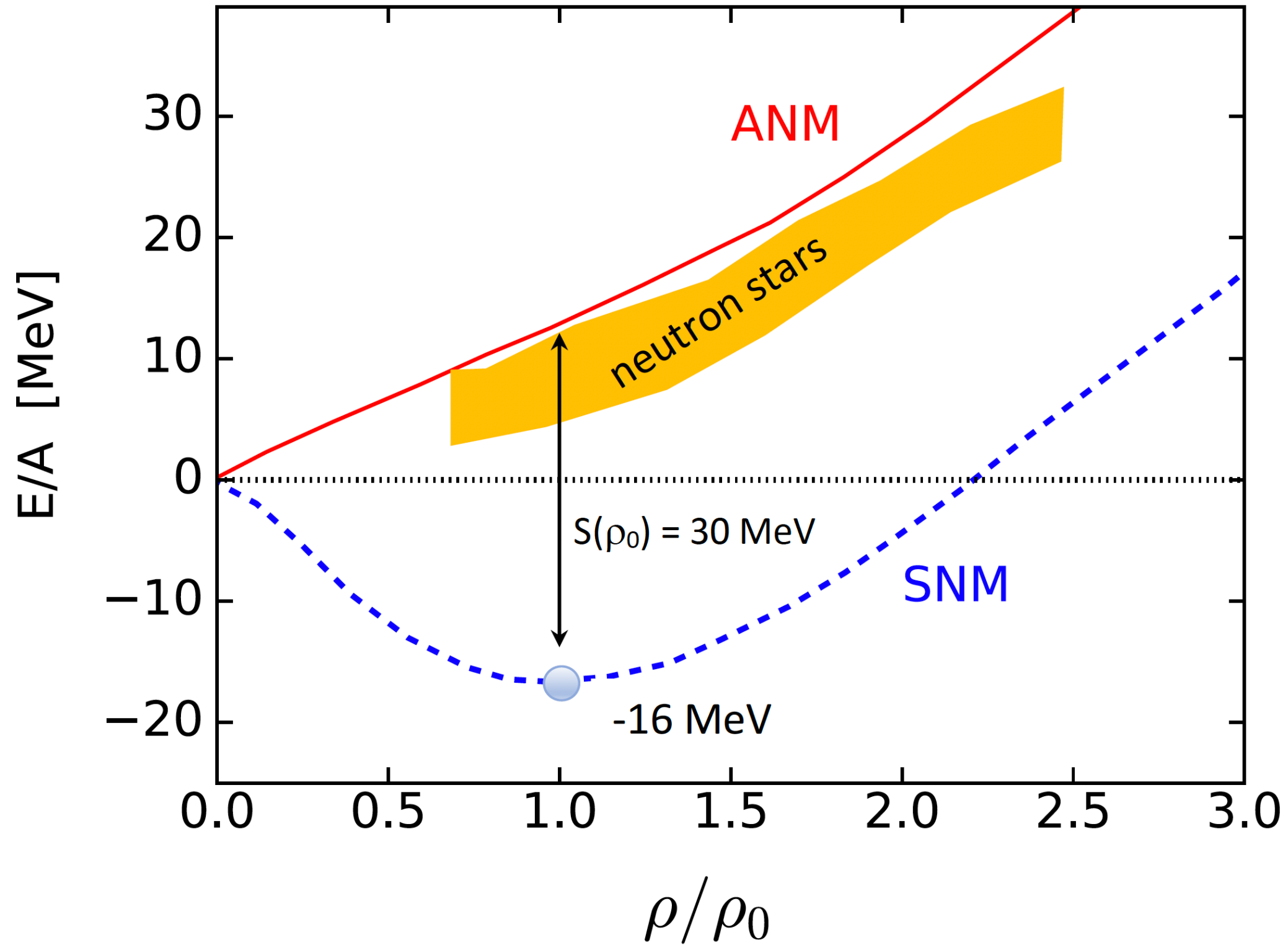
$$L = 3\rho_0 \frac{dS(\rho)}{d\rho} \Big|_{\rho_0}, \quad \delta = \frac{\rho_n - \rho_p}{\rho}, \quad x = \frac{(\rho - \rho_0)}{3\rho_0}$$

$$\text{For } \rho \sim \rho_0 \text{ and } \delta \sim 1 \Rightarrow p = \frac{L\rho_0}{3}$$

Skyrme	ρ_0	E_0	K_∞	J	L	K_{sym}
SLy5	0.161	-15.99	229.92	32.01	48.15	-112.76
Skxs20	0.162	-15.81	201.95	35.50	67.06	-122.31
SkI5	0.156	-15.82	255.57	36.63	129.27	-155.94

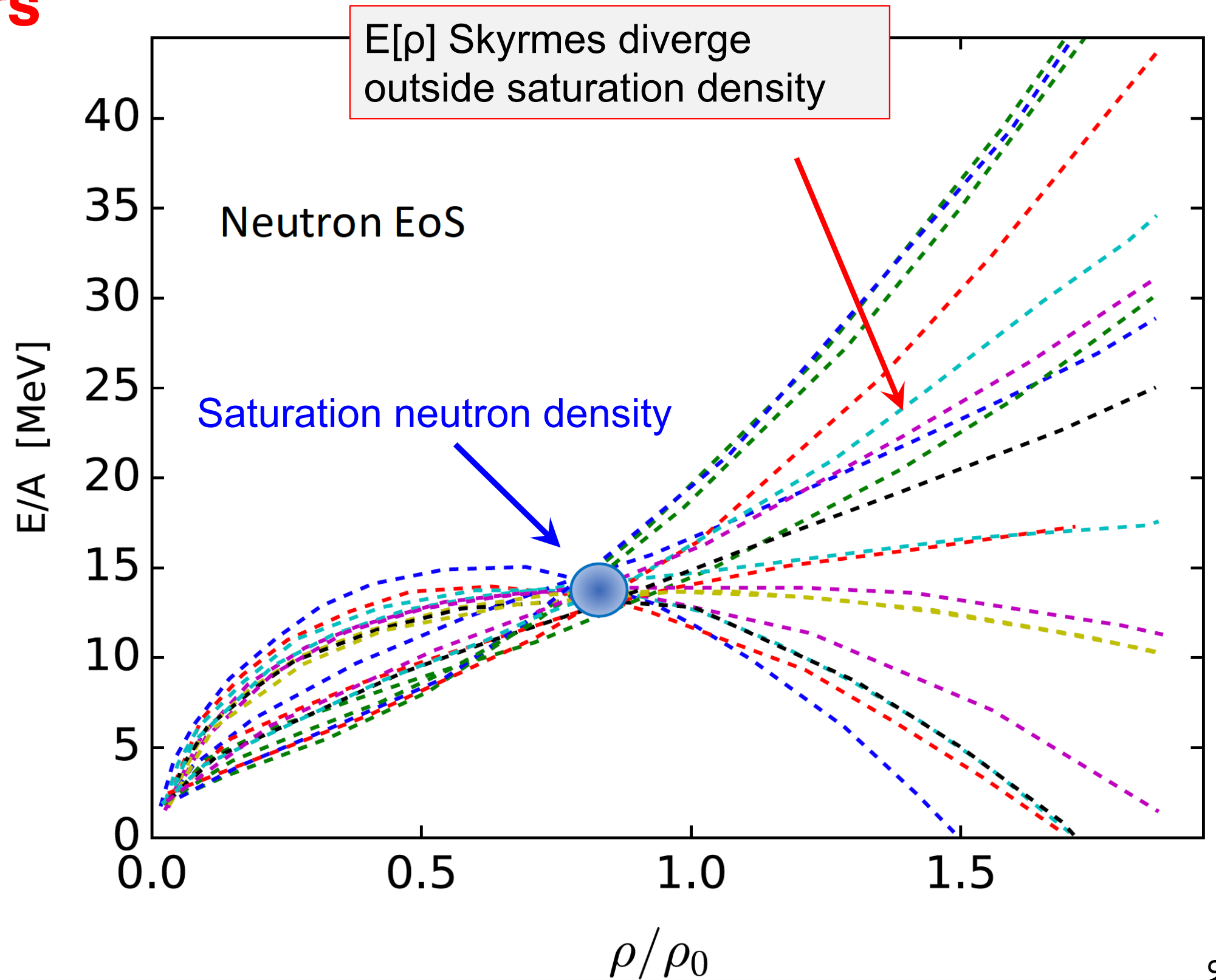
L crucial for neutron matter

EOS of neutron stars



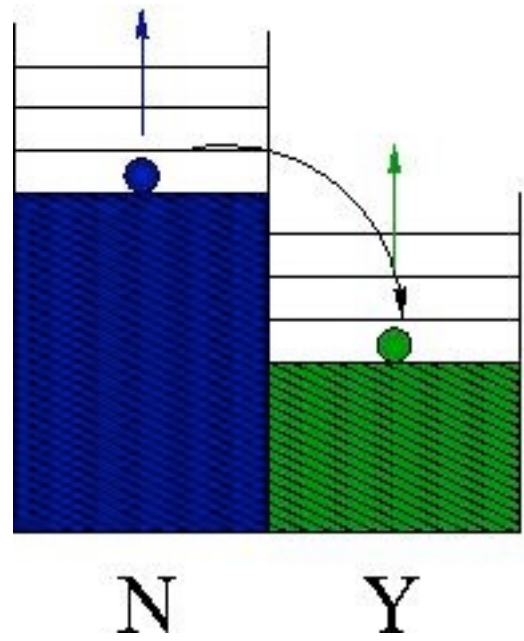
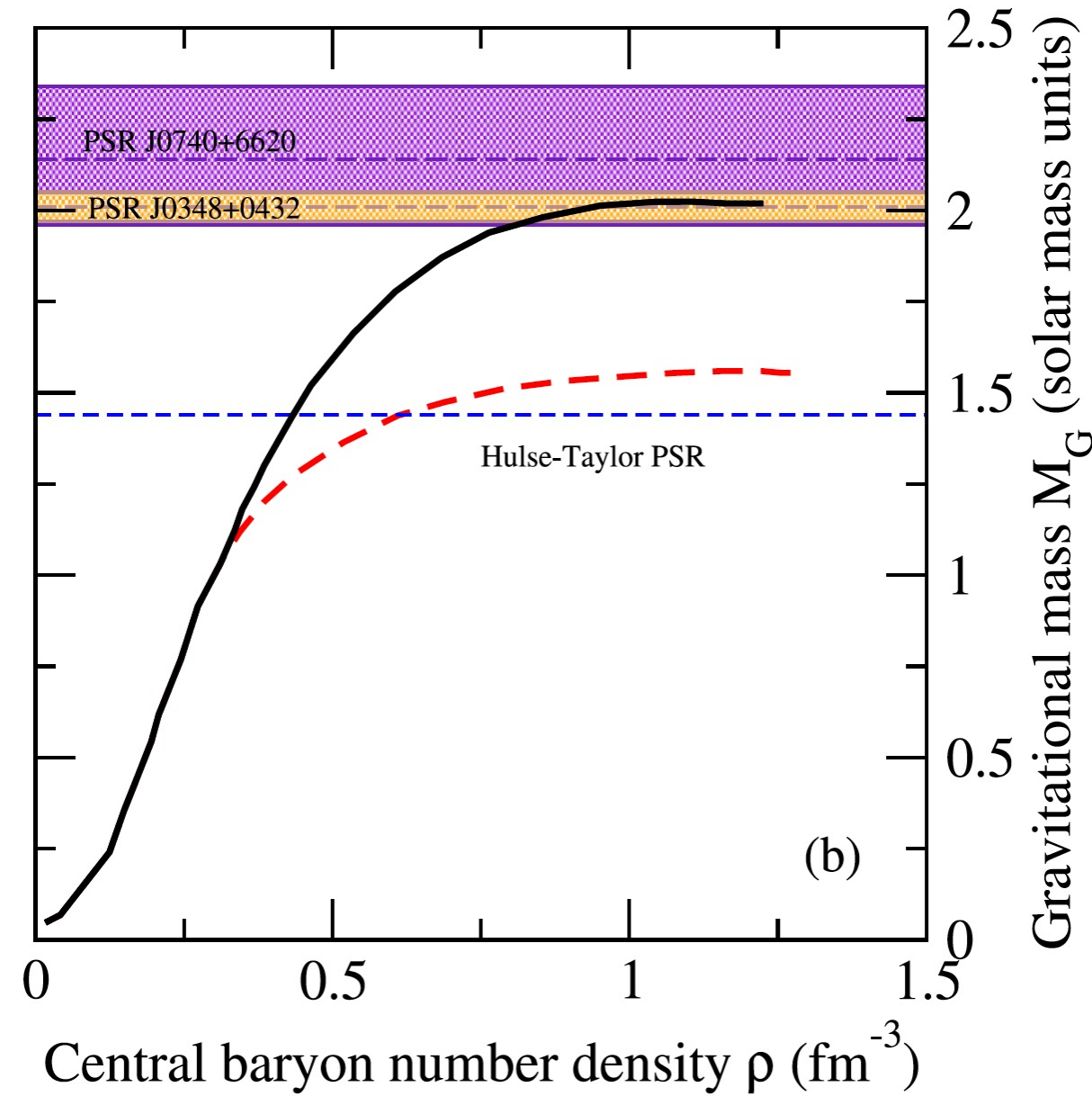
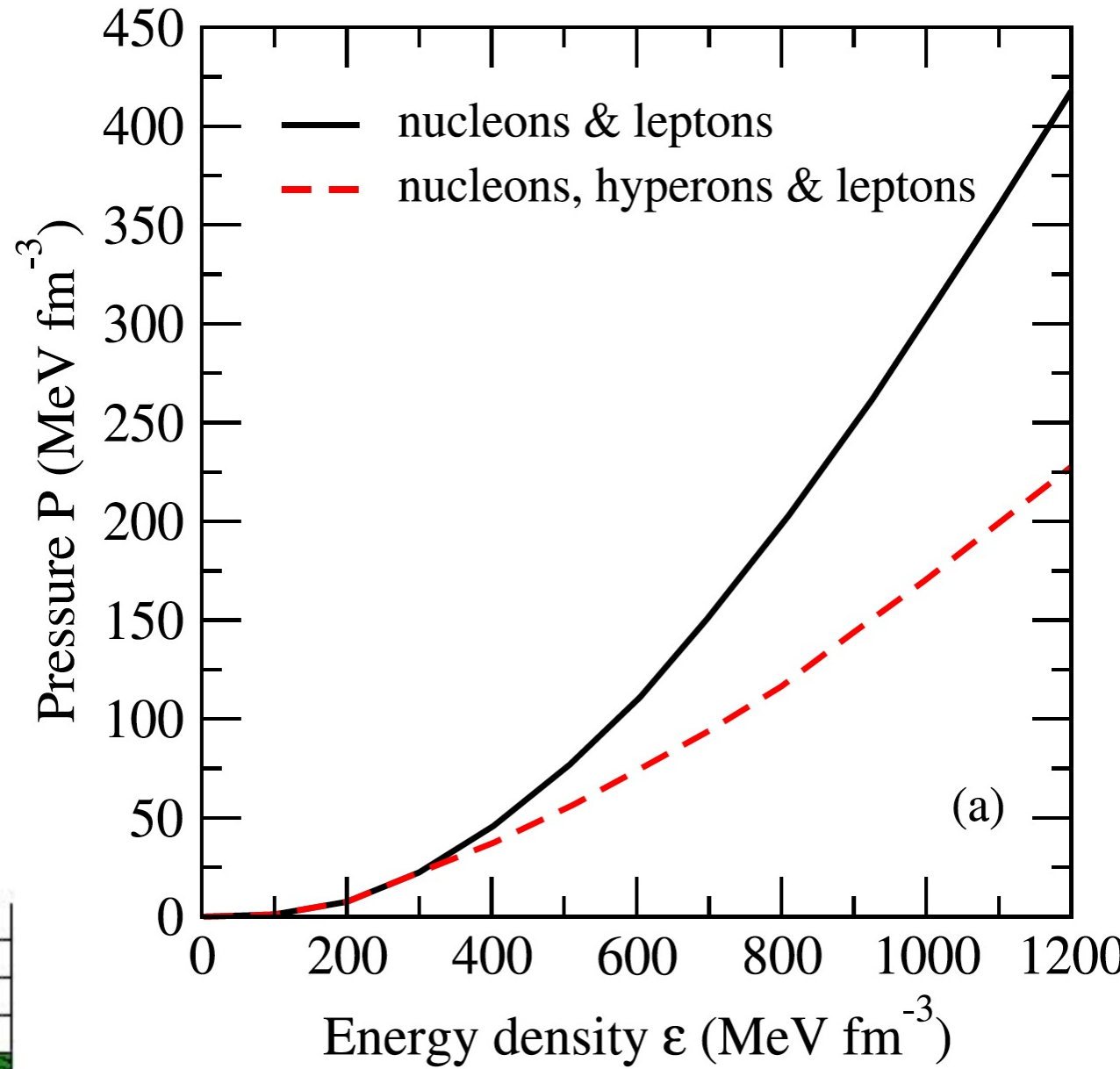
EOS & Neutron stars

Pethick, Ravenhall,
ARNPS 45 (1995) 429



Hyperons and neutron stars

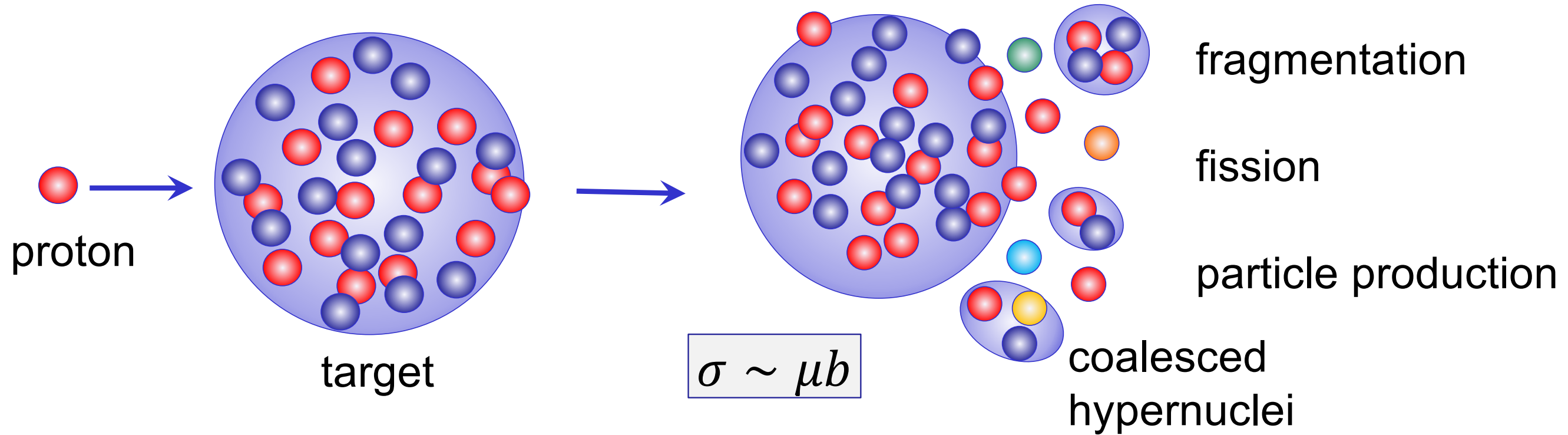
Hyperons make the EoS softer → reduction of the mass



Hyperon "puzzle"

Tolos, Fabbietti, PPNP 112 103770 (2020)

Hypernuclei in the lab



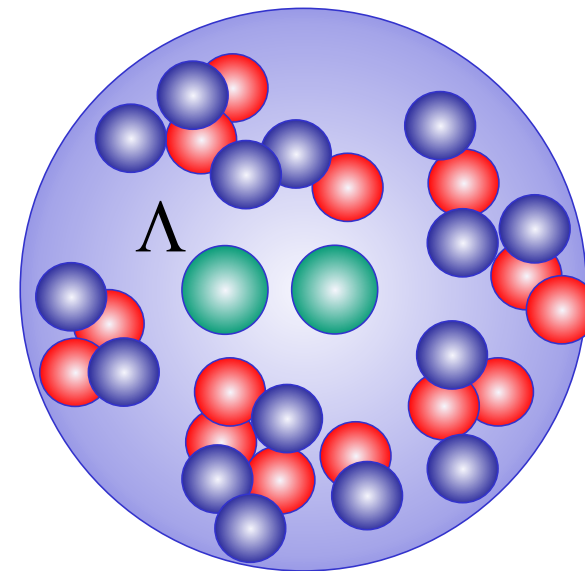
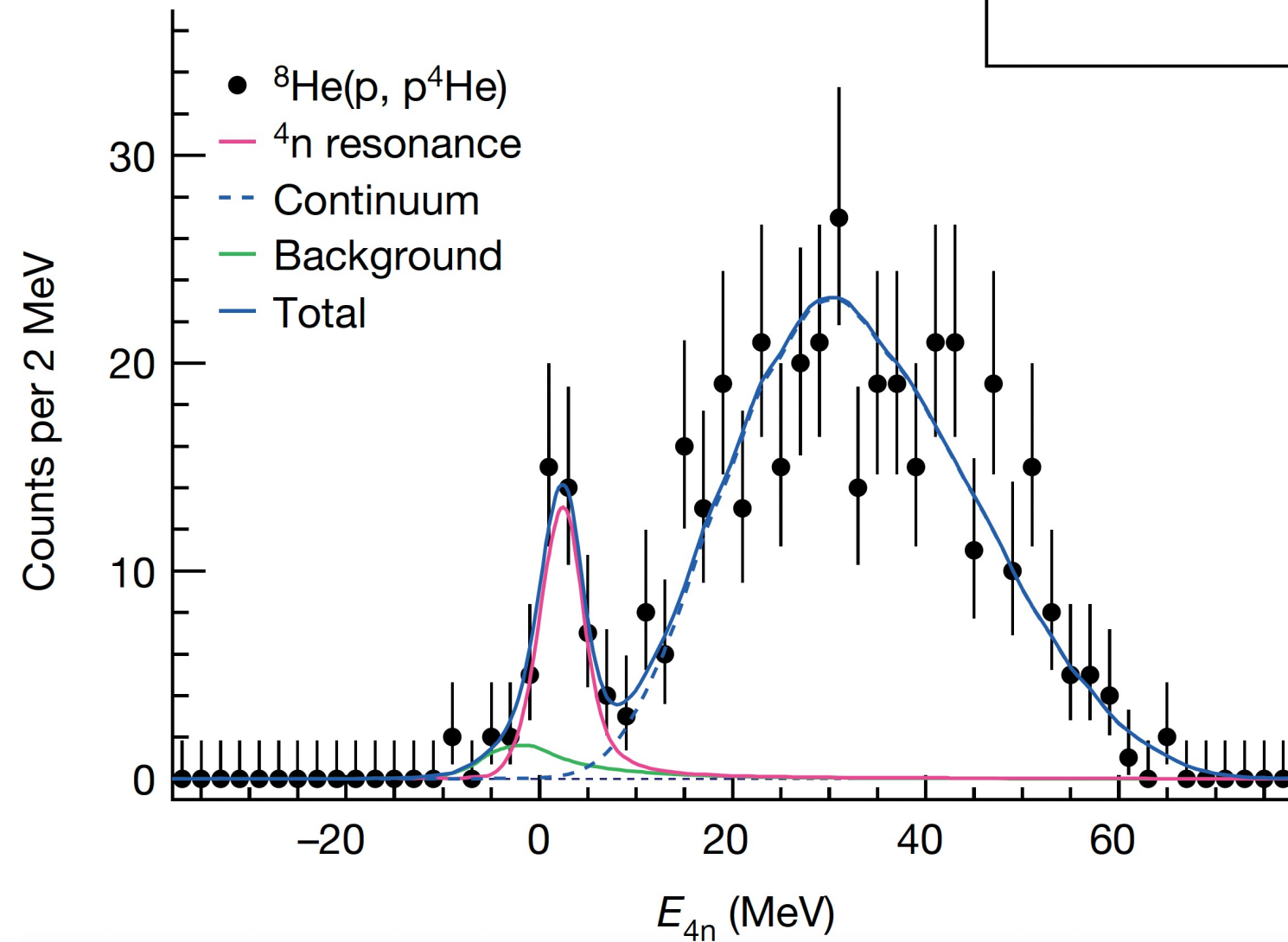
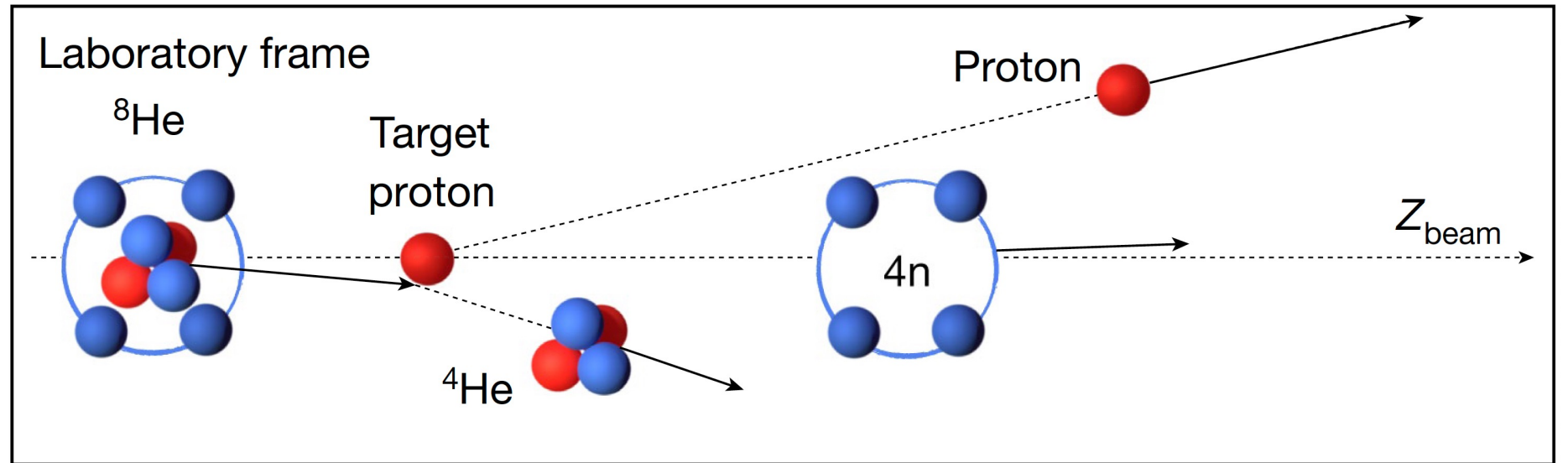
Particles produced coalesce into nuclei if they are close in space and momentum.

$$C_A = \frac{2J_A + 1}{2^A} \frac{1}{\sqrt{A} m_T^{A-1}} \left(\frac{2\pi}{R^2 + \left(\frac{r_A}{2}\right)^2} \right)^{\frac{3}{2}(A-1)}$$

R = source size, r_A = nuclear size
 m_T = transverse mass of coalesc. part.

Nucleon clusters and $N\Lambda$ clusters in the lab

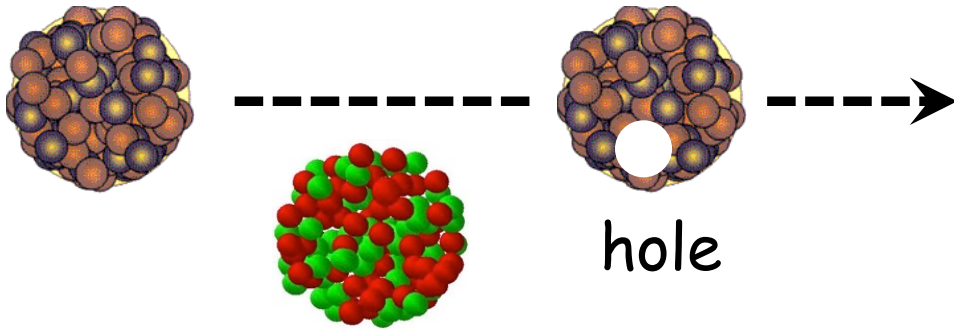
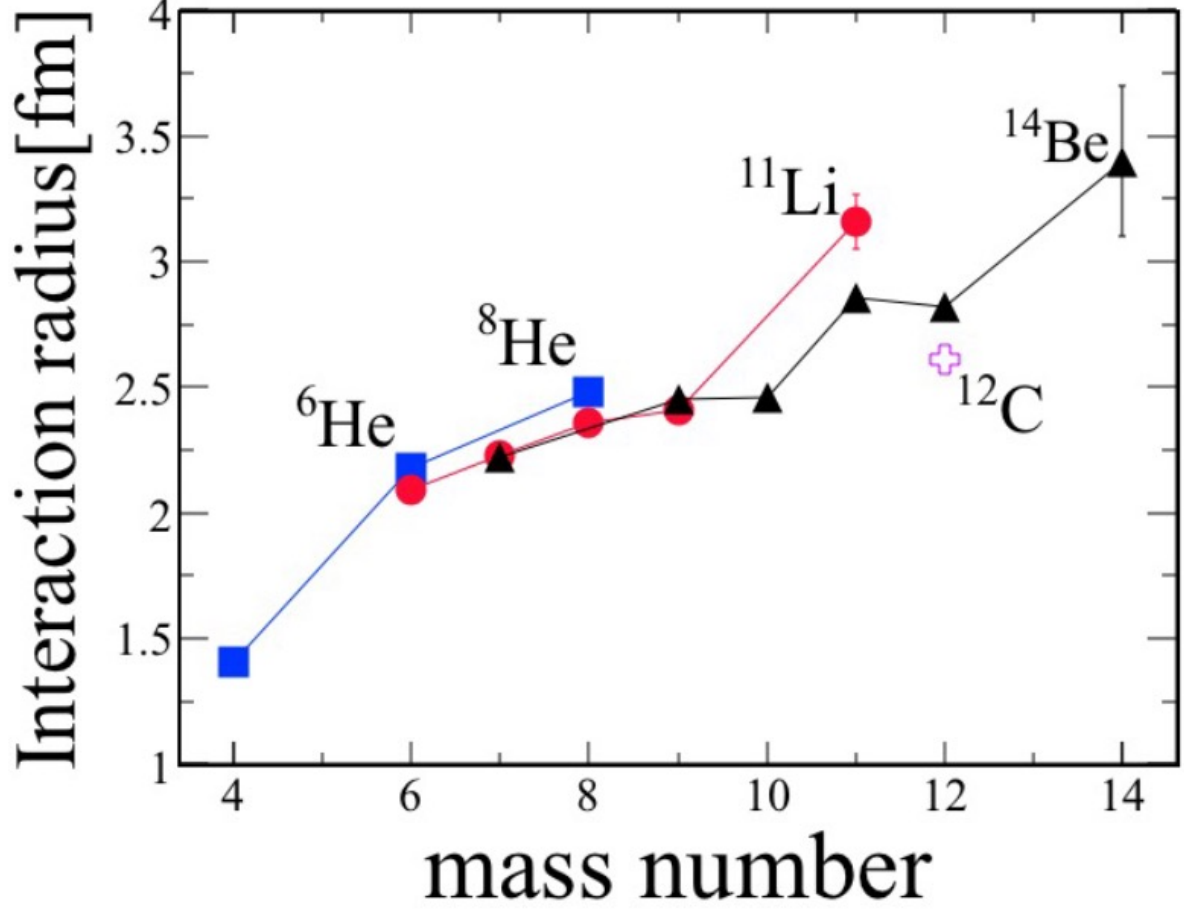
Duer, et al.,
Nature 606, 678 (2022)



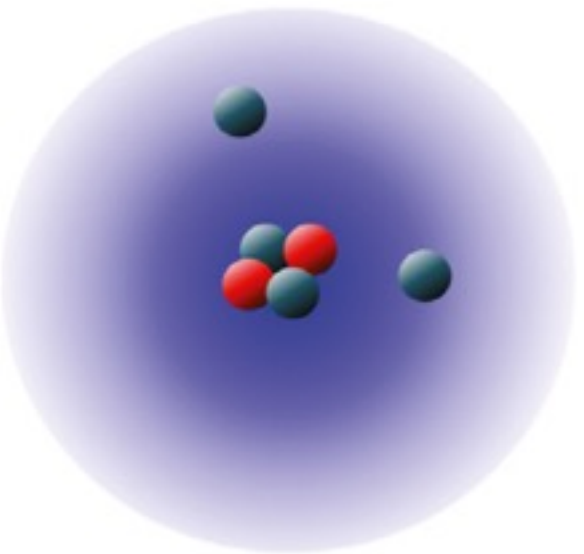
Hypernuclei spectroscopy
→ $N\Lambda$ interaction

Difficult task

Nuclear halos

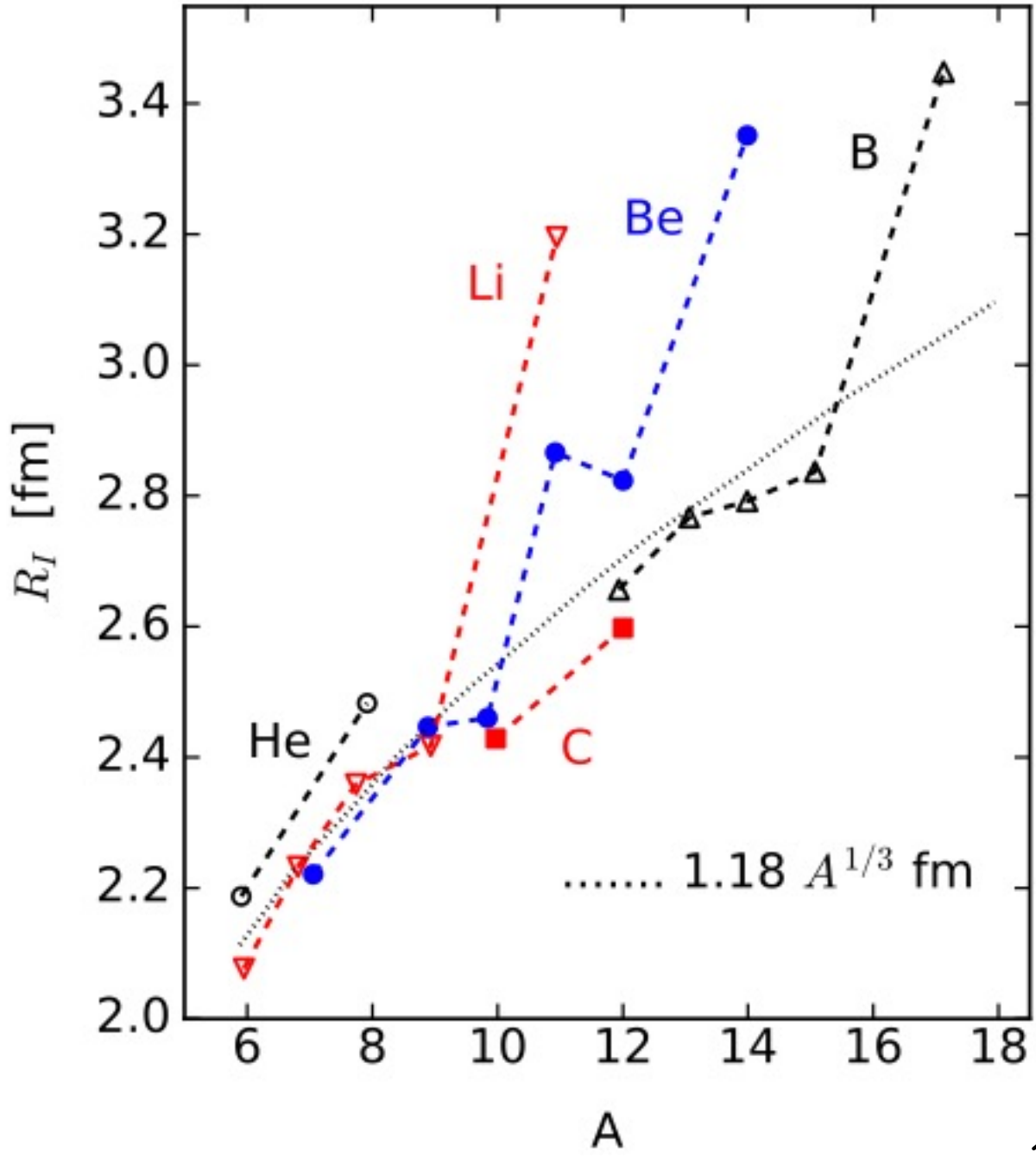


$$\sigma_I = \pi [R_I(P) + R_I(T)]^2$$



⁶He

Tanihata et al.,
PRL 55, 2676 (1985)



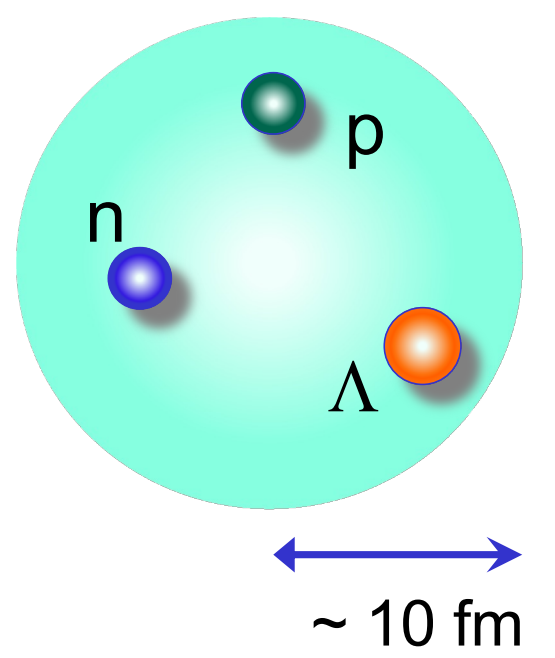
Hypertriton halo

$$\tau_{\Lambda} = 263 \text{ ps}$$

$$\tau_{\Lambda^3\text{H}} = 253 \pm 11(\text{stat.}) \pm 6(\text{sys.}) \text{ ps}$$

Philipp Eckert, et al., EPJ Web Conf. 271 (2022) 01006

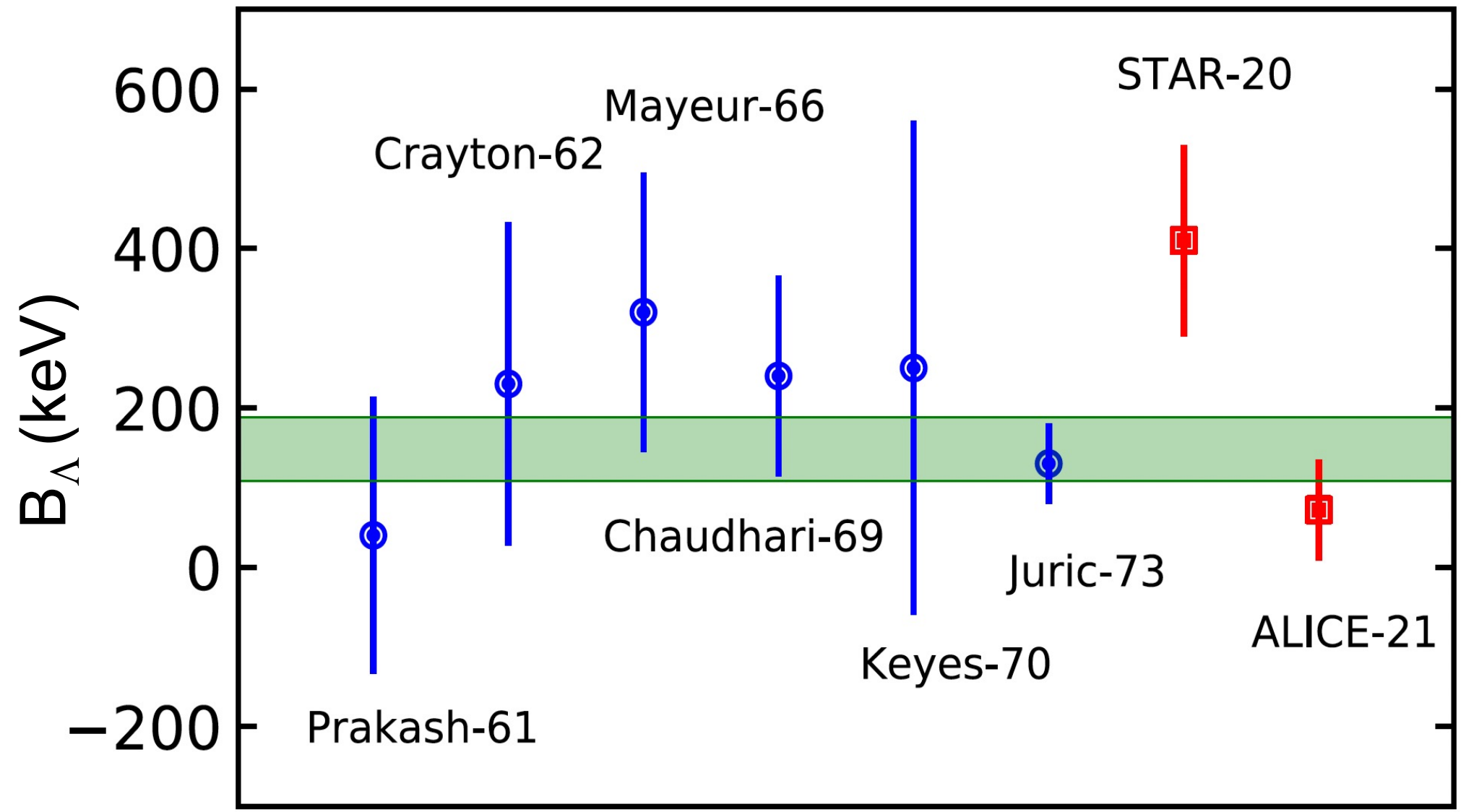
<https://hypernuclei.kph.uni-mainz.de>



Halo

${}^6_{\Lambda}\text{He}$ ($S_n = 0.17 \text{ MeV}$)

${}^7_{\Lambda}\text{Be}$ ($S_{2p} = 0.67 \text{ MeV}$)



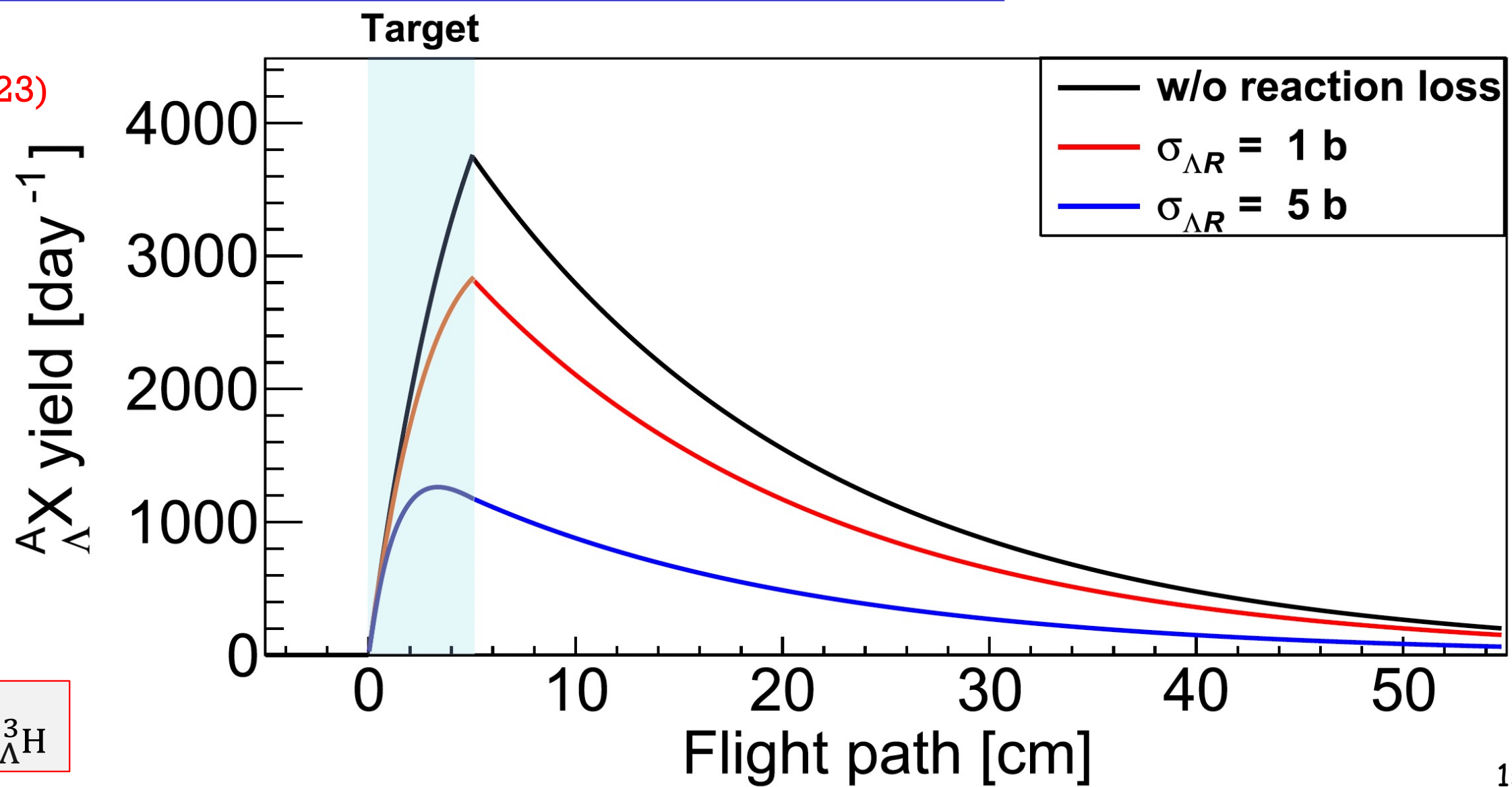
Production & Decay of Hypertriton

- Use active target to:
- (a) Produce hypertriton
 - (b) Reconstruct hypertriton by measuring weak decay (${}^3_{\Lambda}\text{H} \rightarrow \pi^- + {}^3\text{He}$)
 - (c) Interaction cross section through meson decay vertex distribution

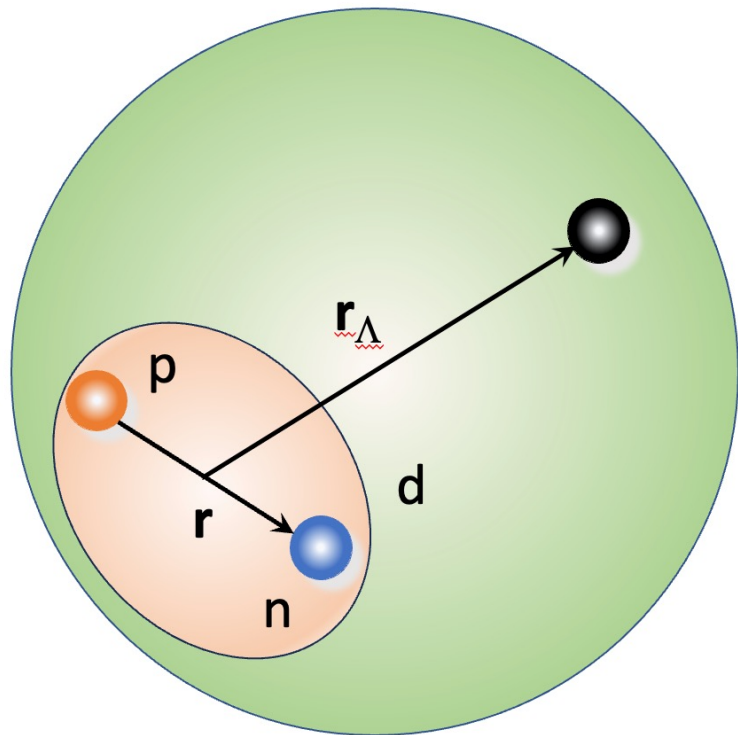
Velardita et al.,
 Eur. Phys. J. A 59,139 (2023)

$\sigma_I = \sigma_{\Lambda R} \sim 1.8 \text{ b}$
 $\tau \sim 200 \text{ ps}$

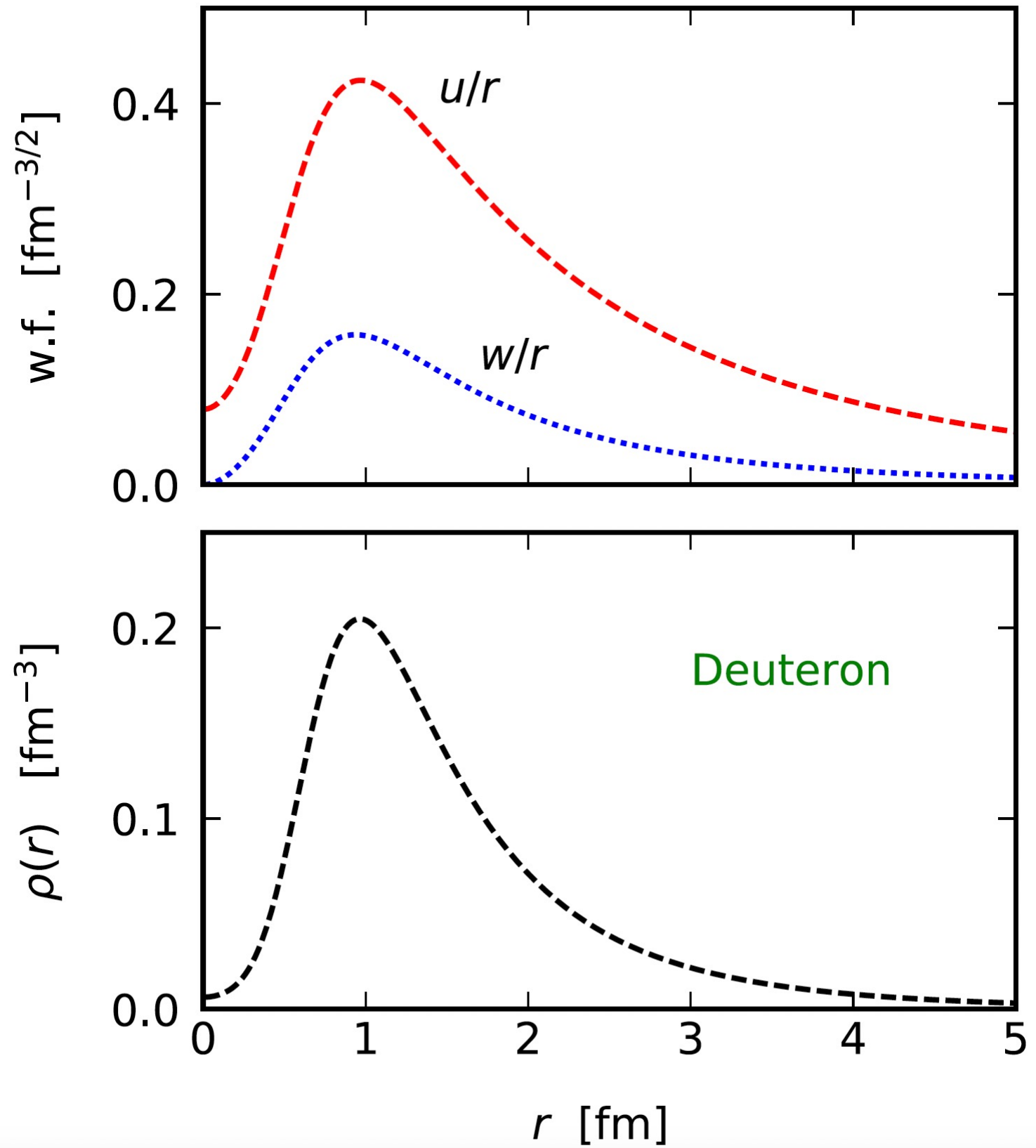
Experiment $\rightarrow \sigma_I \rightarrow R_{{}^3_{\Lambda}\text{H}}$



Hypertriton model

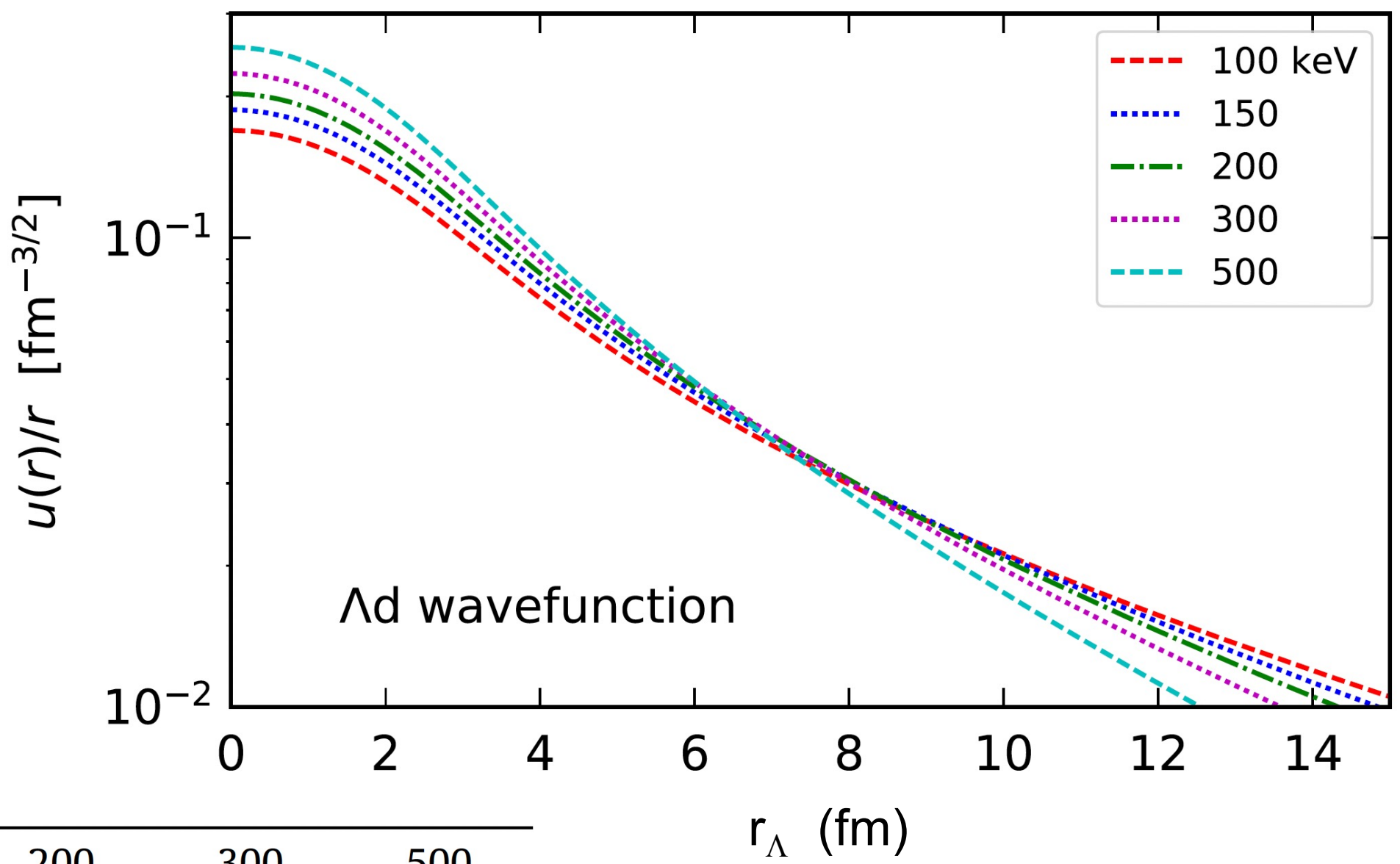
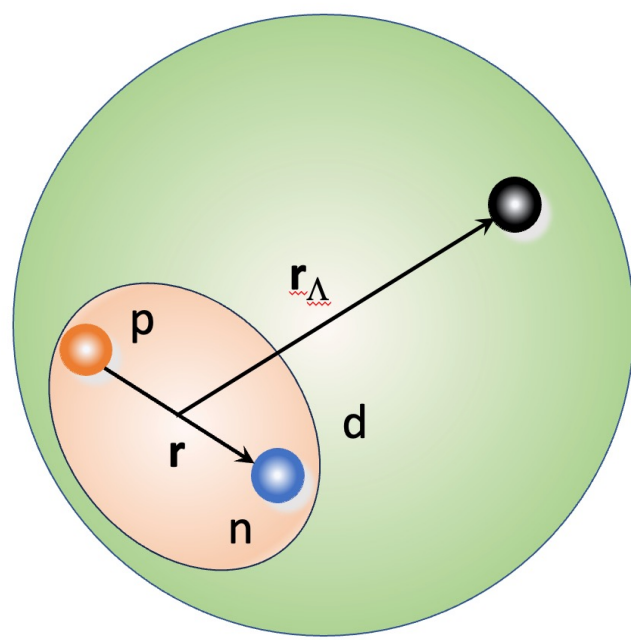


Deuteron radial s-wave, $u(r)/r$, and d-wave, $w(r)/r$ as a function of the proton-neutron distance r using Av18 interaction.



Hypertriton model

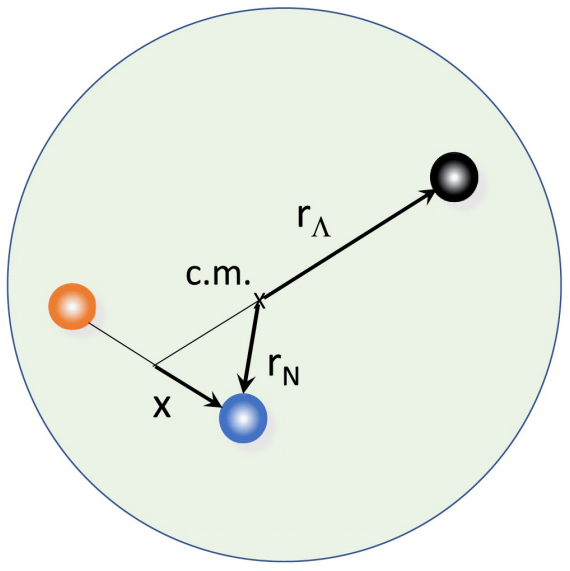
CB, PLB 837, 137639 (2023)



B_Λ (keV)	100	150	200	300	500
V_0 [MeV]	-11.8	12.2	-12.6	-13.2	-14.3

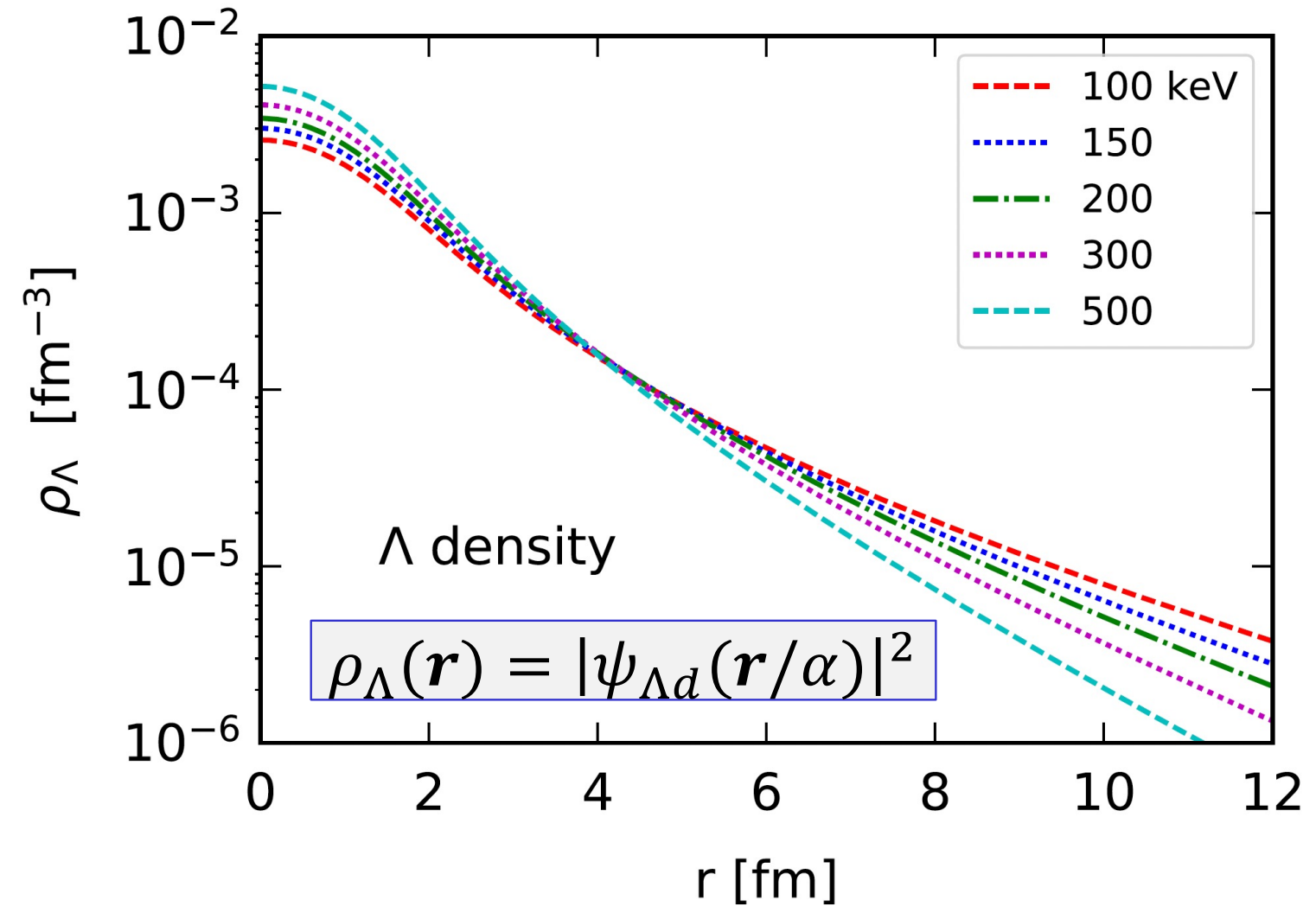
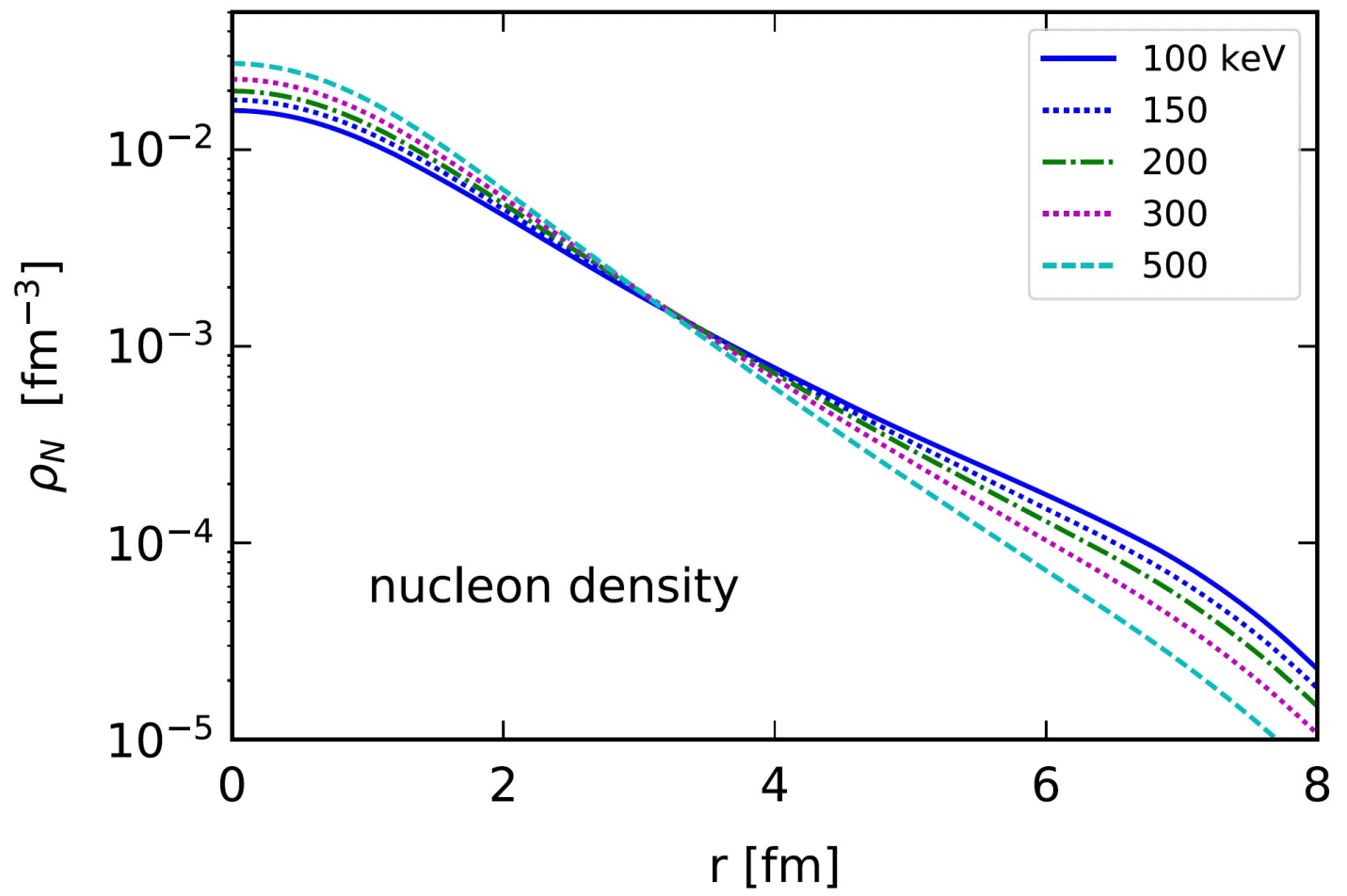
Λ -deuteron wavefunction - Woods-Saxon, radius $R = 2.5$ fm, diffuseness $a = 0.65$ fm.
 $u(r)/r$ for the s-wave and binding energies $B = 100, 150, 200, 300$ and 500 keV.

Hypertriton + nucleon density



$$\alpha = \frac{m_d}{m_\Lambda + m_d}$$

$$\beta = \frac{m_\Lambda}{m_\Lambda + m_d}$$

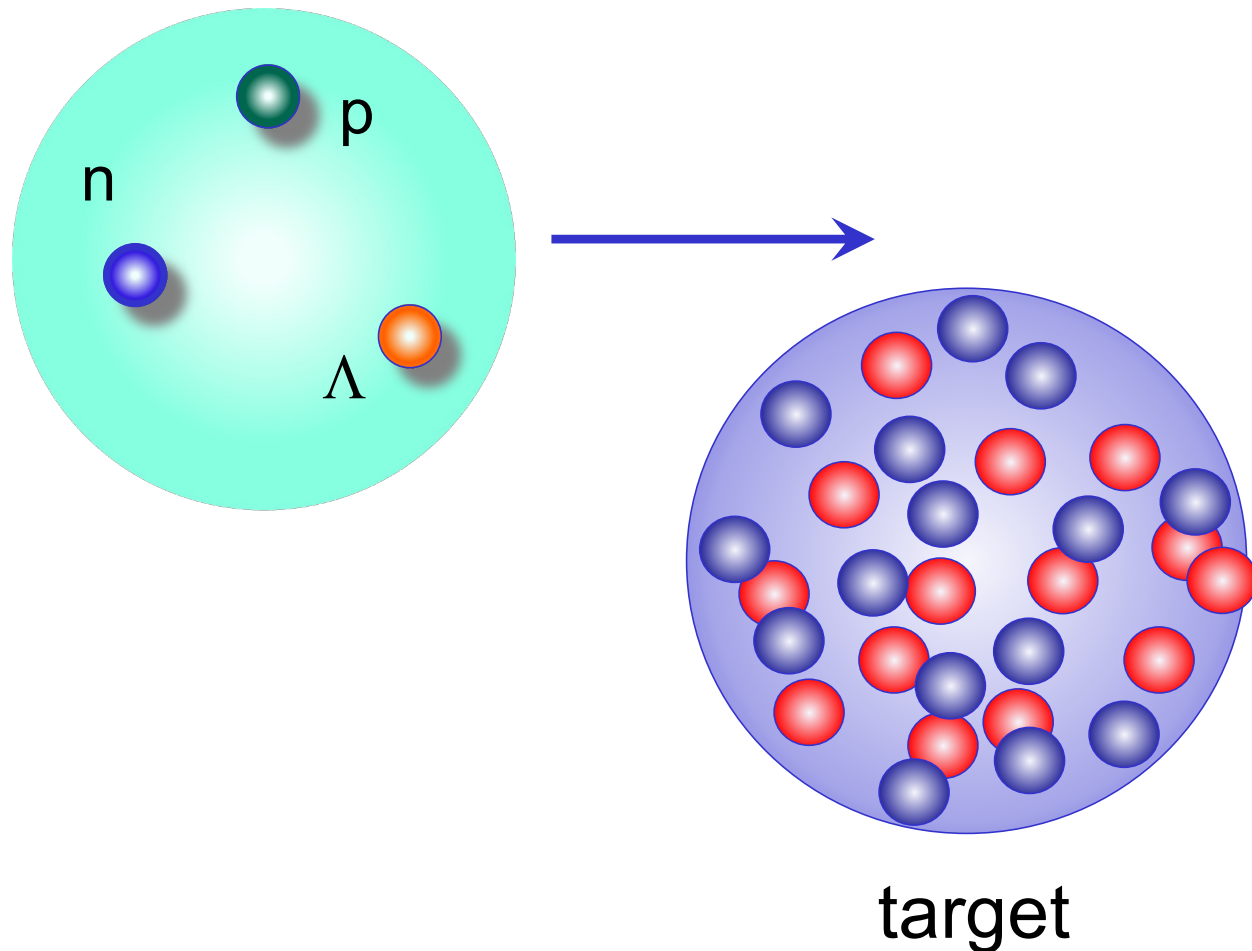


$\rho_1(\mathbf{r}_\Lambda) = |\psi_{\Lambda d}(\mathbf{r}/\beta)|^2$ Λ dist. within ${}^3_\Lambda\text{H}$
 $\rho_2(\mathbf{r}_p) = |\psi_{deut}^{free}(2\mathbf{x})|^2$ p dist. within deut.
 $\rho_N(\mathbf{r}_N) = \int \rho_1(|\mathbf{r} - \mathbf{x}|) \rho_2(\mathbf{x})$
 nucleon distribution within ${}^3_\Lambda\text{H}$

Hypertriton destruction

$$T(b) = T_{\Lambda}(b) T_p(b) T_n(b)$$

Transmission probability



$$\begin{aligned} T_i(b) &= \int d^2s_i dz_i (z_i, \mathbf{s}_i - \mathbf{b}) \\ &= \exp \left[-\sigma_{pi} Z_T \int dz' \rho_p^T(z', \mathbf{s}) \right] \\ &= \exp \left[-\sigma_{ni} N_T \int dz' \rho_n^T(z', \mathbf{s}) \right] \end{aligned}$$

$i = \Lambda, p, \text{ or } n$

1.5 GeV/nucleon ${}^3_{\Lambda}\text{H}$ incident on ${}^{12}\text{C}$, ${}^{120}\text{Sn}$, ${}^{208}\text{Pb}$

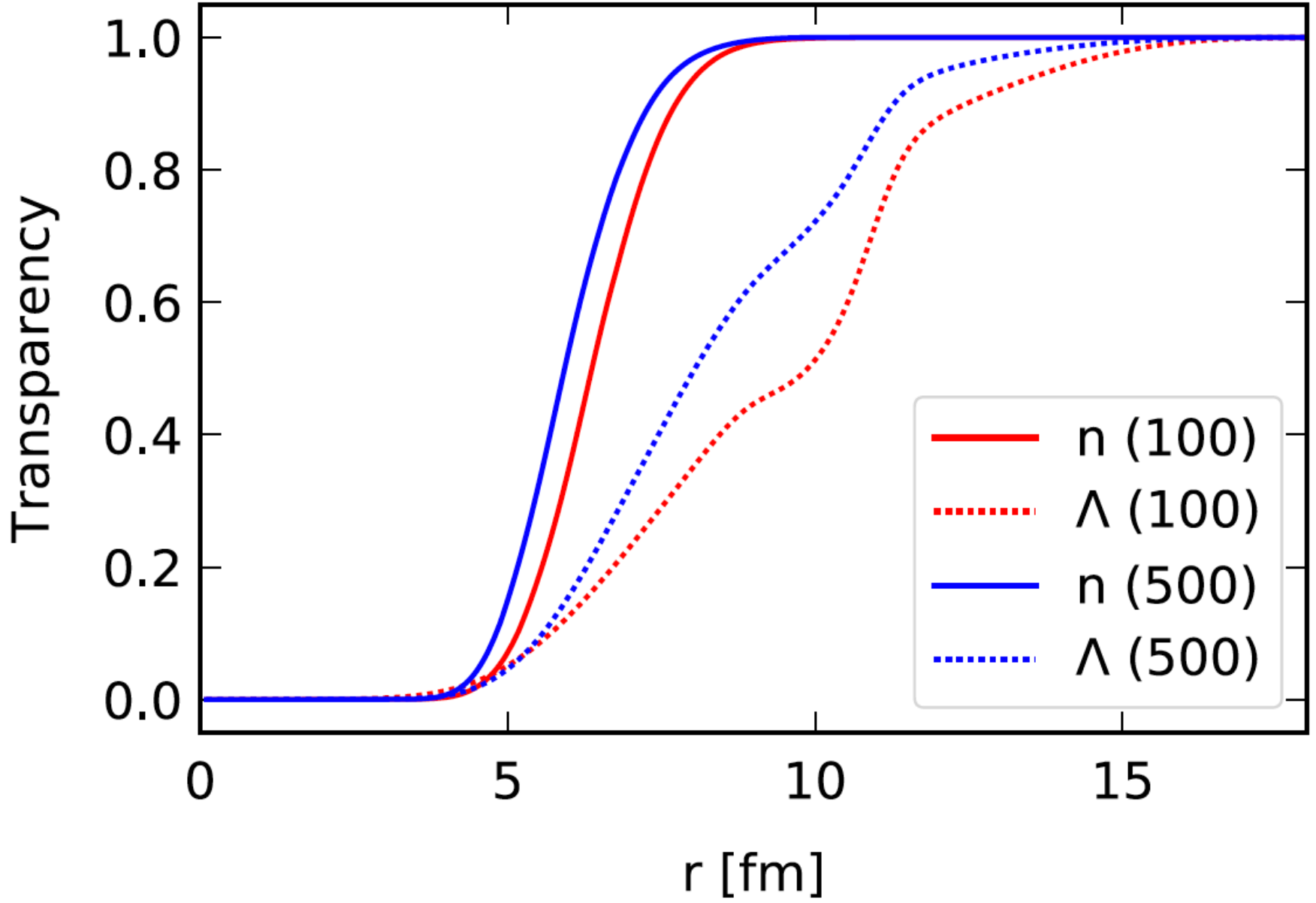
$$\sigma_{np} = 45.8 \text{ mb}$$

$$\sigma_{pp} = 40 \text{ mb}$$

$$\sigma_{\Lambda p} = 35 \text{ mb}$$

Hypertriton destruction

Transmission probability



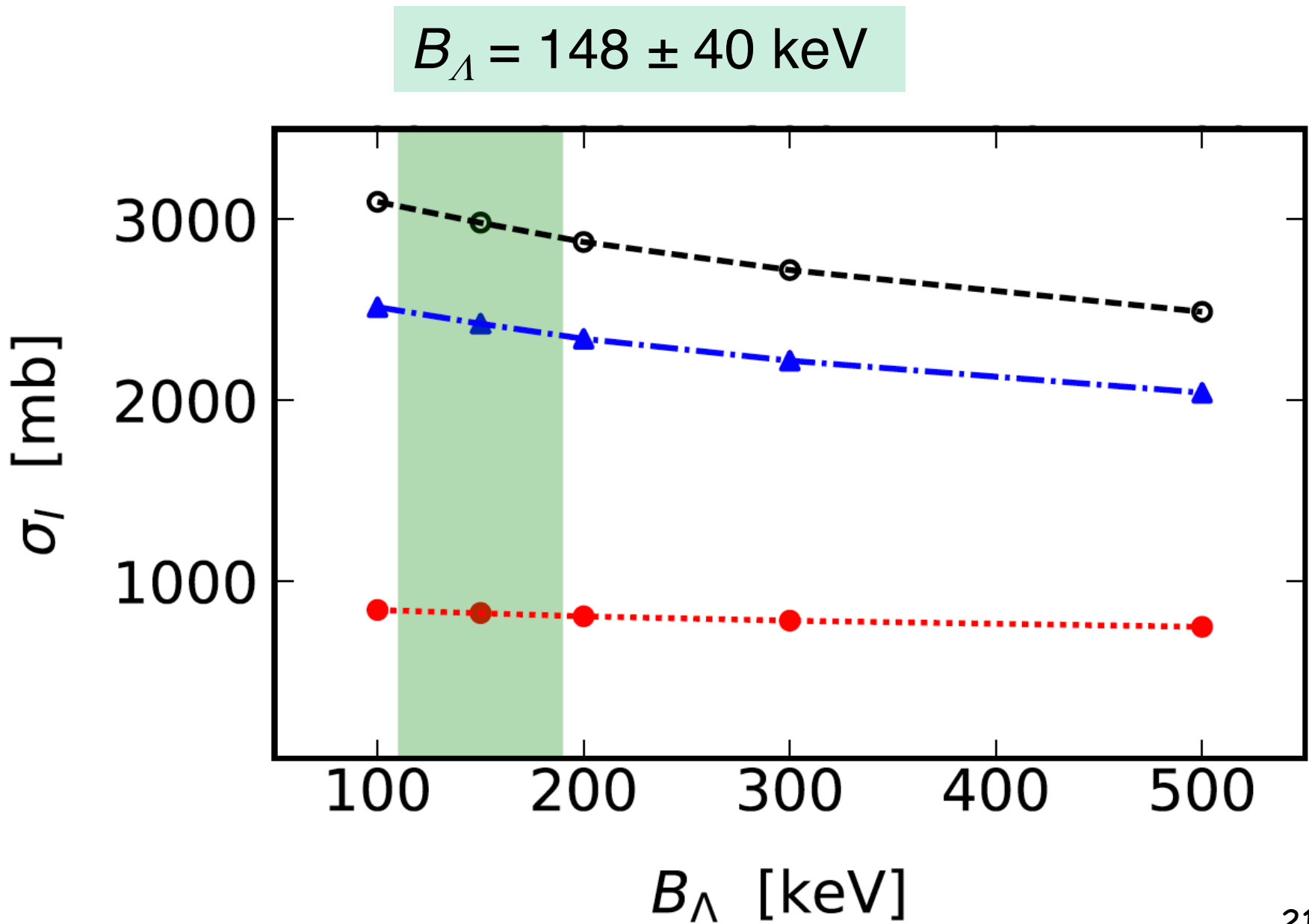
Transition from full opaque-ness to full transparency displays changes in the slope due to structure of the deuteron within ${}^3_{\Lambda}\text{H}$.

Sensitivity to hypertriton interaction cross sections

1.5 GeV/nucleon ${}^3_{\Lambda}\text{H}$ incident on ${}^{12}\text{C}$, ${}^{120}\text{Sn}$, ${}^{208}\text{Pb}$

B_{Λ} (keV)	$\sigma_I(\text{C})$	$\sigma_I(\text{Sn})$	$\sigma_I(\text{Pb})$
100	842.	2516.	3098.
150	824.	2424.	2982.
200	807.	2341.	2876.
300	783.	2220.	2721.
500	749.	2043.	2490.

For a C target: a 12% reduction of the cross section σ_{AI} from $B = 100$ MeV to $B = 500$ MeV.



Nuclear astrophysics

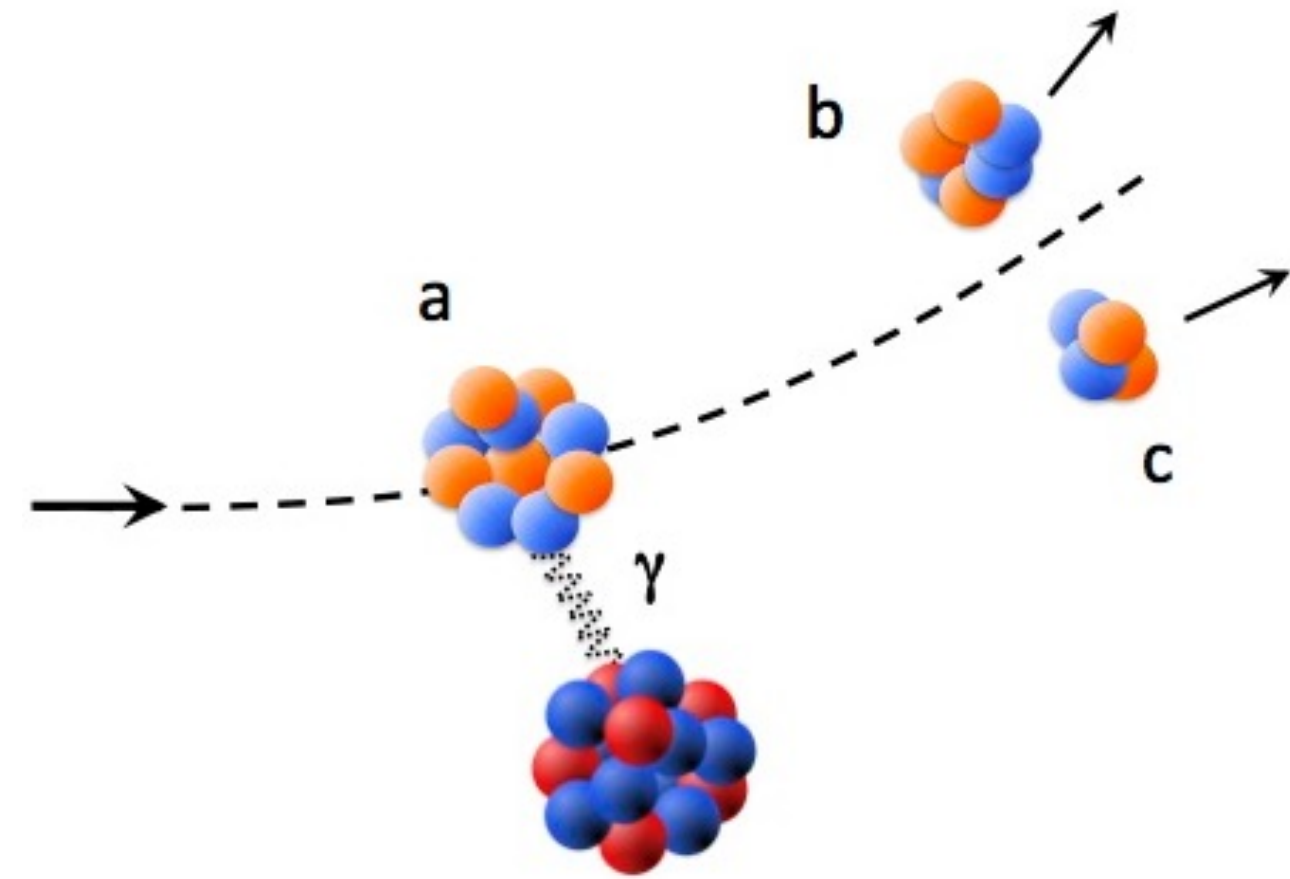
Baur, CB, Rebel, NPA (1986)

$$\frac{d\sigma}{dE_\gamma d\Omega} = \frac{1}{E_\gamma} \sum_1 \frac{dn_1(E_\gamma, \Omega)}{dE_\gamma d\Omega} \sigma_{\gamma + a \rightarrow b + c}(E_\gamma)$$

Theory

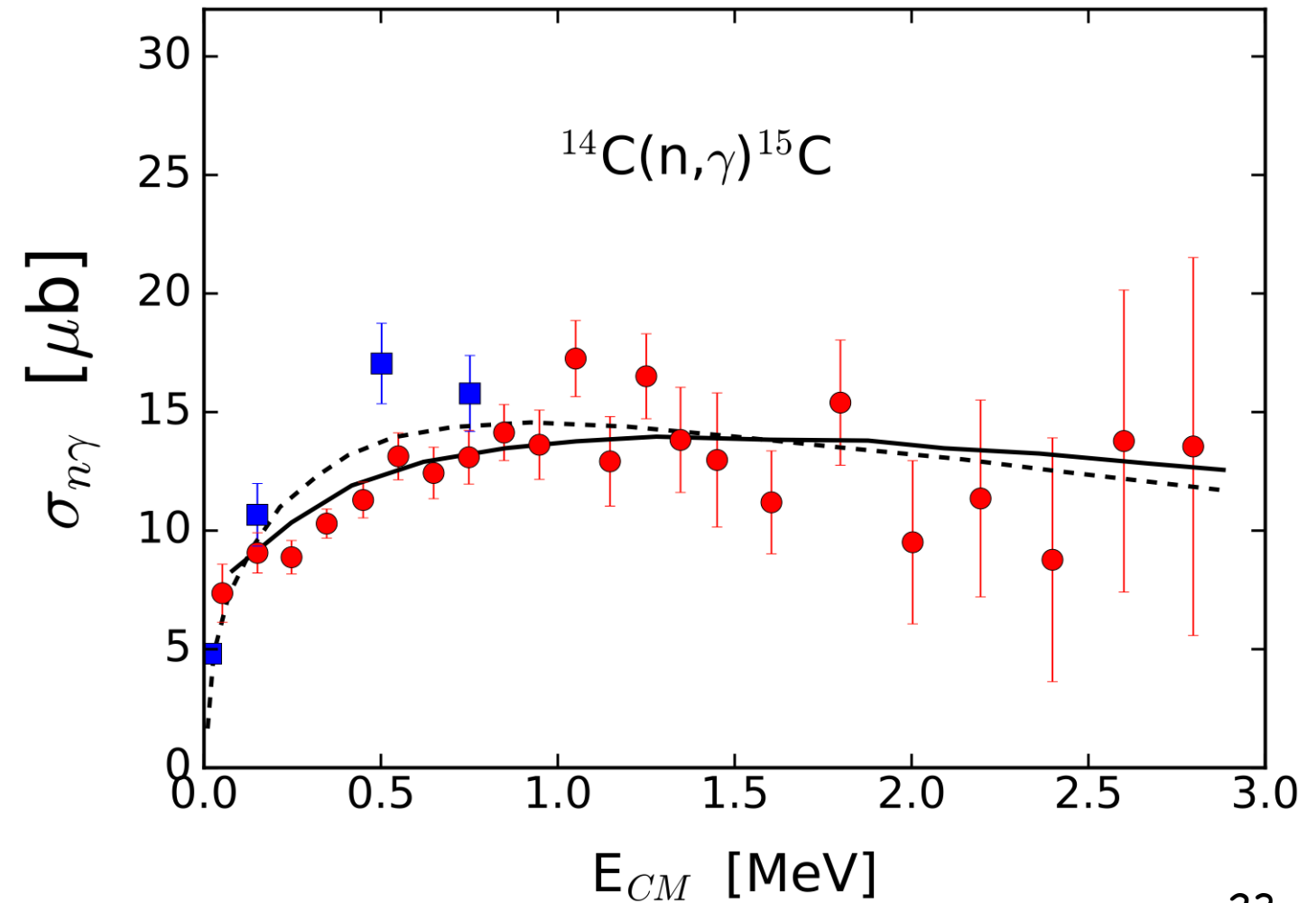
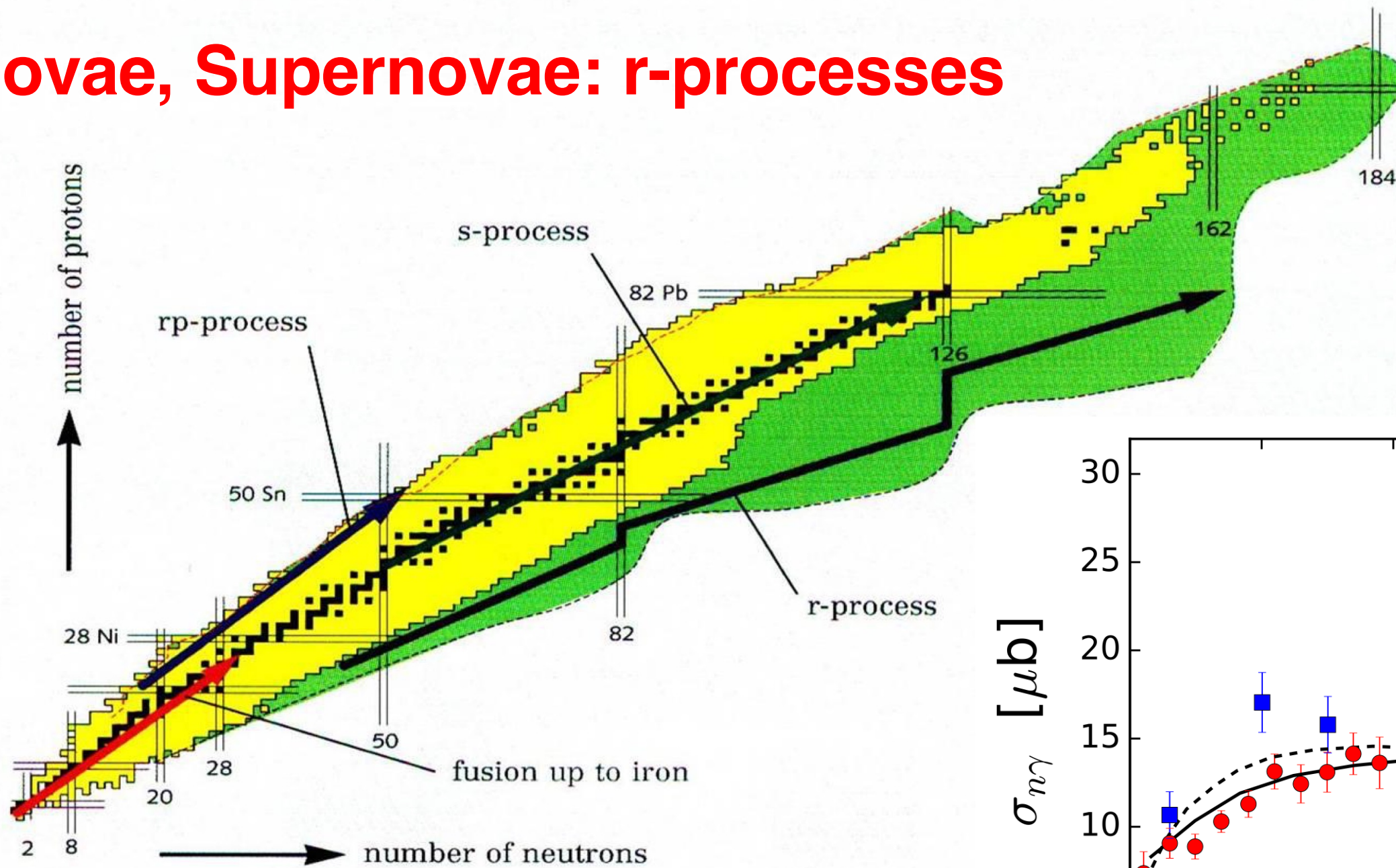
detailed balance

$$\sigma_{b+c \rightarrow a+\gamma} = \frac{2(2j_a + 1)}{(2j_b + 1)(2j_c + 1)} \frac{k_{bc}^2}{k_\gamma^2} \sigma_{\gamma+a \rightarrow b+c}$$



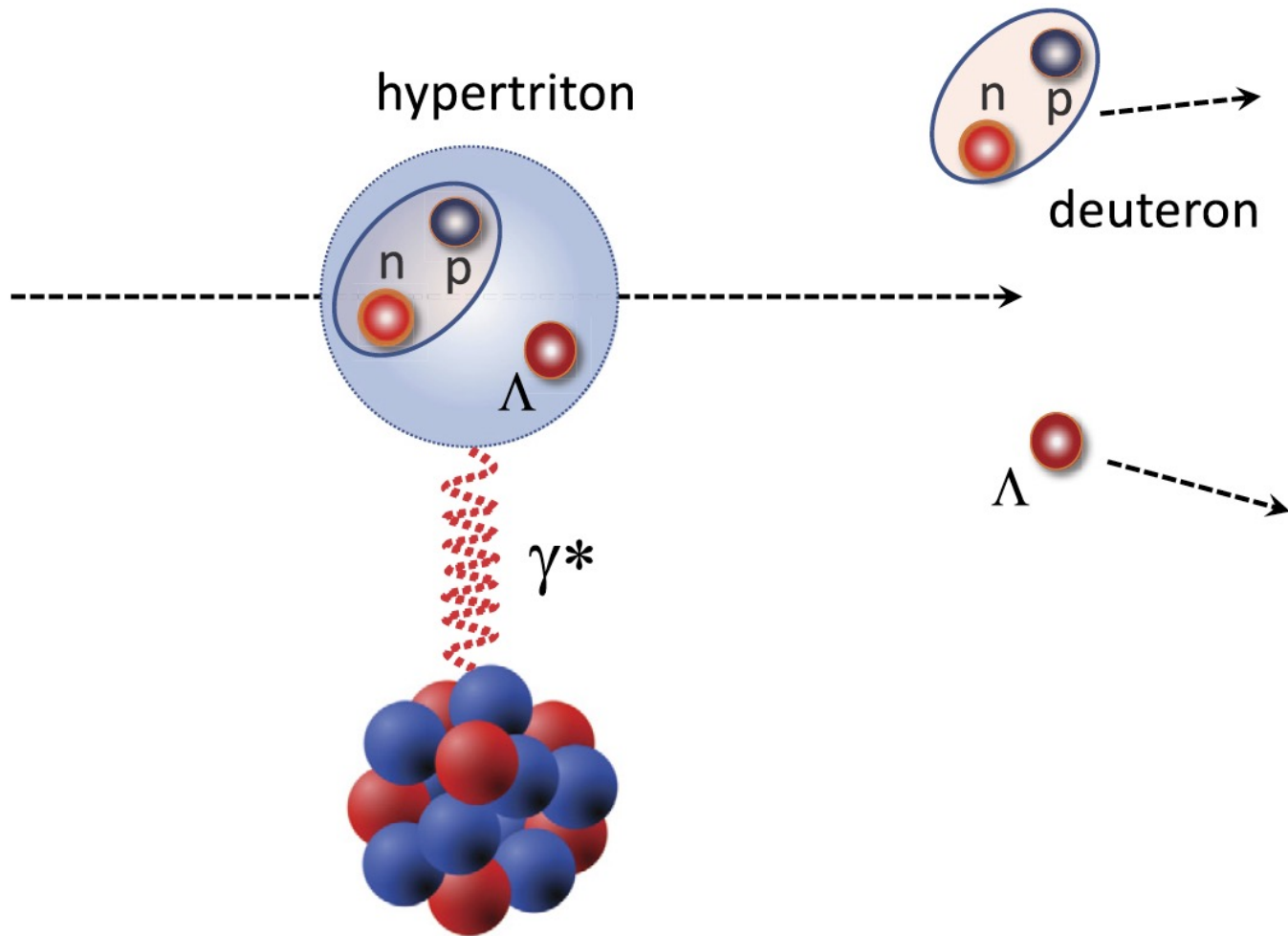
Applications to radiative capture (n,γ) and (p,γ) reactions in nuclear astrophysics

Novae, Supernovae: r-processes



Aumann, Nakamura,
Phys. Scr. T152 (2013) 014012

Electromagnetic response of the hypertriton



$$\frac{d\sigma_c}{dE} = \frac{16\pi^3}{9\hbar c} n(E) \frac{dB(E)}{dE}$$

$$n(E) = \frac{2Z_T^2 \alpha}{\pi} \left(\frac{Ec}{\gamma \hbar v^2} \right)^2 \int_0^\infty db b \left[K_1^2 + \frac{1}{\gamma^2} K_0^2 \right] T(b)$$

$$x = Eb/\gamma v$$

First-order perturbation theory

$$\frac{dB(E)}{dE} = \frac{1}{\hbar} \sqrt{\frac{\mu}{2E}} |\langle g.s. || \mathcal{O}_{E1} || E, l \rangle|^2$$

$$\langle g.s. || \mathcal{O}_{E1} || E, l \rangle = (-1)^l \frac{e_{eff}}{\sqrt{4\pi}} \int_0^\infty dr r u_{g.s.}(r) u_{E,l}(r)$$

$$u_{E,l}(r) \rightarrow \sqrt{2\mu_{\Lambda d}/\pi \hbar^2 k} e^{i\delta_l} \sin(kr + \delta_l)$$

Electromagnetic response of the hypertriton

$$\frac{dB(E)}{dE} = \frac{1}{\hbar} \sqrt{\frac{\mu}{2E}} |\langle g.s. || \mathcal{O}_{E1} || E, l \rangle|^2$$

Analytical model:

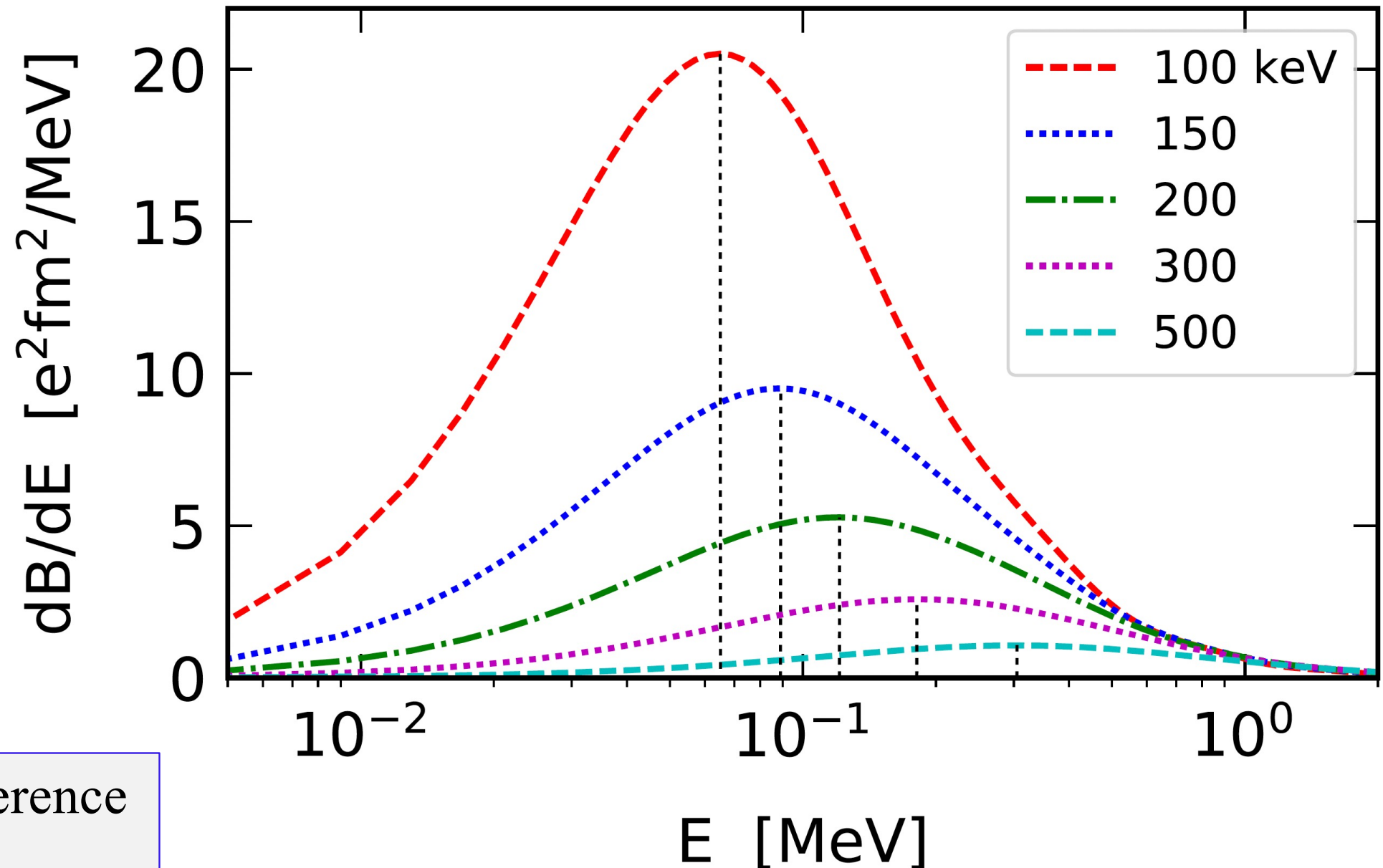
CB, Sustich

Phys. Rev. C 46 (1992) 2340

$$\frac{dB(E)}{dE} = C \sqrt{B_\Lambda} \frac{E^{3/2}}{(E + B_\Lambda)^4}$$

$$E_{max} = \frac{3}{5} B_\Lambda$$

- Excellent agreement < 4% difference
- FSI small

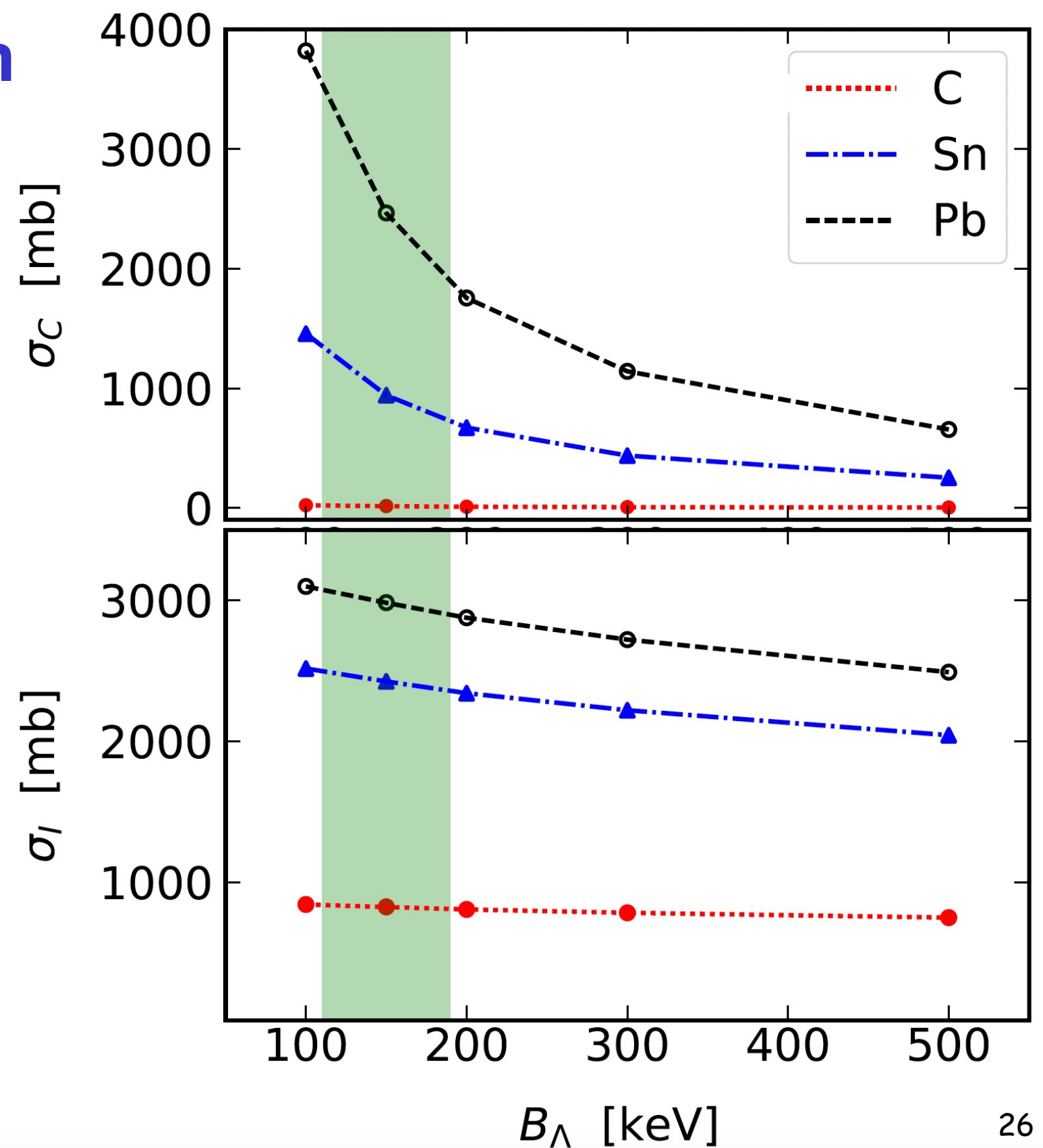


EM response of the hypertriton

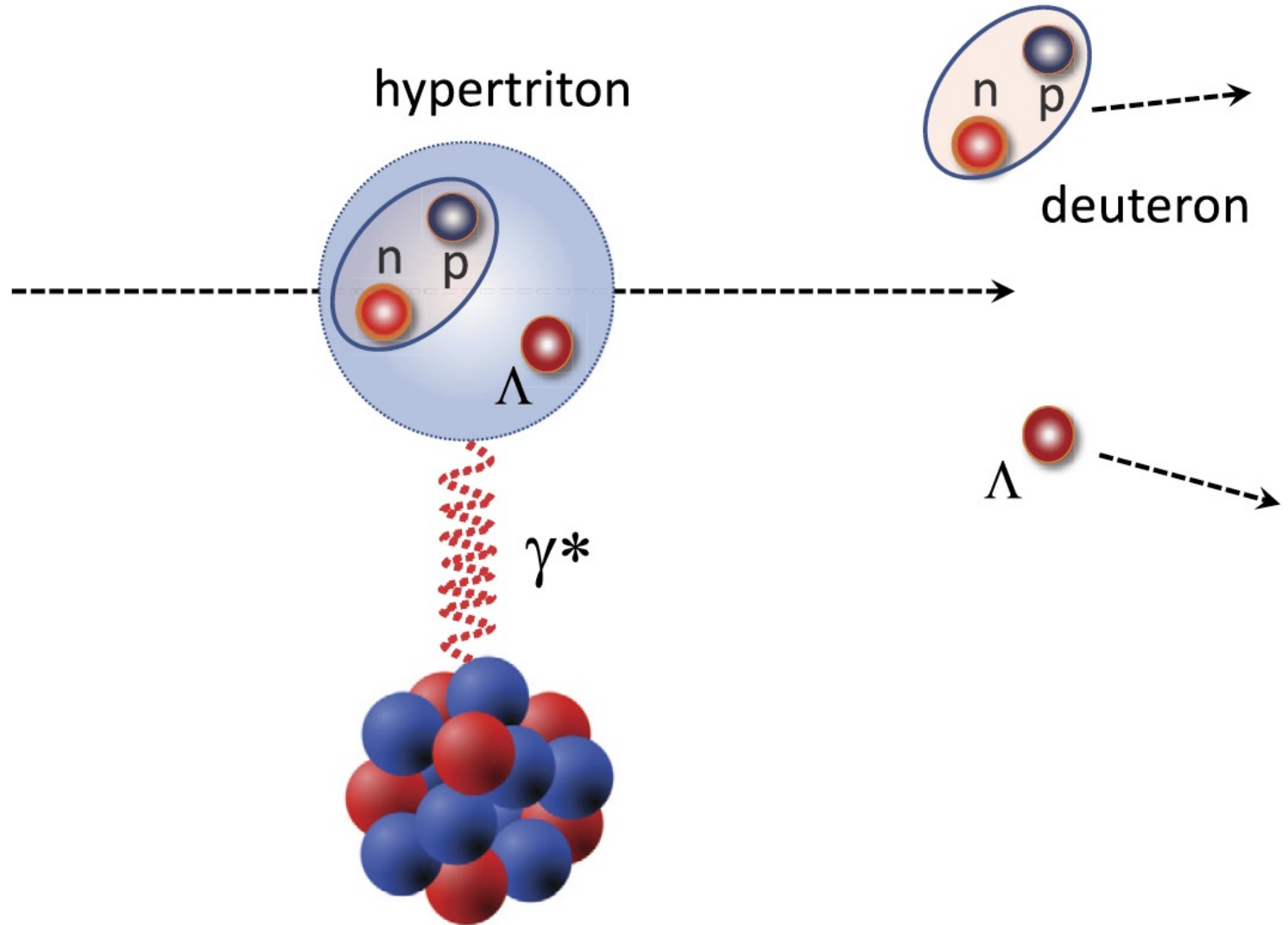
1.5 GeV/nuc. ${}^3_{\Lambda}\text{H}$ incident on ${}^{12}\text{C}$, ${}^{120}\text{Sn}$, ${}^{208}\text{Pb}$

B_{Λ} (keV)	$\sigma_C(\text{C})$	$\sigma_C(\text{Sn})$	$\sigma_C(\text{Pb})$
100	22.9	1457.	3820.
150	14.9	942.	2464.
200	10.7	672.	1755.
300	7.1	438.	1142.
500	4.1	253.	656.

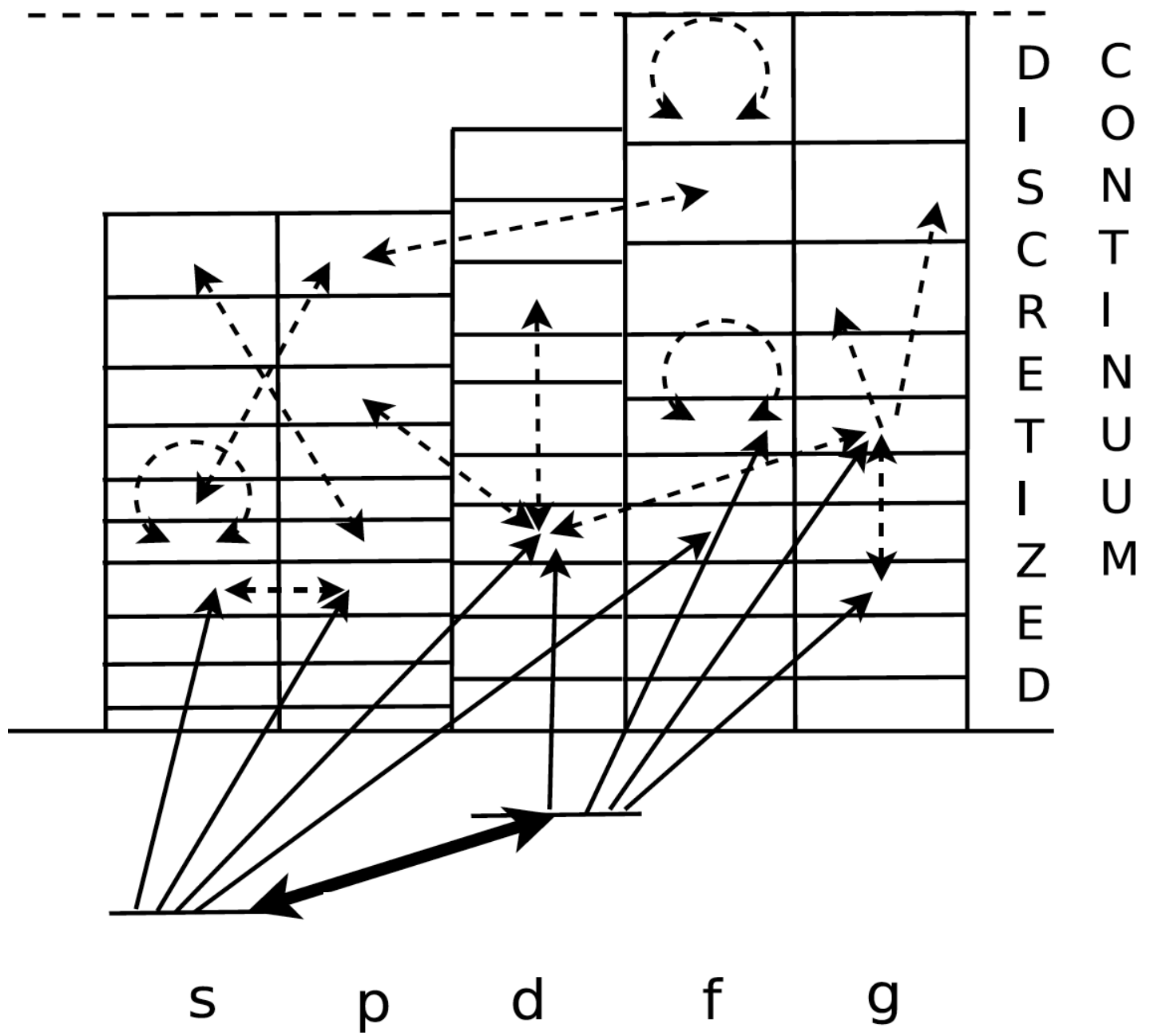
B_{Λ} (keV)	$\sigma_I(\text{C})$	$\sigma_I(\text{Sn})$	$\sigma_I(\text{Pb})$
100	842.	2516.	3098.
150	824.	2424.	2982.
200	807.	2341.	2876.
300	783.	2220.	2721.
500	749.	2043.	2490.



EM response of the hypertriton



- Basis expansion for intrinsic ϕ
- Eikonal scattering waves
- Nuclear + EM potentials
- Relativity



- Continuum discretization
- Coupled-channels (relativistic CDCC)

Electromagnetic response of loosely bound nuclei

$$i\hbar v \frac{d}{dz} S_c(\mathbf{b}, z) = \sum_{c'} \langle \Phi_c | H_{int}(\mathbf{b}, z) | \Phi_{c'} \rangle S_{c'}(\mathbf{b}, z) \exp \left[i \frac{E_{cc'} z}{\hbar c} \right]$$

$$f_c(\mathbf{q}) = -\frac{ik}{2\pi} \int db \exp(i\mathbf{q} \cdot \mathbf{b}) [S_c(\mathbf{b}, z) - \delta_{0c}]$$

$$\frac{d\sigma_c}{d\Omega} = \sum_{M_0, M_c} \left| f_c^{(M_c - M_0)}(\theta, E_c) \right|^2$$

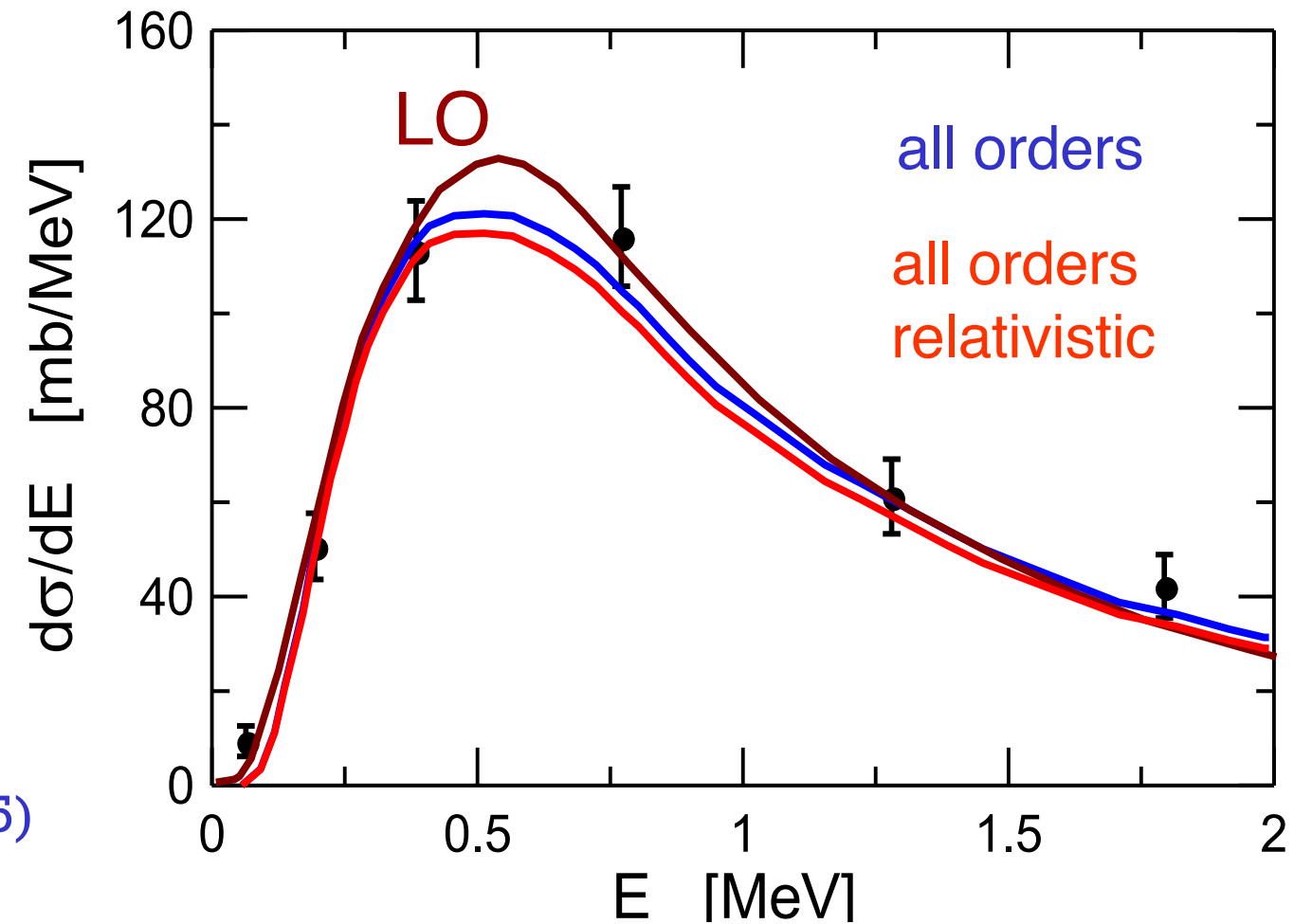
$$|E_c\rangle = \int dE'_c \Gamma(E'_c) |E'_c\rangle$$

$$\Gamma(E_j) = \begin{cases} \frac{1}{\Delta E} & \text{if } (j-1)\Delta E < E_c < j\Delta E \\ 0, & \text{otherwise} \end{cases}$$

$H_{int} = H_{EM} = \text{easy}$

$H_{int} = H_{\text{nucleus-nucleus}}$
= very complicated

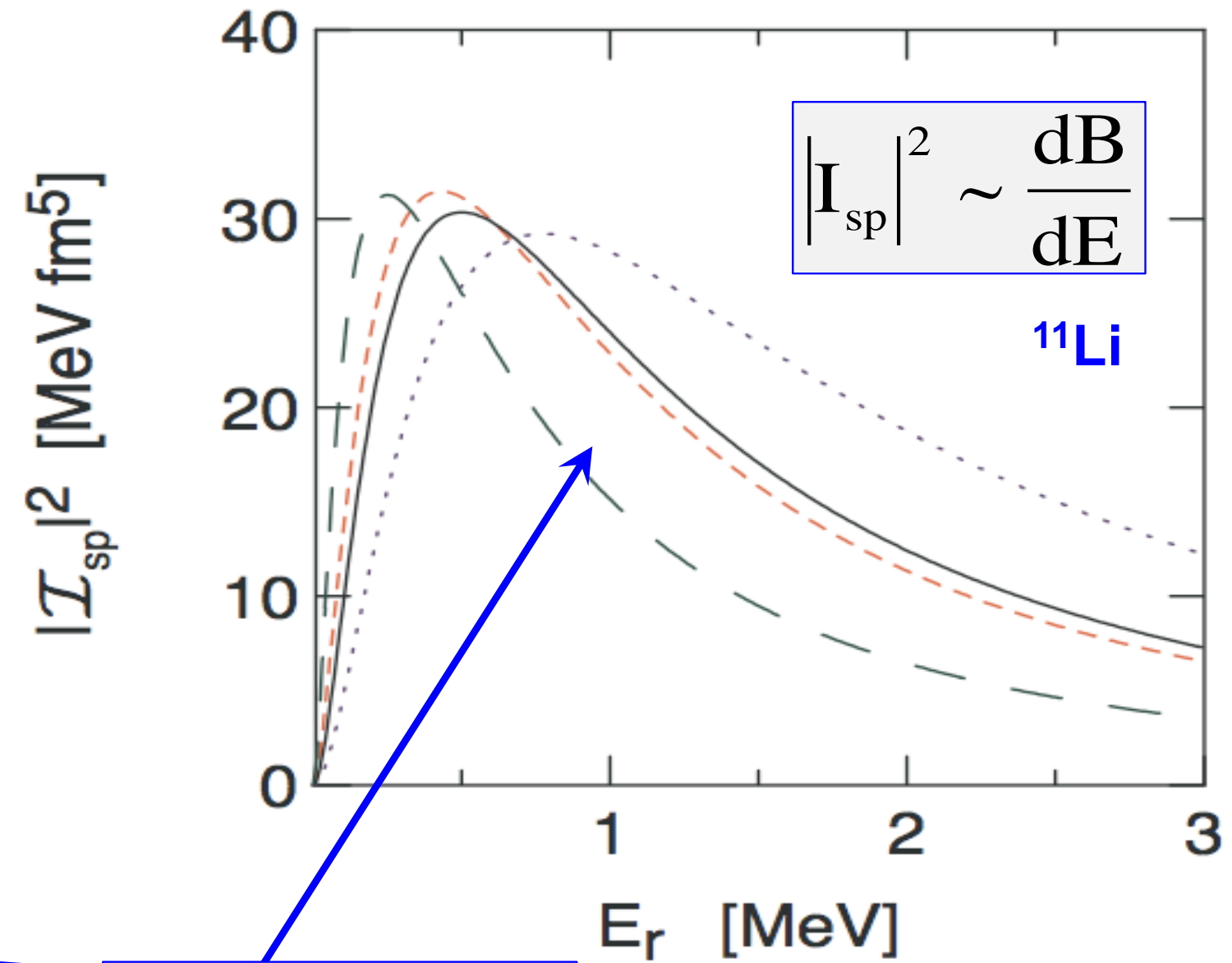
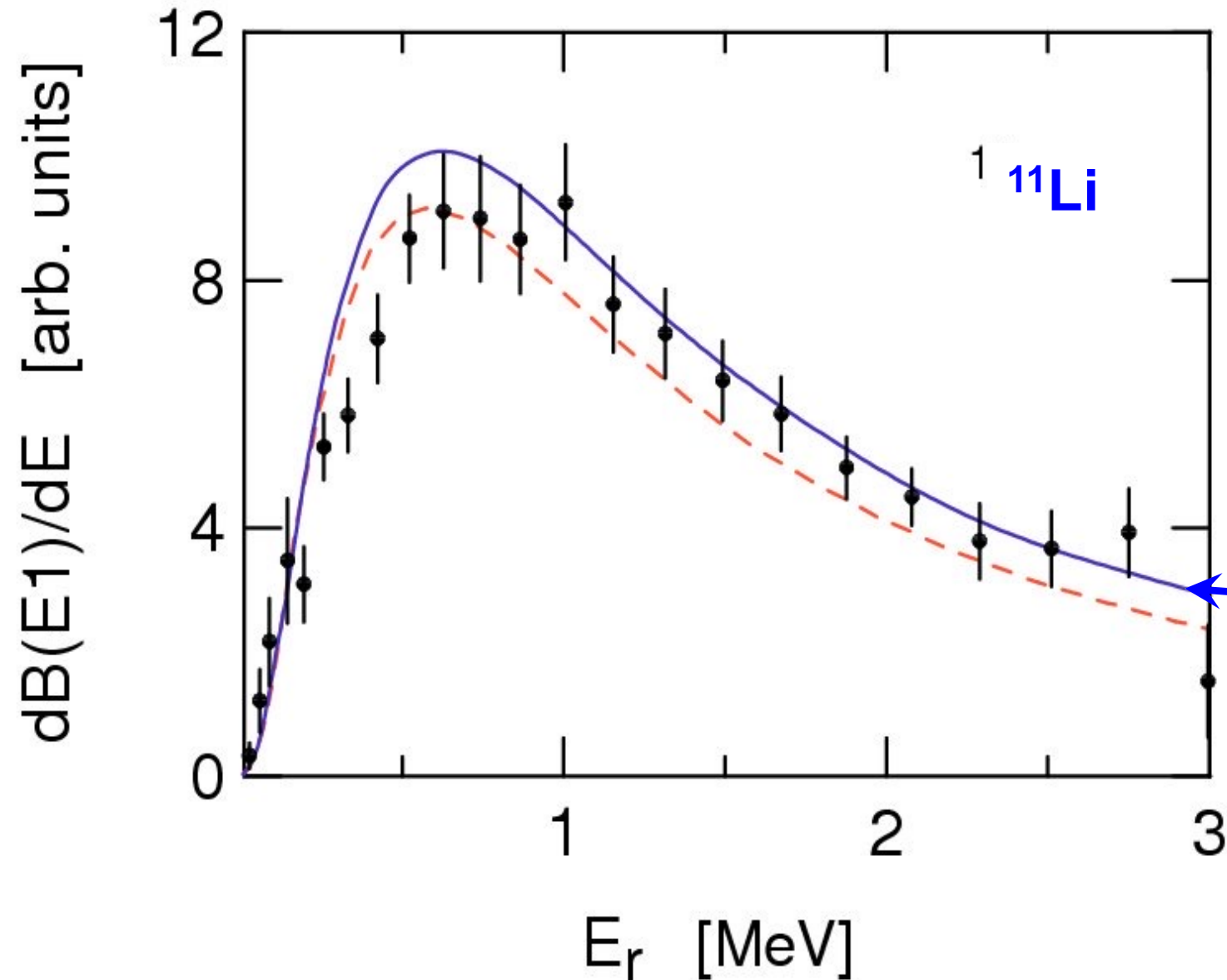
Pb ($^8\text{B}, p^7\text{Be}$) at 100 MeV/nucleon



CB, PRL 94, 072701 (2005)

Final state interactions (FSI)

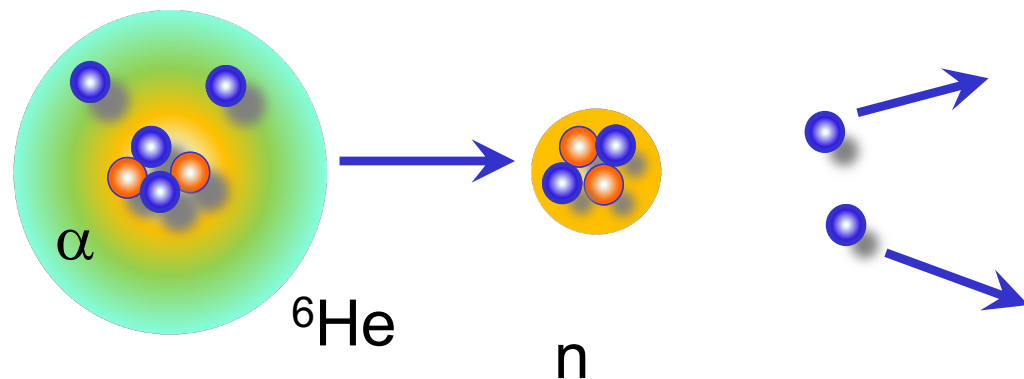
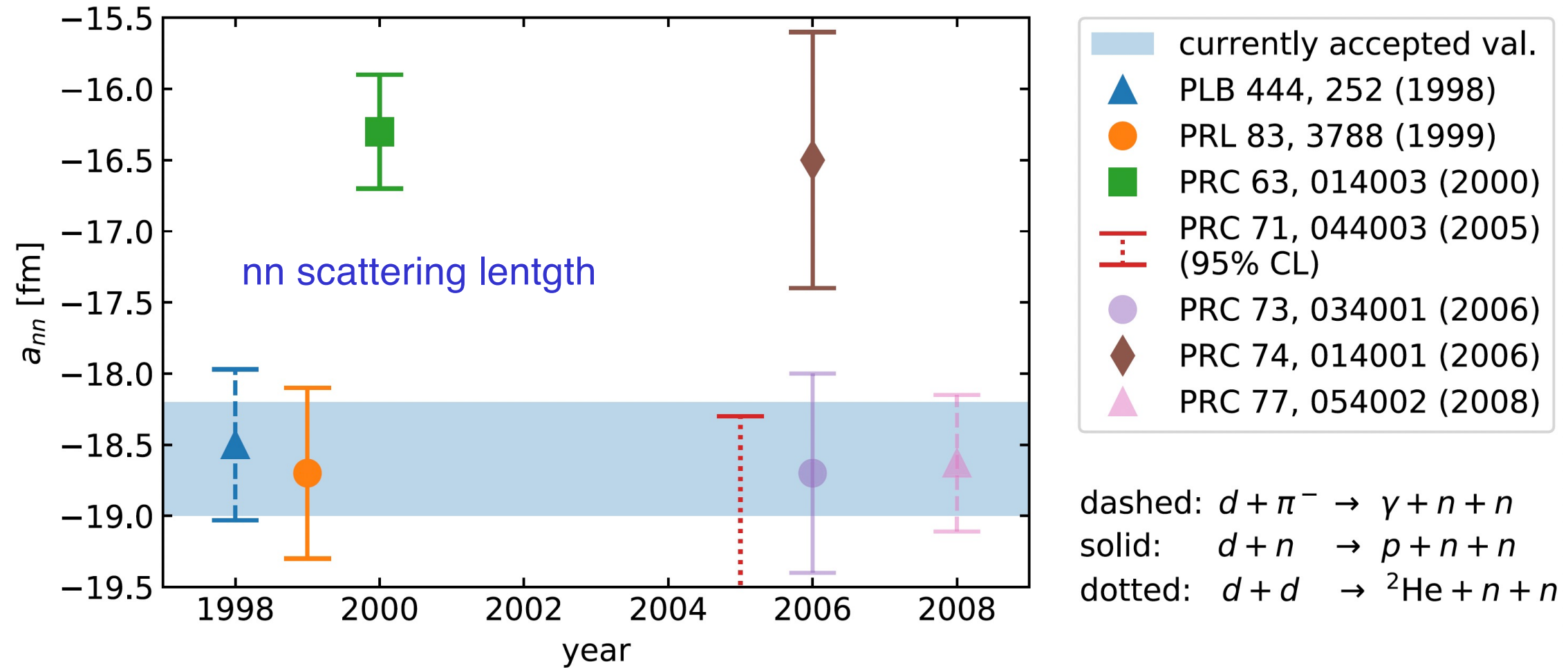
3-body configurations and FSI widen $\frac{dB(E1)}{dE}$



FSI: Different scattering lengths, effective ranges

CB, PRC 75, 024606 (2007)

FSI and nn scattering length



${}^6\text{He}(p,p\alpha)nn$ reaction in inverse kinematics at high energies

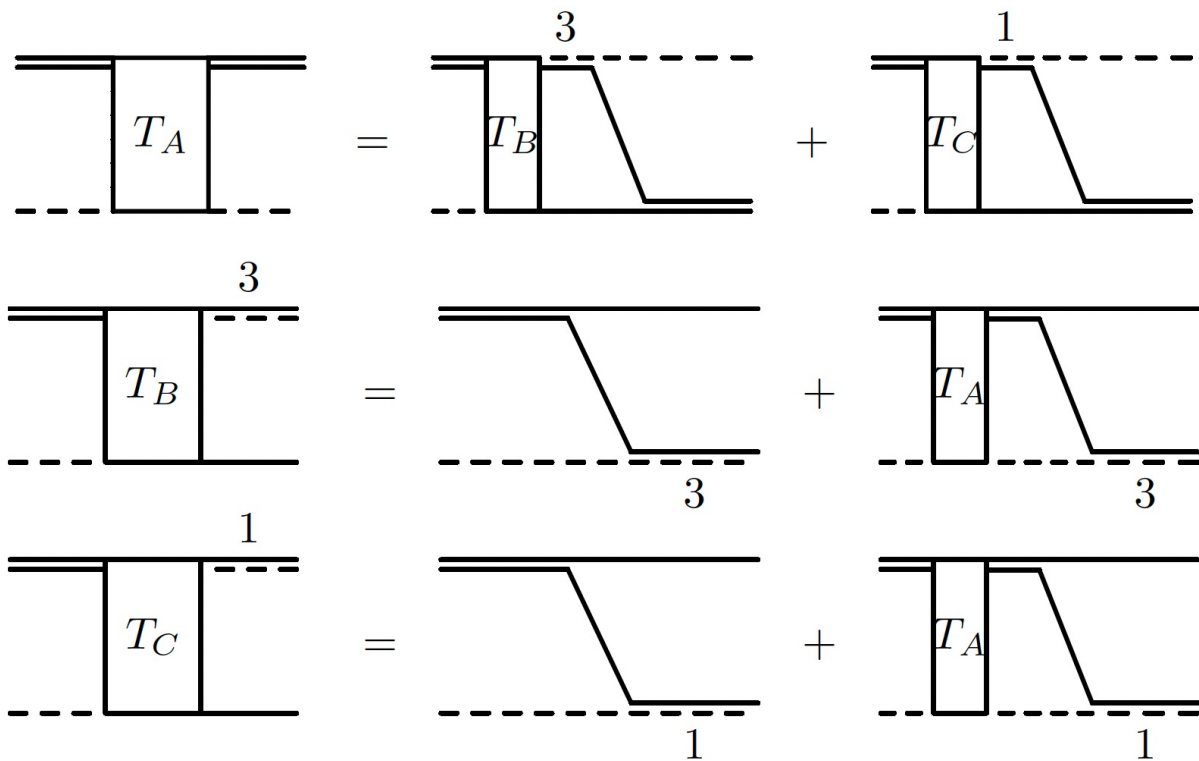
Göbel, et al, PRC 104, 024001 (2021)

Effective Field Theory (EFT)

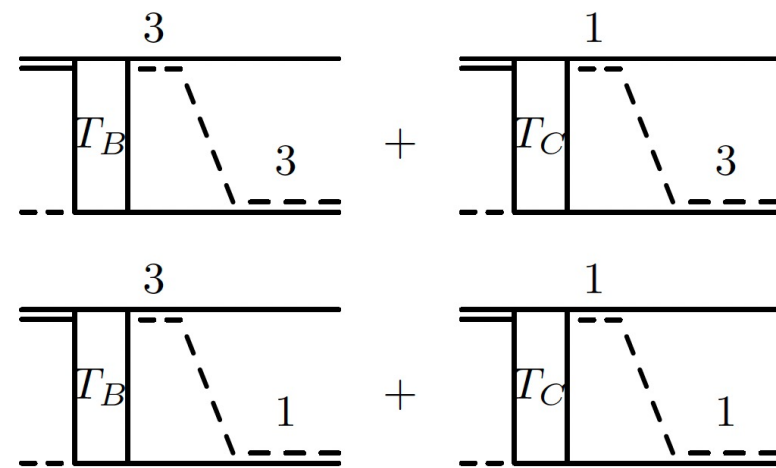
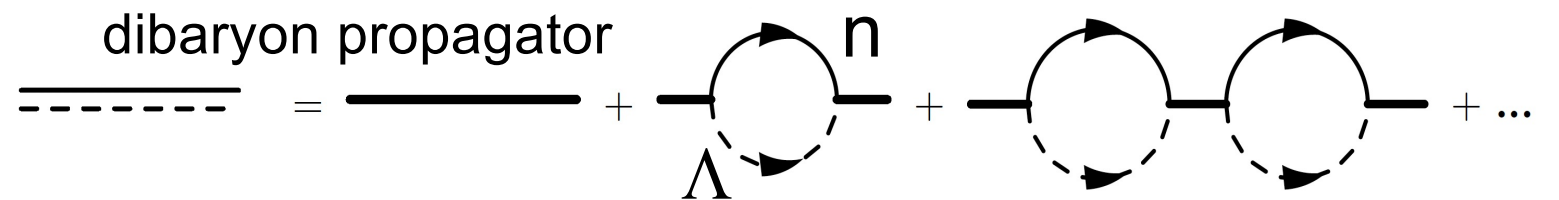
Pionless EFT

- (a) Momentum scales < pion mass
- (b) Dibaryon field Δ_d
- (c) Cutoff parameter Λ_c
- (d) Simplified 3-body force $H(s_0, \Lambda_c)$
- (e) Asymptotic analysis

Hildenbrand, Hammer,
Phys. Rev. C, 100, 034002 (2019)



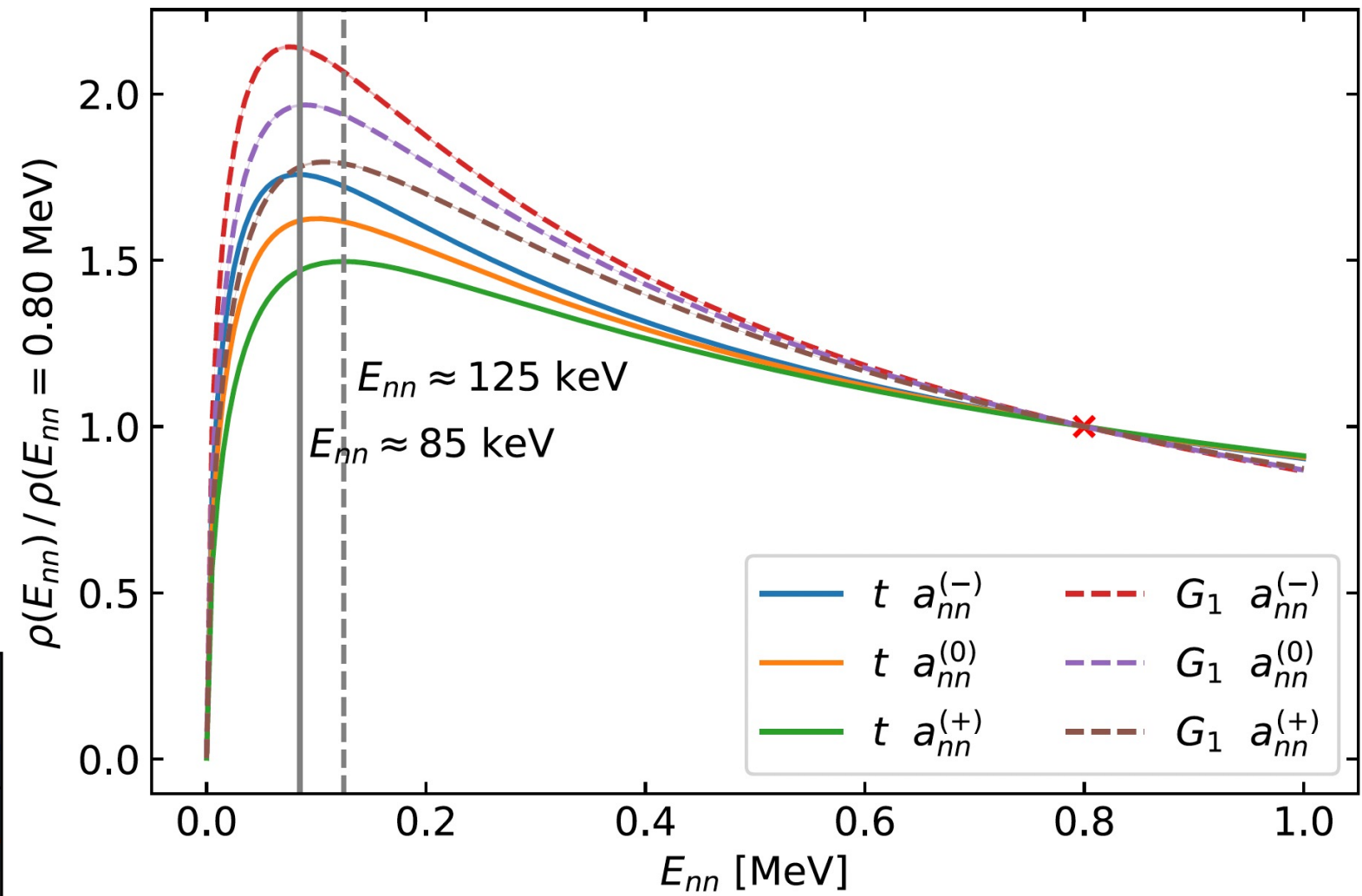
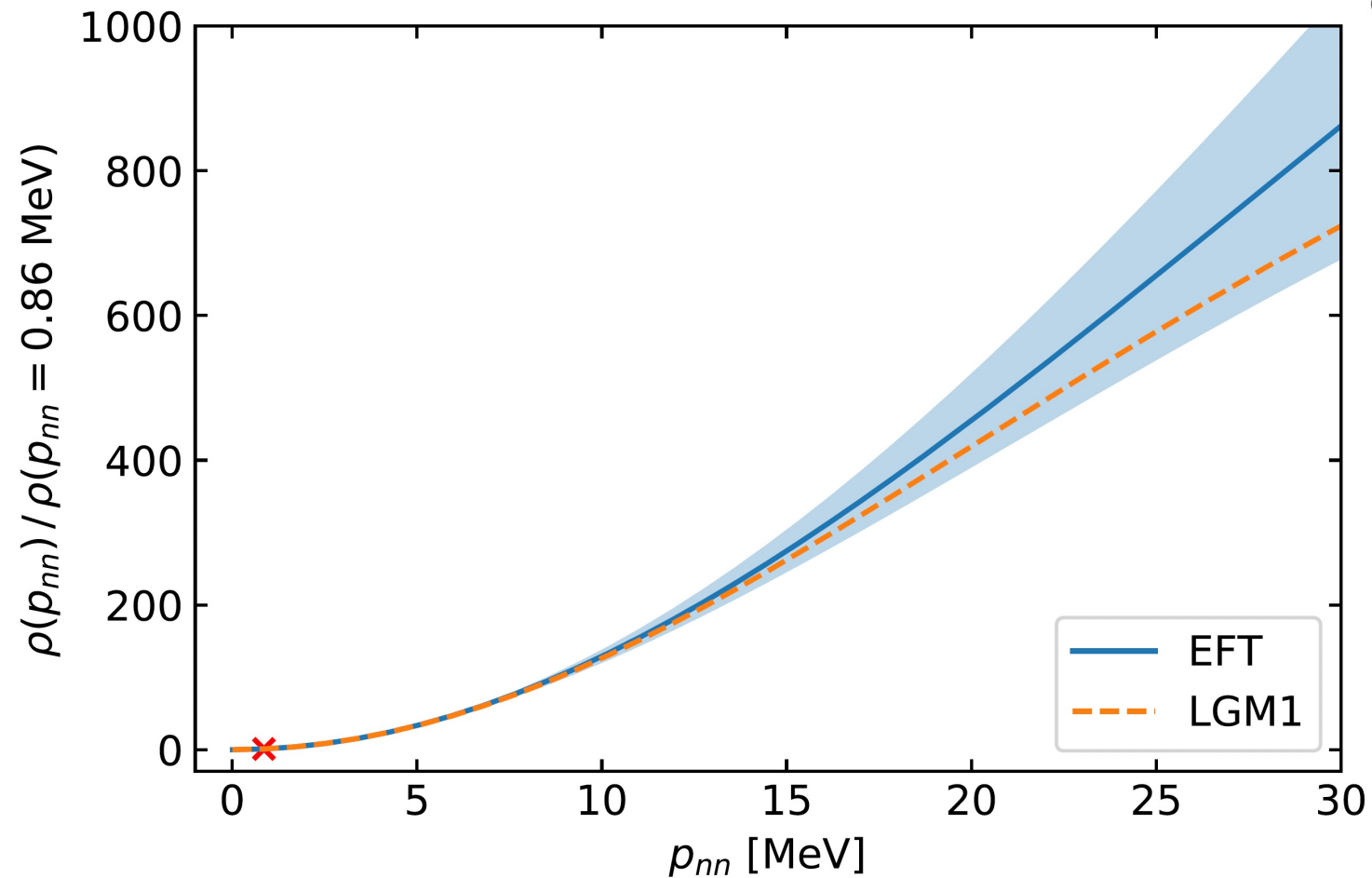
$$\begin{aligned} \mathcal{L} = & N^\dagger \left(i\partial_t + \frac{\nabla^2}{2M} \right) N + \Lambda^\dagger \left(i\partial_t + \frac{\nabla^2}{2M_\Lambda} \right) \Lambda \\ & + \Delta_d d_l^\dagger d_l - \frac{g_d}{2} \left[d_l^\dagger N^T (i\tau_2) (i\sigma_l \sigma_2) N + \text{H.c.} \right] \\ & + \Delta_s s_j^\dagger s_j - \frac{g_s}{2} \left[s_j^\dagger N^T (i\tau_j \tau_2) (i\sigma_2) N + \text{H.c.} \right] \\ & + \Delta_3 (u_l^3)^\dagger u_l^3 - g_3 \left[i (u_l^3)^\dagger \Lambda^T (i\sigma_l \sigma_2) N + \text{H.c.} \right] \\ & + \Delta_1 (u^1)^\dagger u^1 - g_1 \left[i (u^1)^\dagger \Lambda^T (i\sigma_2) N + \text{H.c.} \right] + \dots \end{aligned}$$



nn scattering length

Göbel, et al, PRC 104, 024001 (2021)

Halo EFT \rightarrow nn configuration
in ${}^6\text{He}$ \rightarrow E_{nn} density



LGM1 = Faddeev calculations with local Gaussian potentials

pp scattering length

v_{NN} charge independence violation: $m_{\pi^\pm} \neq m_{\pi^0}$

v_{NN} charge symmetry violation: $m_{down} \neq m_{up}$

$p + d \rightarrow p + p + n \rightarrow p + p$ scattering

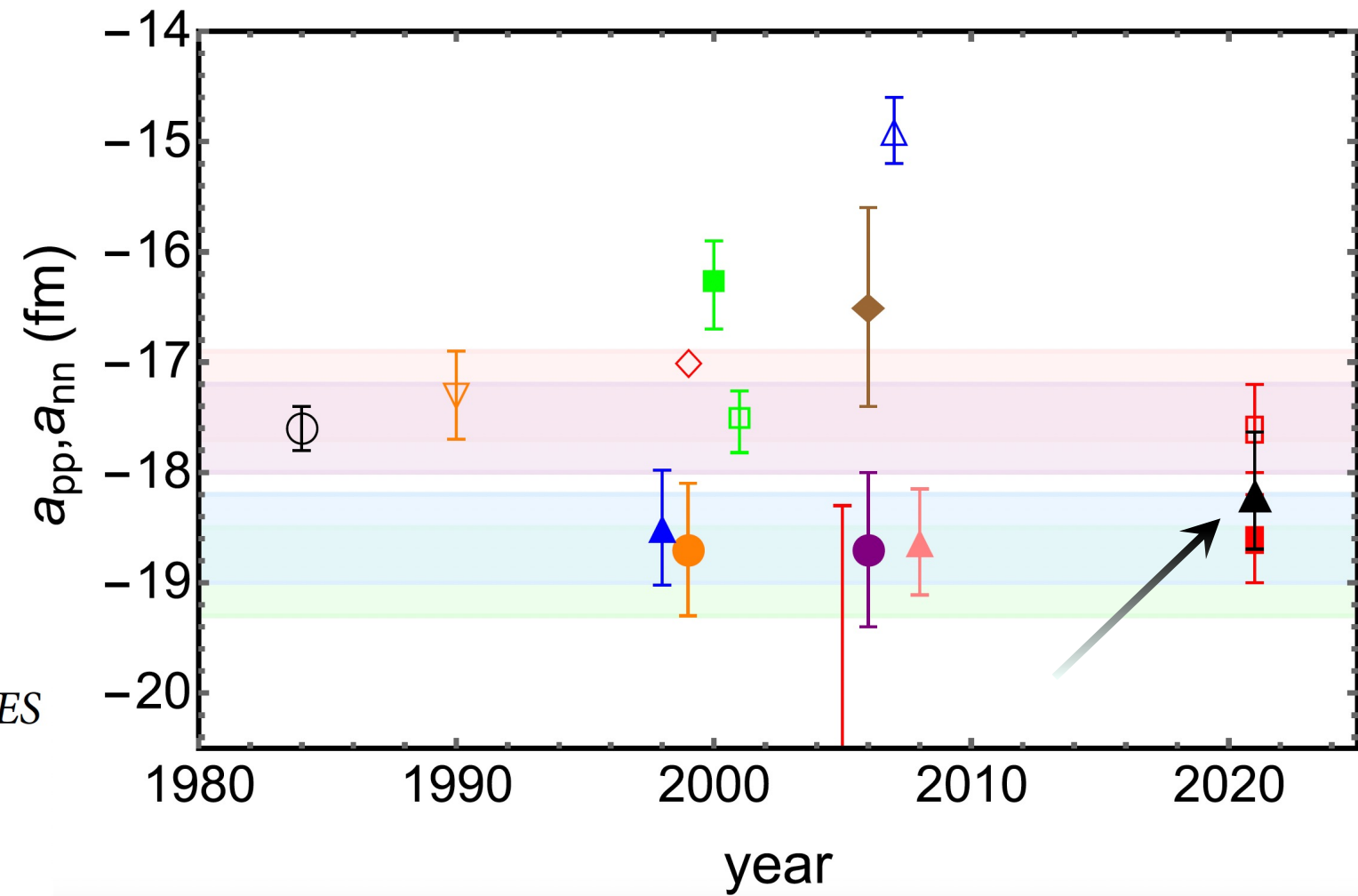
Tumino, et al,
Nature Comm. Phys. 6, 106 (2023)

$$\frac{d^3 \sigma}{d\Omega_B d\Omega_b dE_B} = (KF) \cdot |\phi(p_{xs})|^2 \cdot \left[\frac{d^2 \sigma_{xA \rightarrow bB}}{dE_{c.m.} d\Omega} \right]^{HOES}$$

$$\left(\frac{d\sigma}{d\Omega_{c.m.}} \right)^{HOES} = \frac{1}{4k^2} \left(|F(\mathbf{p}, \mathbf{k}) - 2T_{CN}(p, k)|^2 + 3|F(\mathbf{p}, \mathbf{k})|^2 \right)$$

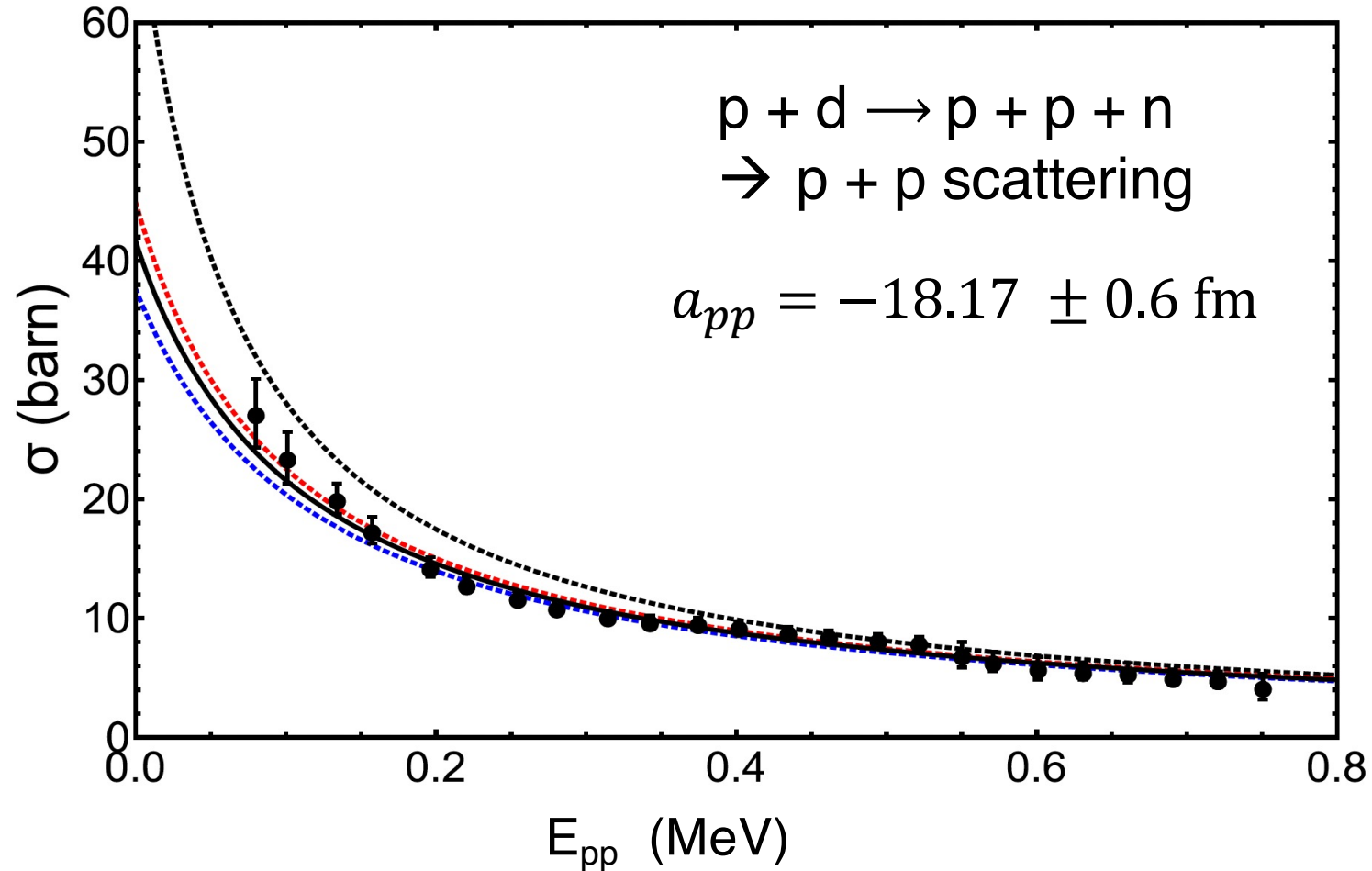
$$F(\mathbf{p}, \mathbf{k}) = m_p e^2 e^{-\pi\eta} \Gamma(1 + i\eta) (p^2 - k^2)^{i\eta} g(\mathbf{p}, \mathbf{k})$$

$$g(\mathbf{p}, \mathbf{k}) = (\mathbf{p} - \mathbf{k})^{-2(1+i\eta)} \pm (\mathbf{p} + \mathbf{k})^{-2(1+i\eta)}$$



Energy differences between mirror nuclei small as compared to experiment (Nolen-Schiffer anomaly)

pp scattering length



NN s-wave phase shift

$$k \cot \delta = -\frac{1}{a} + \frac{1}{2} r_0 k^2$$

$$\sigma = \frac{4\pi}{\left(\frac{1}{a} - \frac{1}{2} r_0 k^2\right)^2 + k^2}$$

$$V_{NN}(R) = V_0 e^{-\frac{r^2}{r_G^2}} + \frac{e_{NN}^2}{r}$$

disable EM \rightarrow d from short-range
universal window

Table 2 The effect of electromagnetic terms. Low-energy parameters with and without the inclusion of the electromagnetic terms for the two potential models indicated.

	Argonne v_{18}	w/o v^{EM}		Argonne v_{18}	w/o v^{EM}
$^1a_{nn}(\text{fm})$	-18.487	-18.818	$^1a_{pp}(\text{fm})$	-7.806	-17.164
$^1r_{nn}(\text{fm})$	2.840	2.834	$^1r_{pp}(\text{fm})$	2.788	2.865
	Gaussian	w/o v^{EM}		Gaussian	w/o v^{EM}
$^1a_{nn}(\text{fm})$	-18.487	-18.89 ± 0.02	$^1a_{pp}(\text{fm})$	-7.806	-17.19 ± 0.03
$^1r_{nn}(\text{fm})$	2.85 ± 0.07	2.83 ± 0.07	$^1r_{pp}(\text{fm})$	2.77 ± 0.08	2.86 ± 0.08

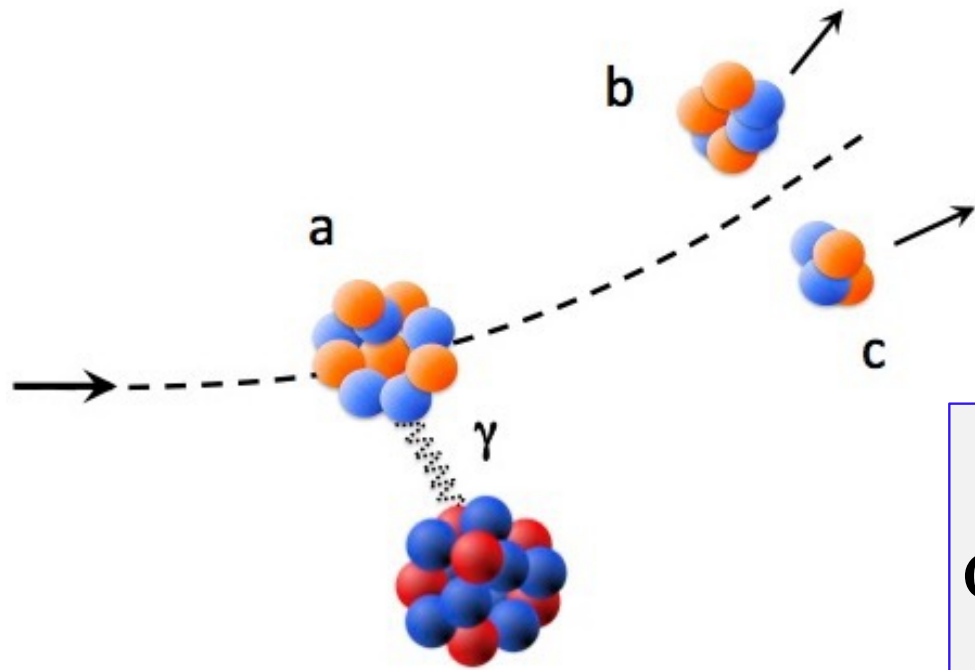
Pigmy resonances & Dipole polarizability

Rossi et al.

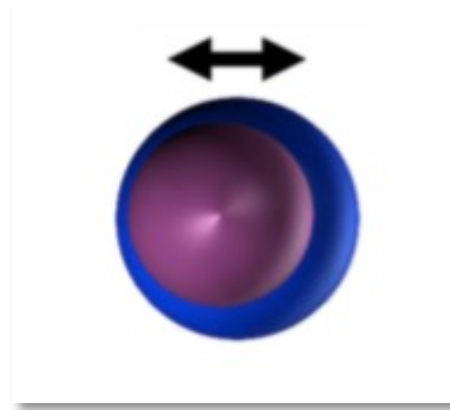
PRL 111 (2013) 242503

Wieland et al.

PRL 102, 092502 (2009)

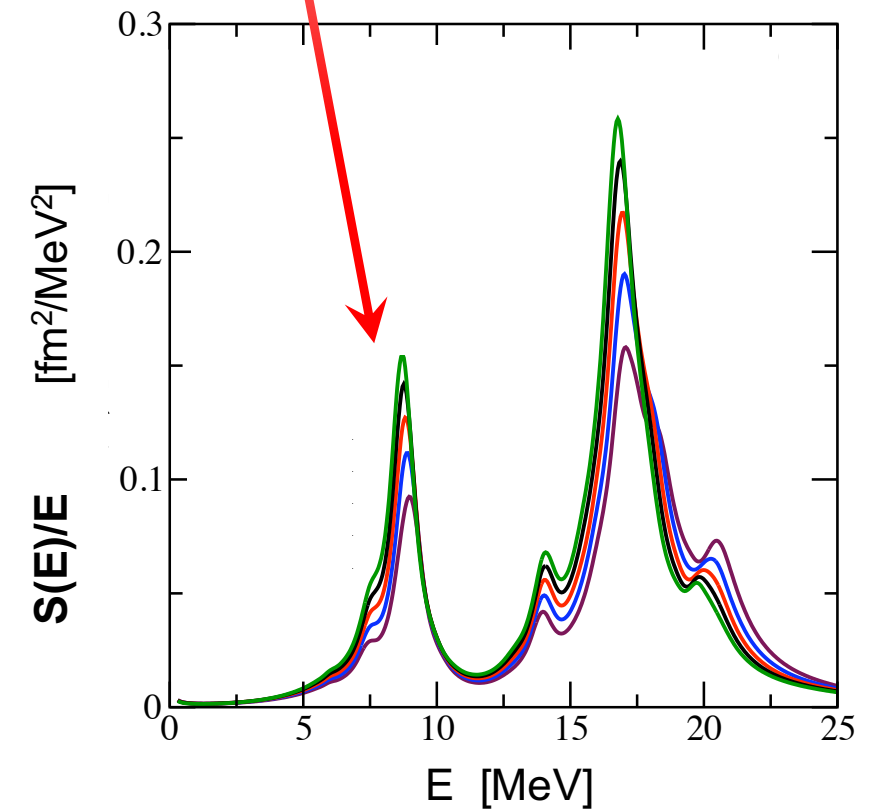
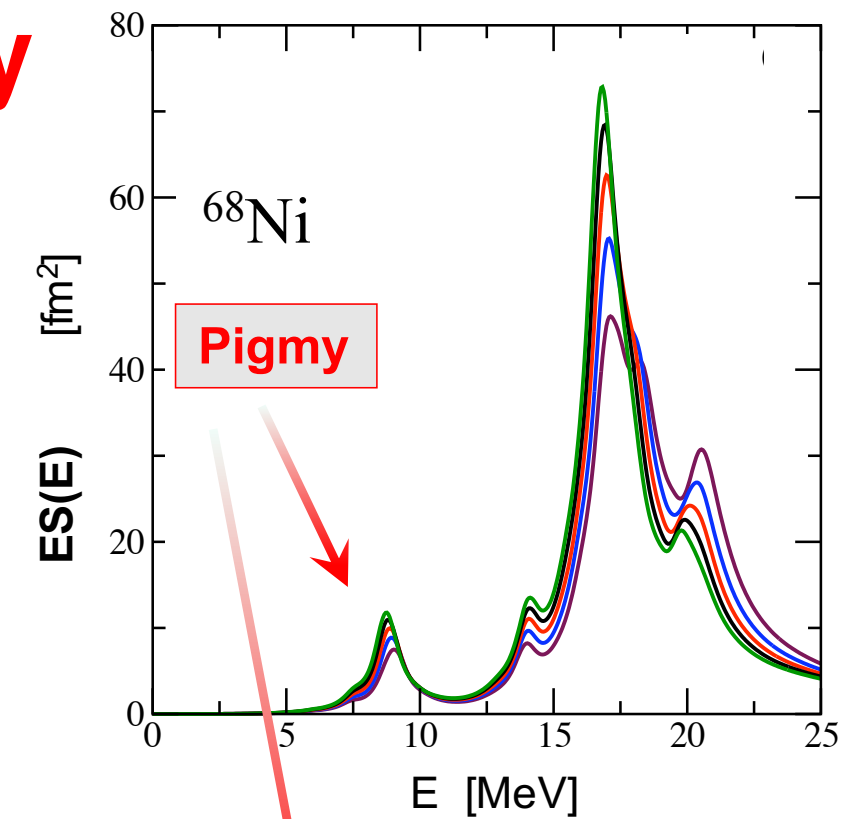


$$\sigma_C \sim (\dots) \int_0^\infty \frac{\sigma_\gamma(E)}{E^2} dE$$



$$\alpha_D = \frac{\hbar c}{2\pi^2} \int_0^\infty \frac{\sigma_\gamma(E)}{E^2} dE$$

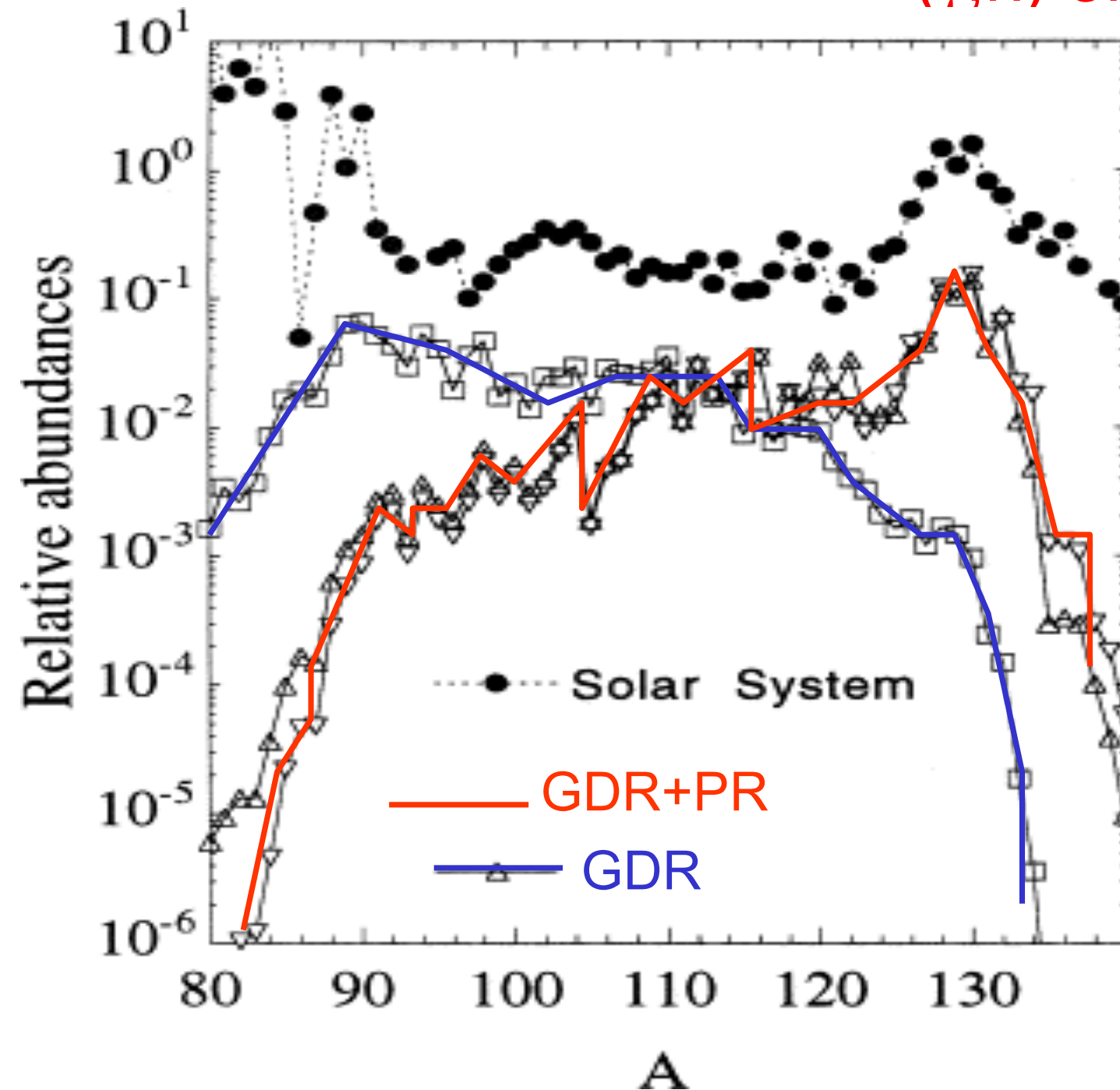
$$= \frac{8\pi}{9} \int \frac{B(E1, E_x)}{E_x} dE_x$$



Impact of pygmies on nucleosynthesis (??!)

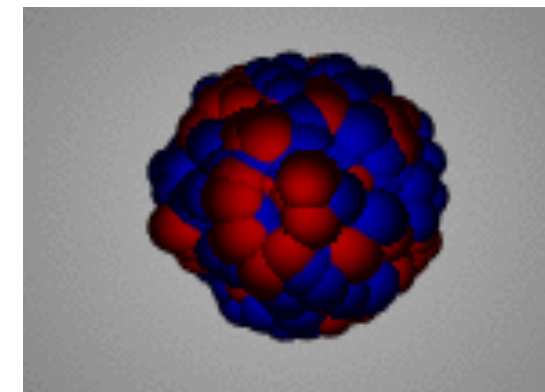
Goriely, PLB 436, 10 (1998)

(γ, n) or (n, γ) cross sections in the r-process

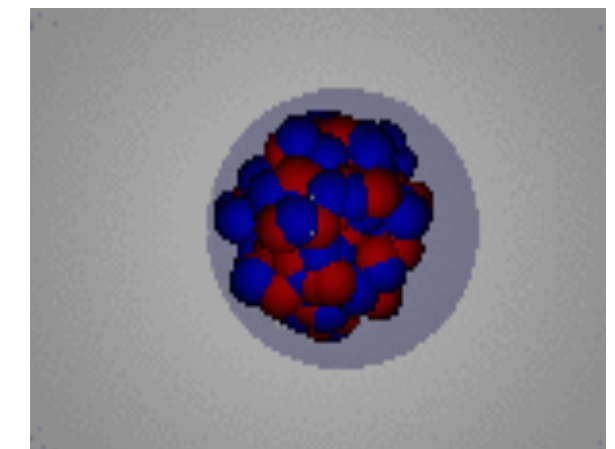


Impact: r-process abundances

- Calculation for $T = 10^9$ K, $N_n = 10^{20}$ cm⁻³, $\tau = 2.3$ s
- Under some conditions, PDR can enhance production in some regions

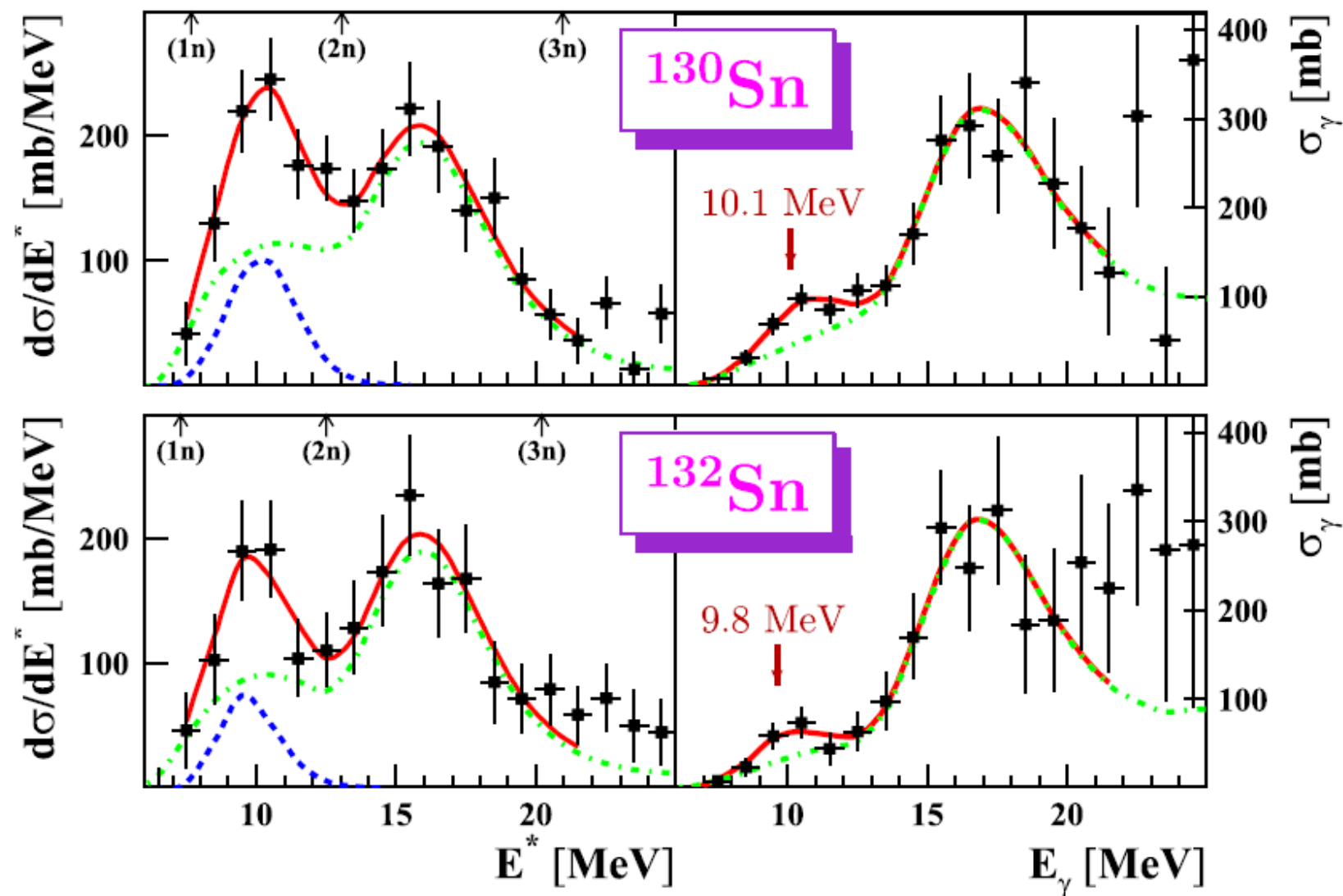


Giant dipole



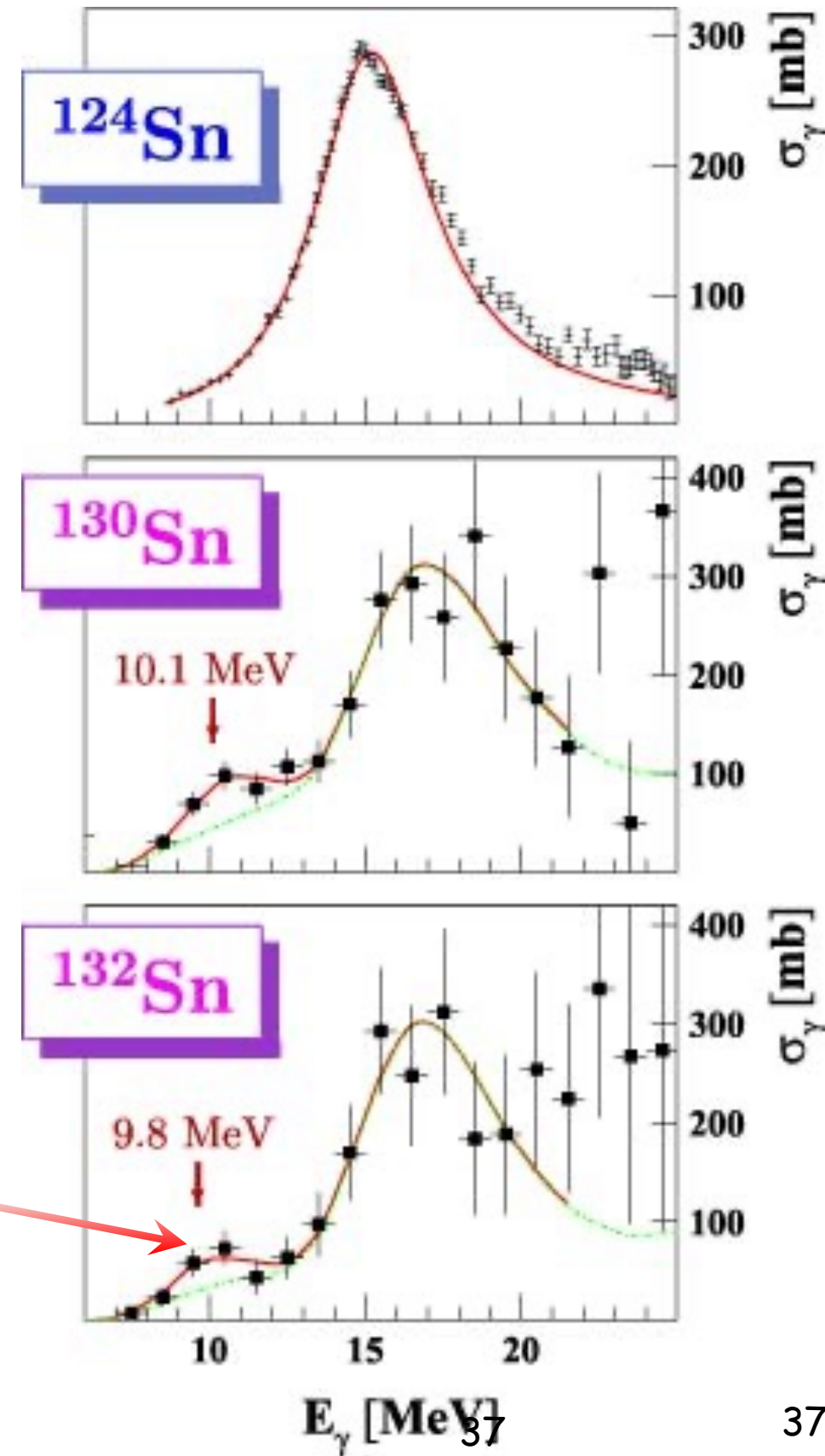
Pygmy dipole

Dipole polarizability

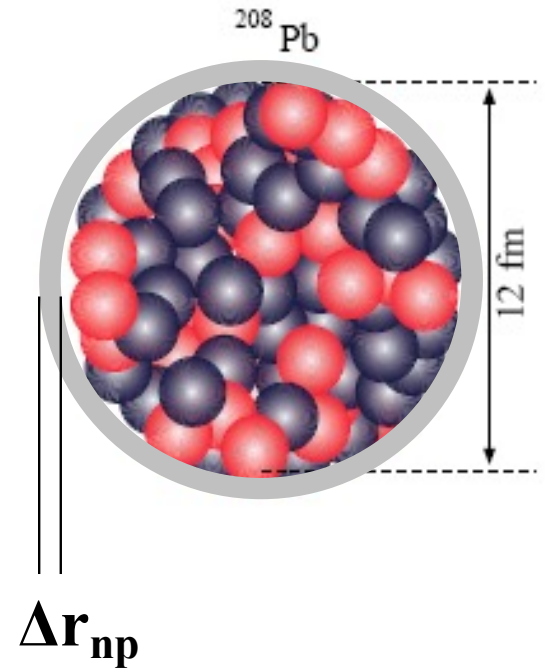
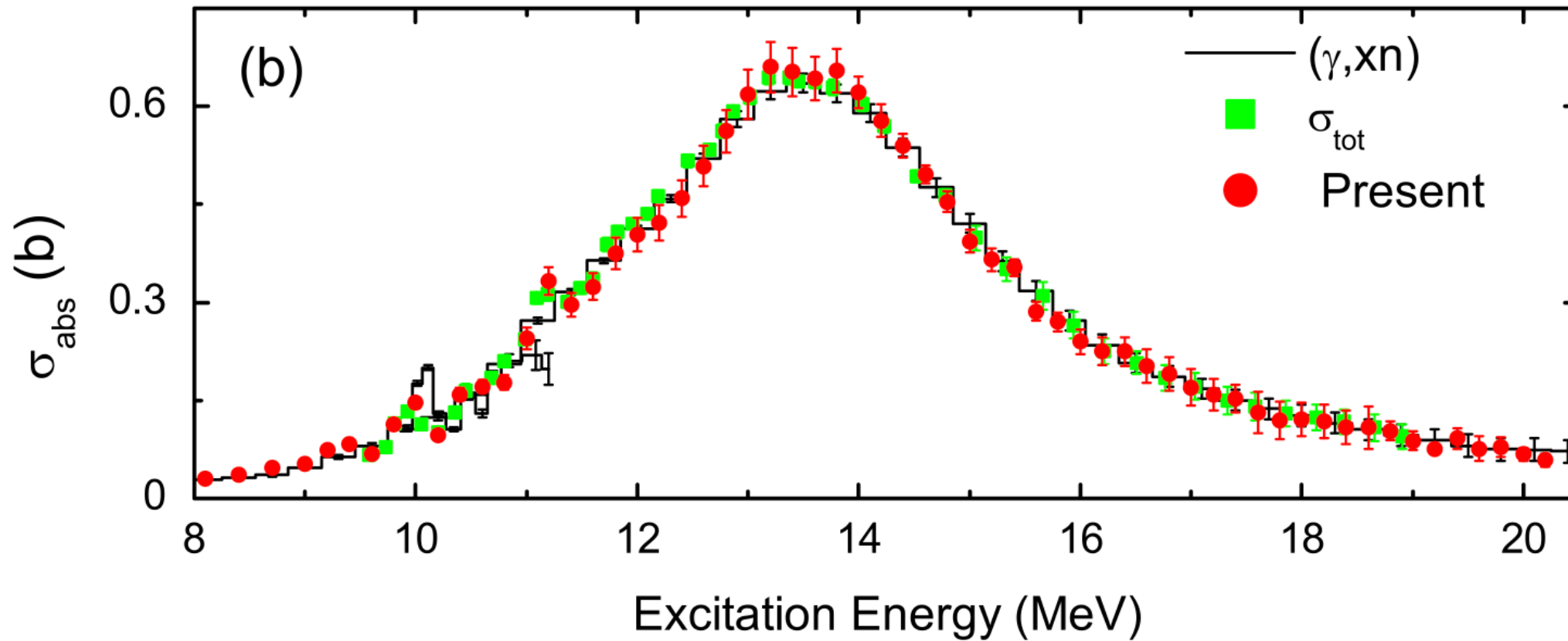


Adrich et al., PRL 95, 132501 (2005)

Pigmy



Dipole polarizability & neutron skin

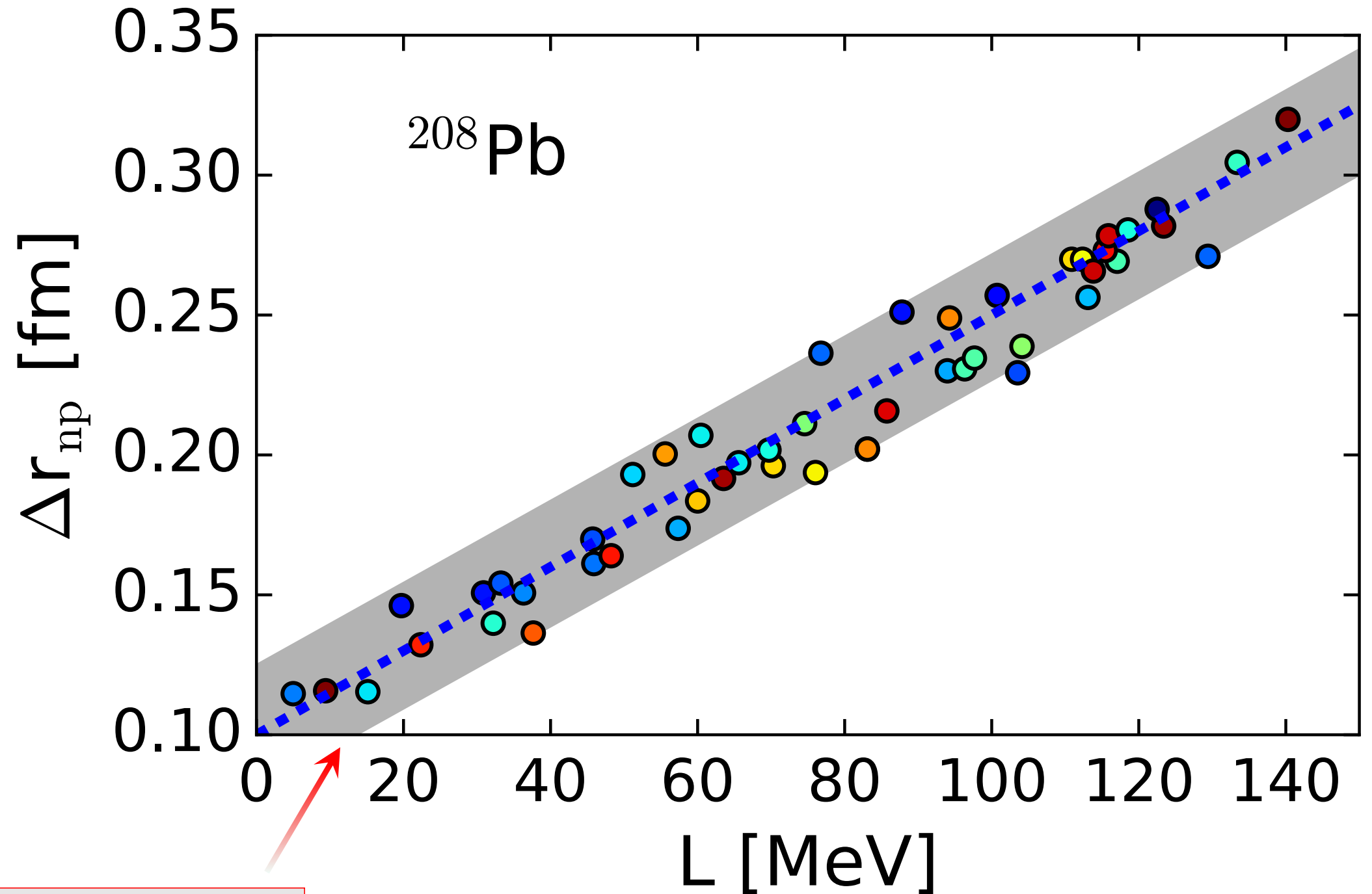
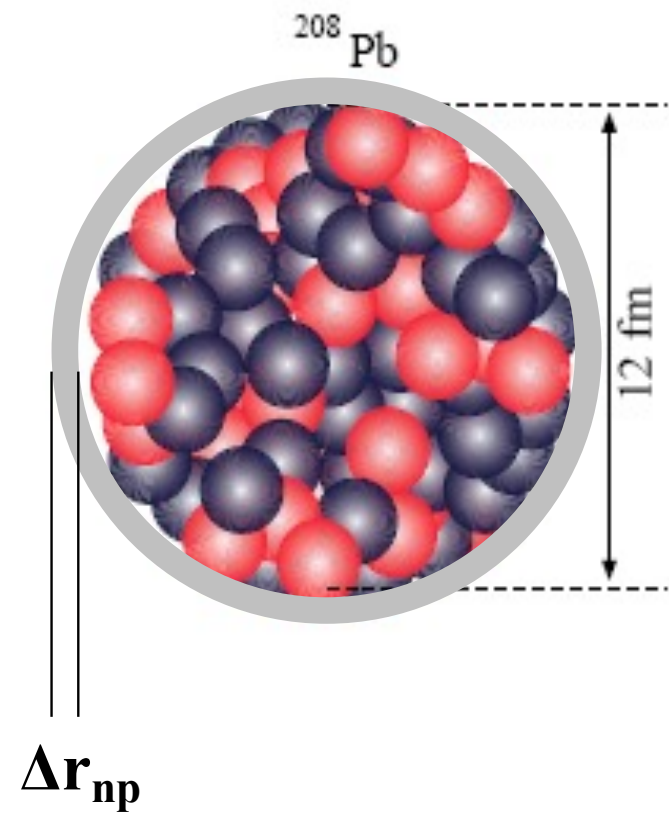


Tamii et al.,
PRL 107, 062502 (2011)

$$\alpha_D = \frac{\hbar c}{2\pi^2} \int_0^\infty \frac{\sigma_\gamma(E)}{E^2} dE$$

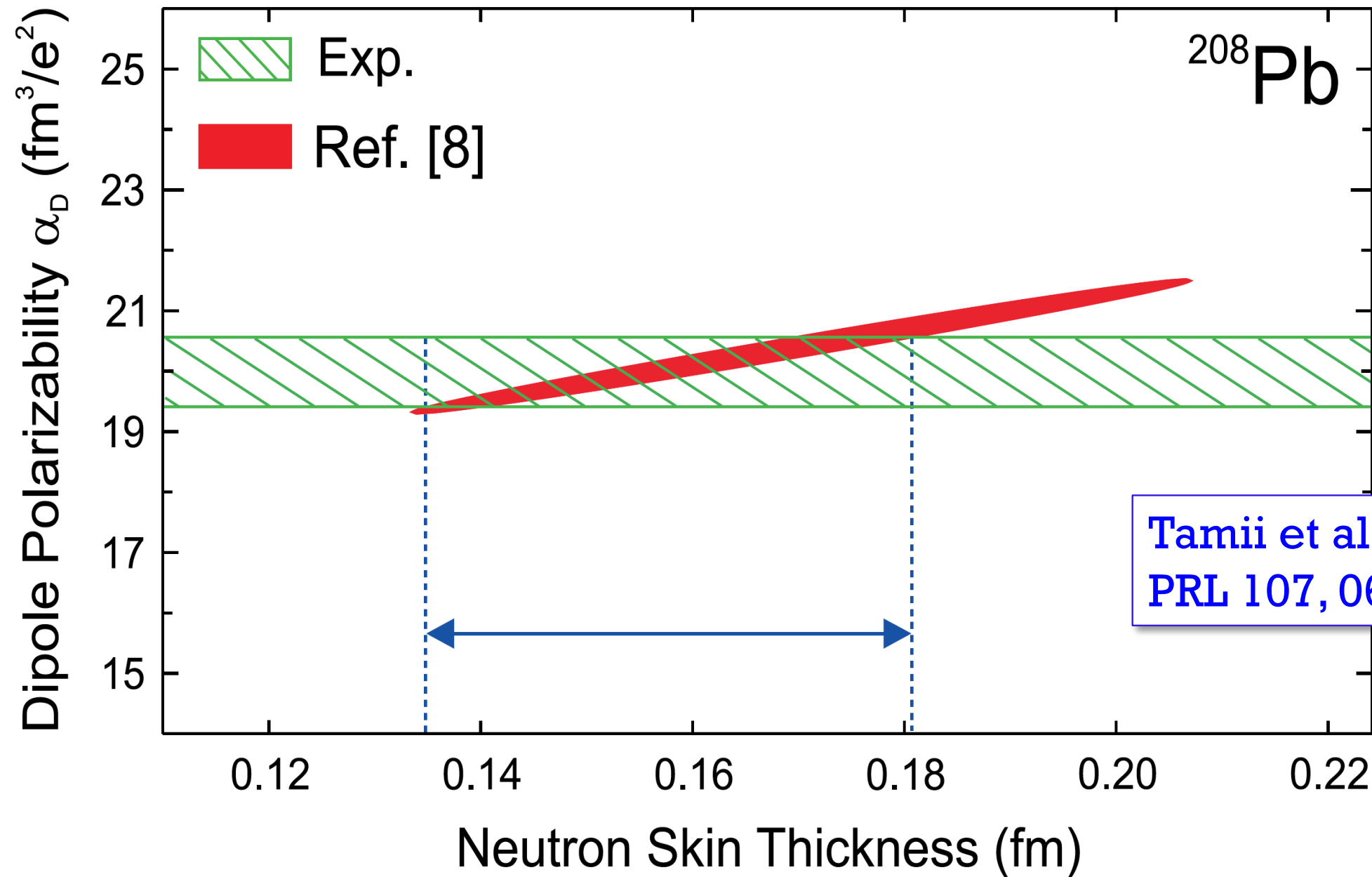
$$= \frac{8\pi}{9} \int \frac{B(E1, E_x)}{E_x} dE_x$$

Correlation between symmetry energy & neutron skin



Numerous EDF

Dipole polarizability & neutron skin



Reinhard, Nazarewicz,
PRC 81, 051303(R) (2010)

Tamii et al.,
PRL 107, 062502 (2011)

EFT:

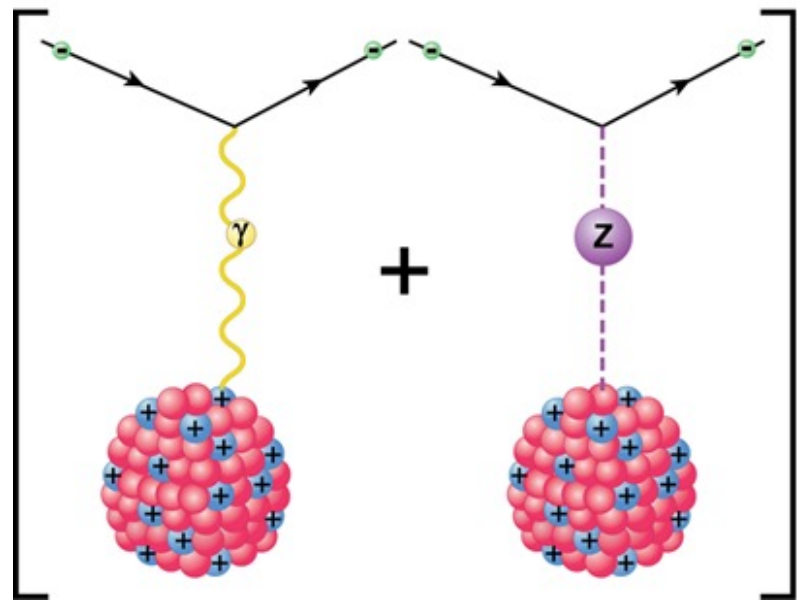
Hebeler et al.,
PRL 105, 161102 (2010)

Experiment:

$$\Delta r_{np} \sim 0.156 \text{ fm}$$

$$\Delta r_{np} \sim 0.17 \text{ fm}$$

n-skin from PV e⁻ scattering



Abrahamyan et al,
PRL 108, 112502 (2012)

Howowitz et al,
PRC 85, 032501(R) (2012)

$$A_{PV} = \frac{d\sigma_R - d\sigma_L}{d\sigma_R + d\sigma_L}$$

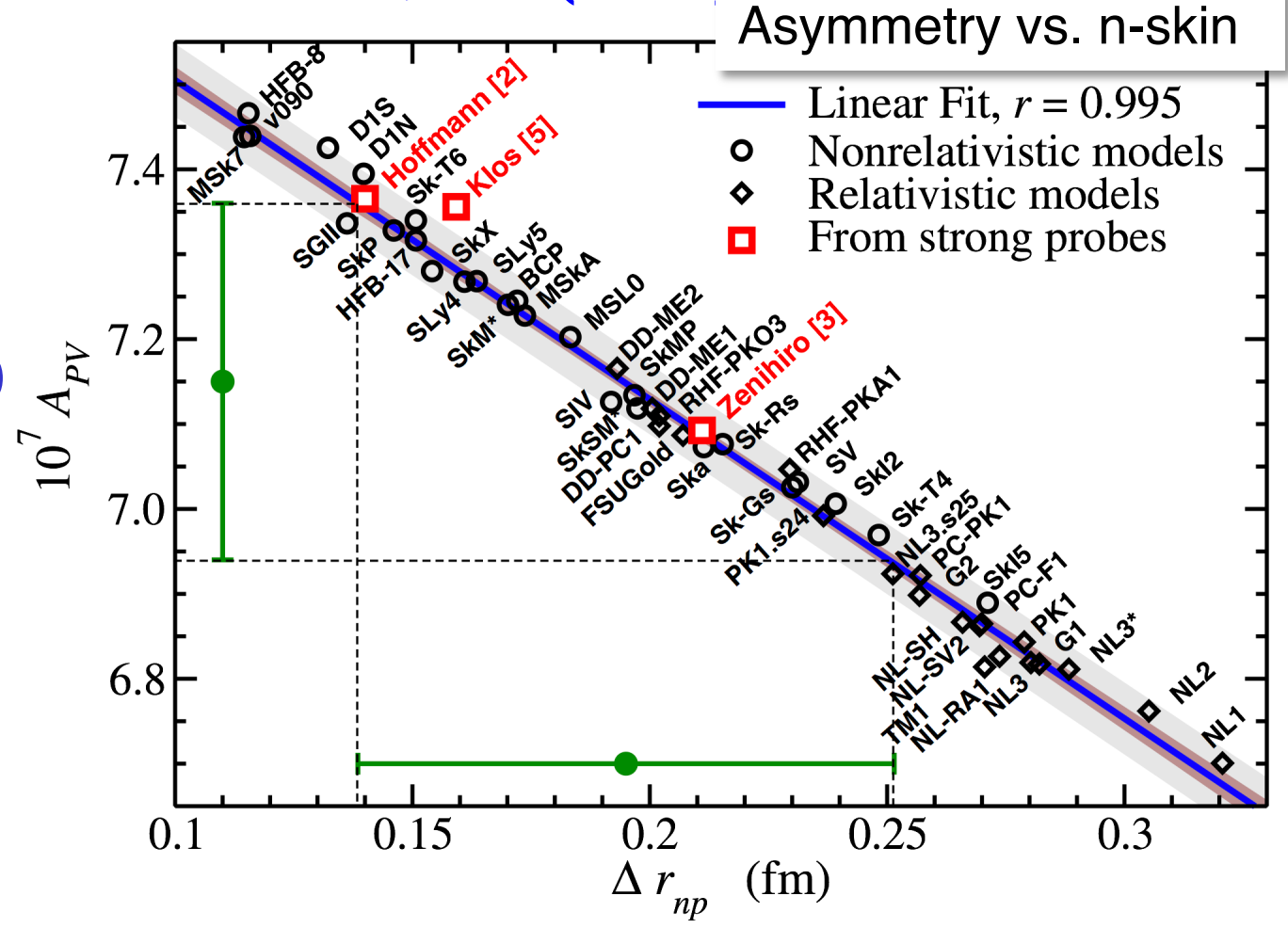
$$A_{PV}(Q^2) \sim \frac{G_F Q^2}{4\pi e^2 \sqrt{2}} \frac{F_W(Q)}{F_{ch}(Q)}$$

$$F_W = \frac{1}{Q_w} \int dr \frac{\sin(Qr)}{Qr} \rho_w(r)$$

$$\rho_w(r) = q_p \rho_{ch}(r) + q_n \int d^3 r' [G_E^p \rho_n + G_E^n \rho_p]$$

$$q_p = 0.0721, \quad q_n = 0.0721,$$

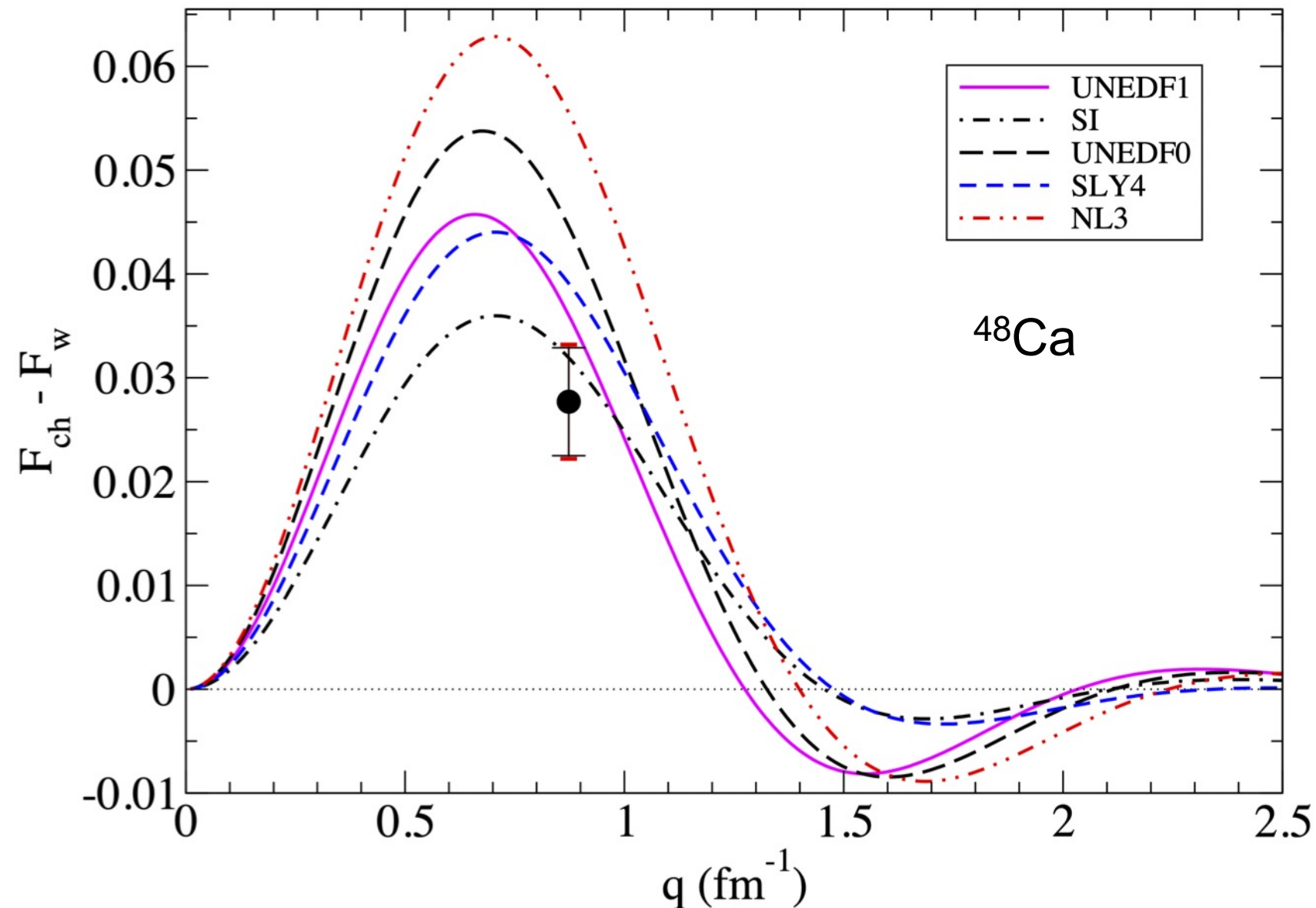
Roca-Maza, PRL (2011)



n-skin from e⁻ PV scattering ⁴⁸Ca

$$F(Q^2) \sim 1 - \frac{1}{6} q^2 \langle r^2 \rangle$$

$$\langle r^2 \rangle \cong -6 \frac{dF(Q^2)}{dQ^2}$$

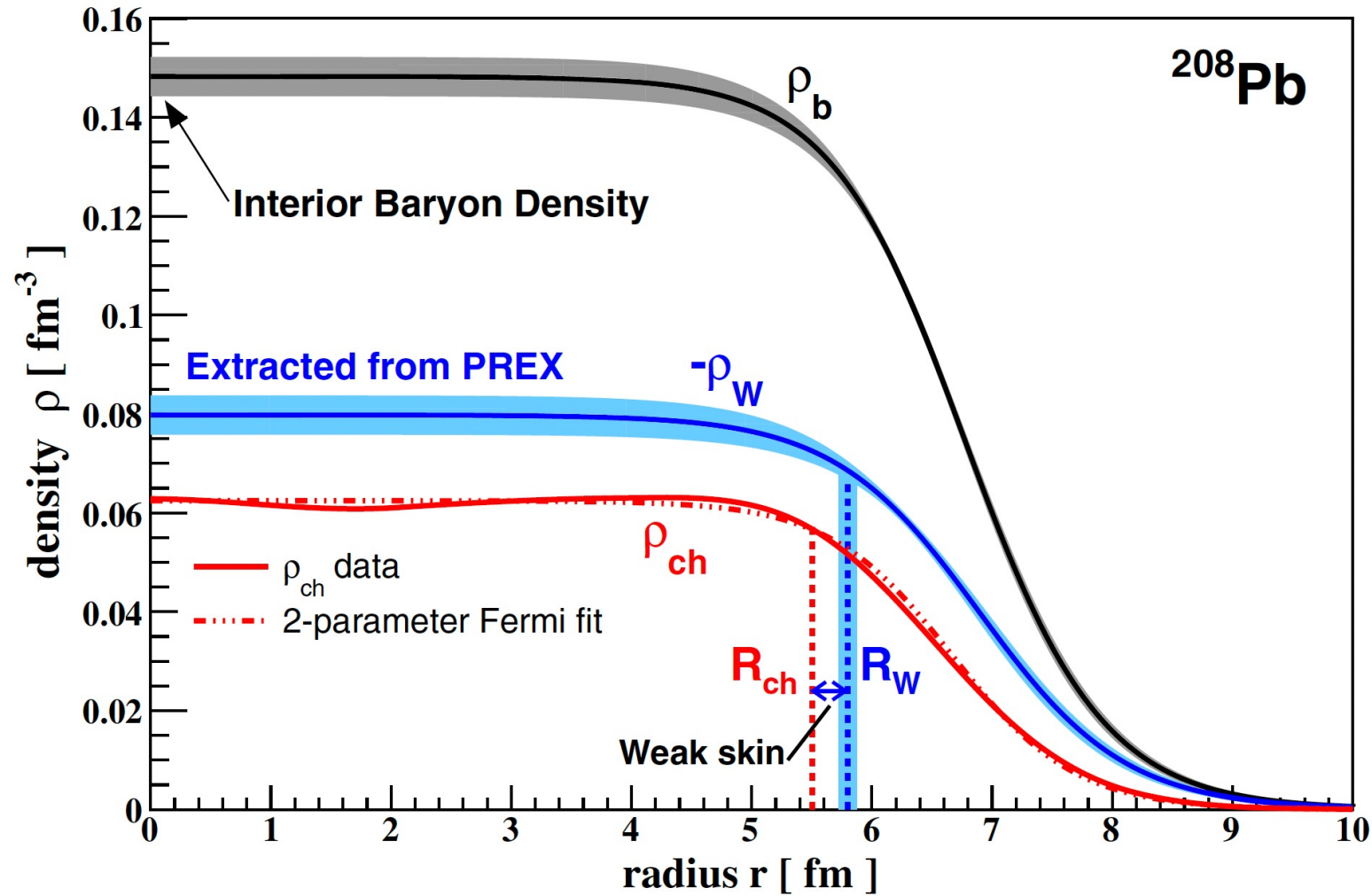


- PREX & CREX: measurement of parity violating asymmetry
- Determine n-skin and/or L by comparison to predictions from DFT

$$(R_n - R_p)_{48\text{Ca}} = 0.121 \pm 0.025 \text{ fm}$$

Adhikari et al, PRL 129, 042501 (2022)

n-skin from e^- scattering ^{208}Pb



$$\Delta r_{np} \sim 0.156 \text{ fm}$$

Dipole polarizability

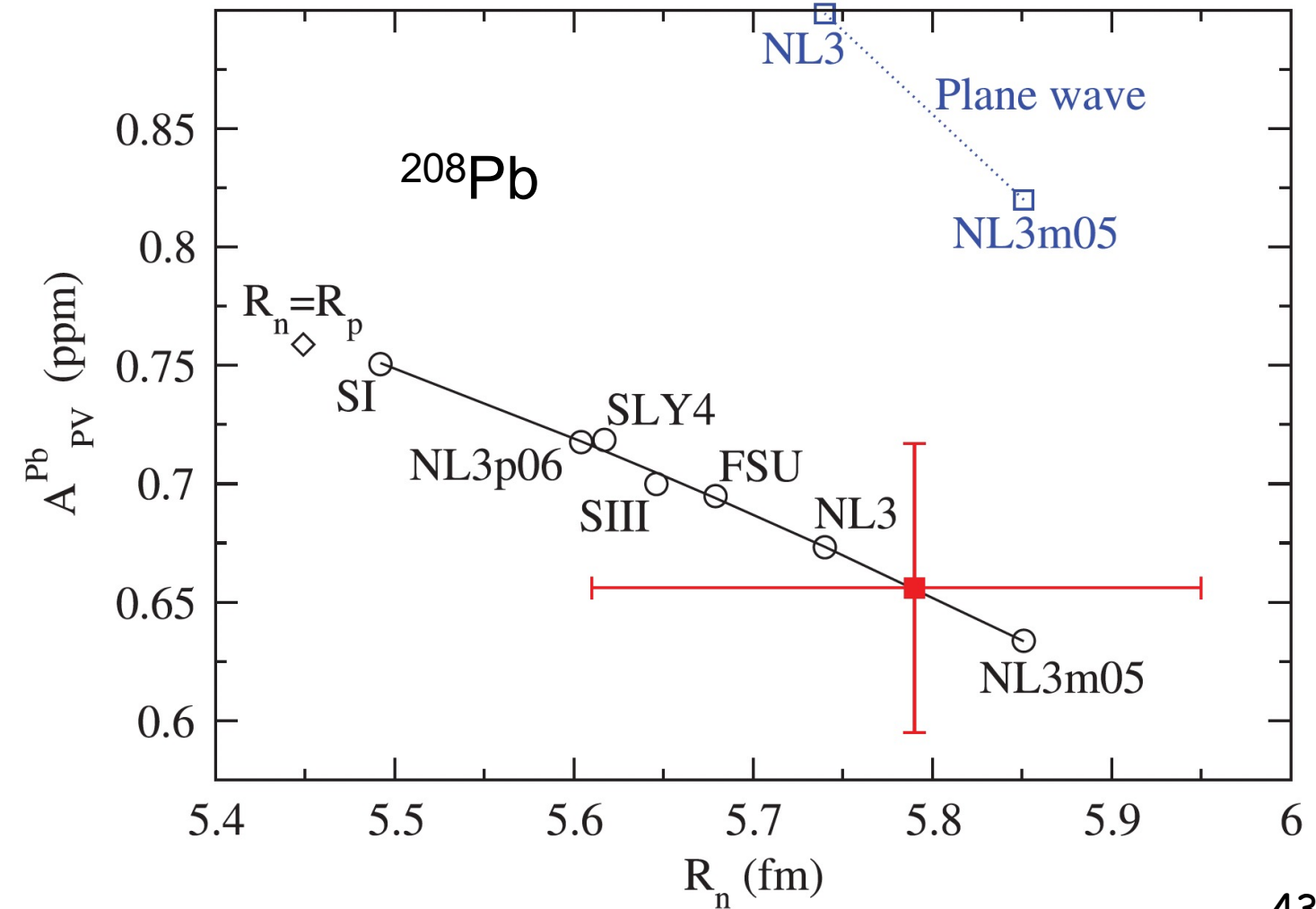
Tamii et al., PRL 107, 062502 (2011)

very large value!

PREX-I

$$R_n - R_p = 0.33 \pm 0.17 \text{ fm}$$

Adhikari et al, PRL 126, 172502 (2021)



Radiative capture, spectroscopic factors

Overlap function

$$I_{lj}(\mathbf{r}_n) = \langle \Psi_{A=B+n}(\xi_B; \mathbf{r}_n) | \Psi_B(\xi_B) \rangle$$

$$\int d^3r_n |I_{lj}(\mathbf{r}_n)|^2 = S(lj)$$

Spectroscopic factor

Asymptotic Normalization Coefficient (ANC)

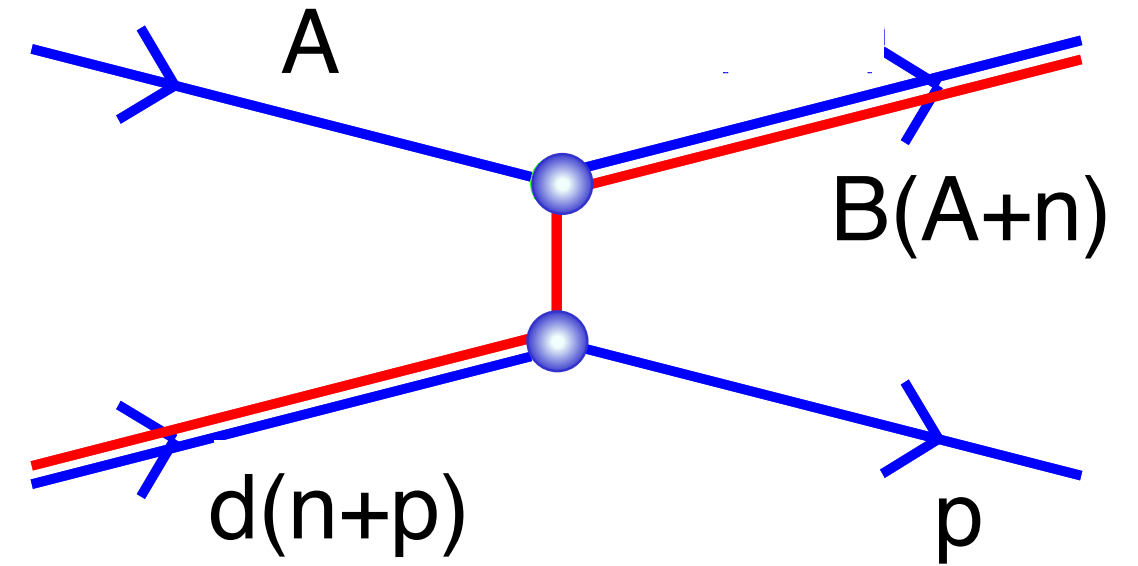
Large r $I_{lj}(r) \rightarrow C_{lj} h_{ij}^{(1)}(ikr)$

If $I_{lj}(r) = \sqrt{S(lj)} \varphi_{lj}^{s.p.}(r)$ and $\varphi_{lj}^{s.p.}(r) \rightarrow b_{lj} h_{ij}^{(1)}(ikr)$
then $S(lj) = \frac{C_{lj}^2}{b_{lj}^2}$ $b_{lj}^2 = \text{s. p. ANC}$

ANC

Assume cross section for $A(d,p)B$

$$\sigma^{DW} = |M|^2 = \left| \langle \psi_f^{(-)} I_{An}^B | V | \phi_{pn} \psi_i^{(+)} \rangle \right|^2$$



With the single particle approximation

$$\sigma^{DW} = S \left| \langle \psi_f^{(-)} \phi_{An}(n_r l j) | V | \phi_{pn} \psi_i^{(+)} \rangle \right|^2$$

If the reaction is peripheral

$$I_{lj}(r) \rightarrow C_{lj} h_{ij}^{(1)}(ikr)$$

$$\frac{d\sigma}{d\Omega} = \left(C_{Bpl_A j_A}^A \right)^2 \left(C_{Bpl_d j_d}^A \right)^2 \frac{\sigma_{l_A j_A l_d j_d}^{DW}}{b_{Bpl_A j_A}^2 b_{Bpl_d j_d}^2}$$

Use of ANCs

- Find a **peripheral transfer reaction**
- Measure angular distribution
- Fit with a **DWBA** calculation
- Determine **ANCs**
- Use ANCs to calculate $\sigma_{\text{astrophysics}}$

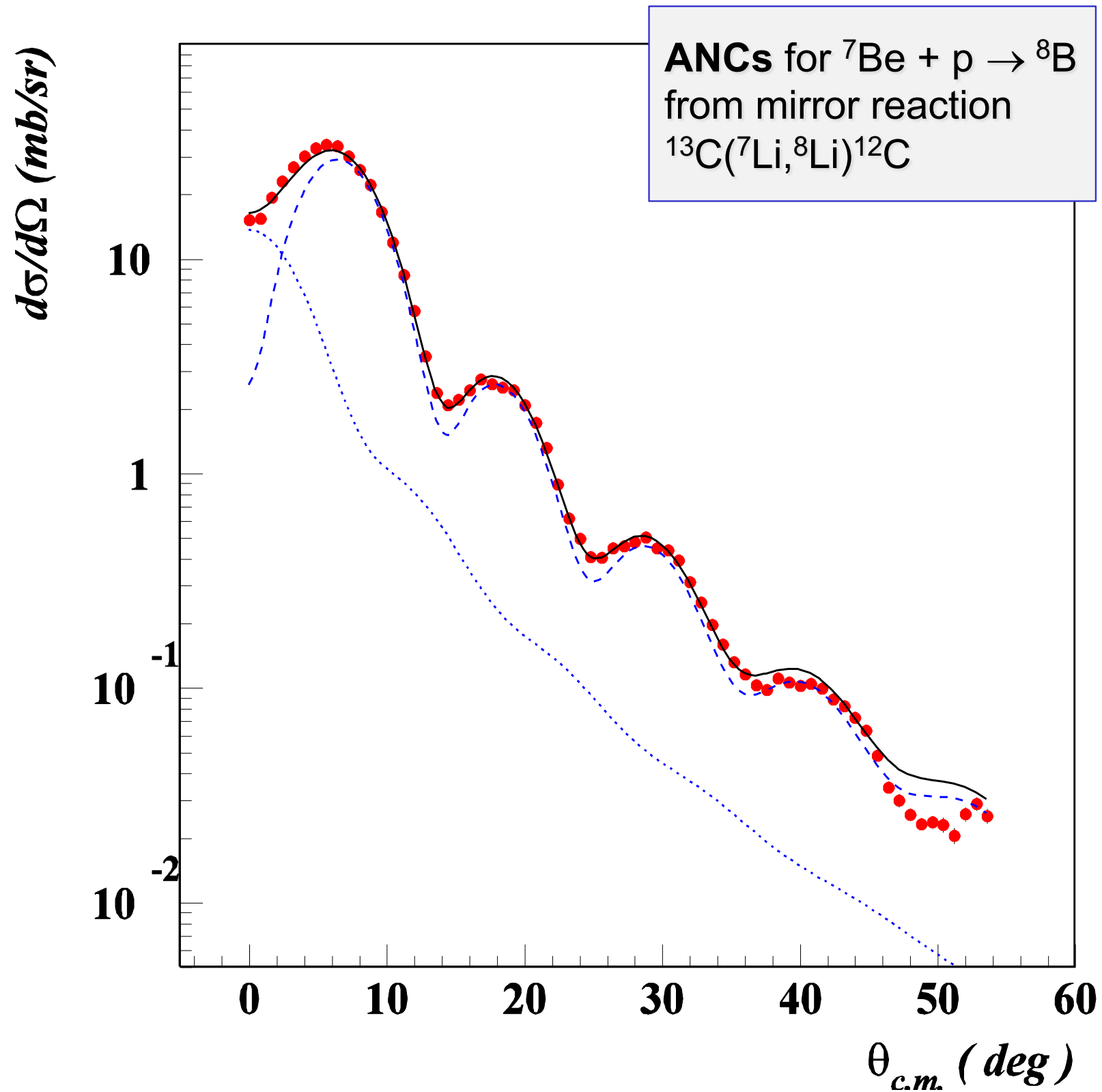
Example: radiative capture reactions



$$\sigma_{E1} \propto |\langle \Psi_a | r Y_1 | \Psi_{b+c} \rangle|^2$$

Only tail of Ψ_a necessary to calculate σ_{E1}

Ψ_{b+c} is rather reliably calculated in a potential model



$$S_{17}(0) = 17.6 \pm 1.7 \text{ eV.b}$$

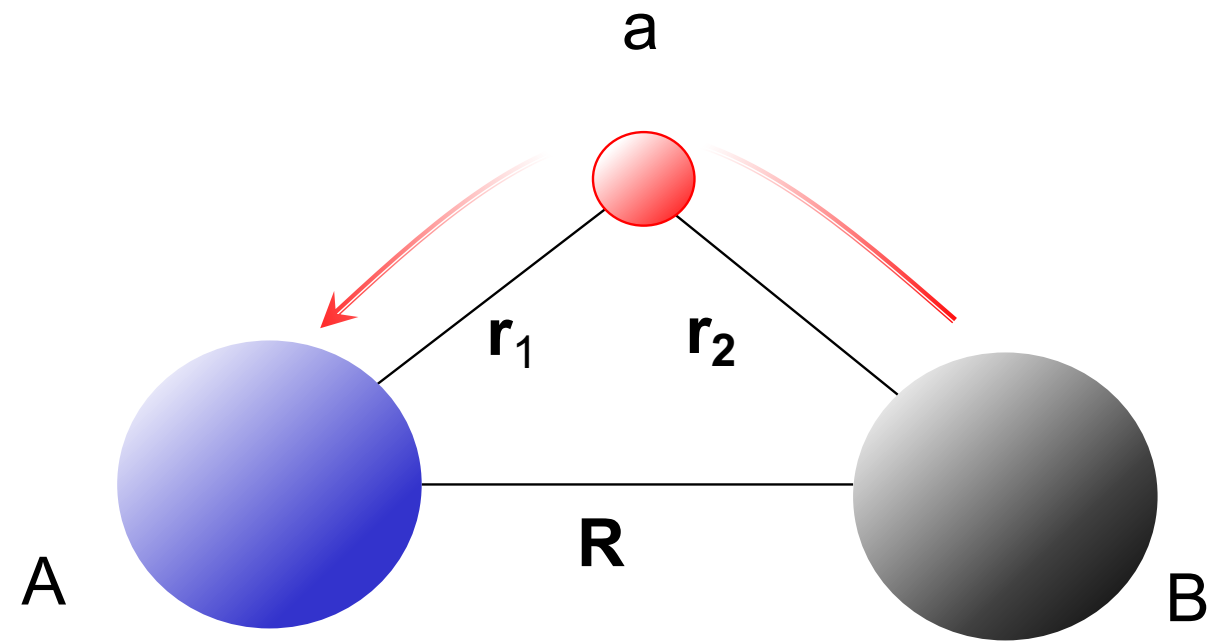
Trache, PRC (2003)

Nucleon transfer, in general

S_x = spectroscopic factors

\mathbf{Q} = momentum transfer

V_{1A} = transfer interaction



$$\left(\frac{d\sigma}{d\Omega}\right)_{PWBA} \sim S_{aA}S_{aB} \left| \int d^3R F_{PWBA}(\mathbf{R}) \right|^2$$

$$F_{PWBA}(\mathbf{R}) \sim \int d^3r_1 e^{i\mathbf{Q}\cdot\mathbf{r}_1} \varphi_a^{(A)}(\mathbf{R} + \mathbf{r}_1) V_{1A} \varphi_a^{(B)}(\mathbf{r}_1)$$

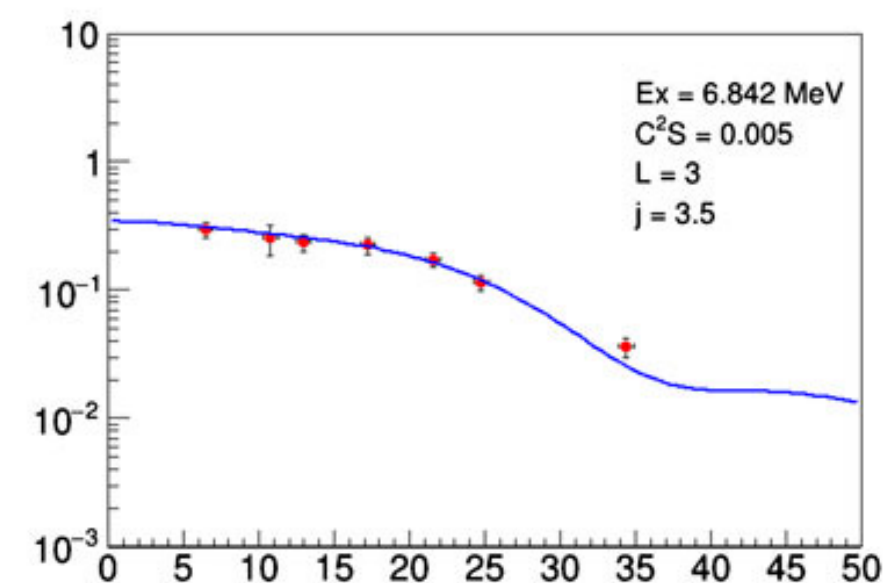
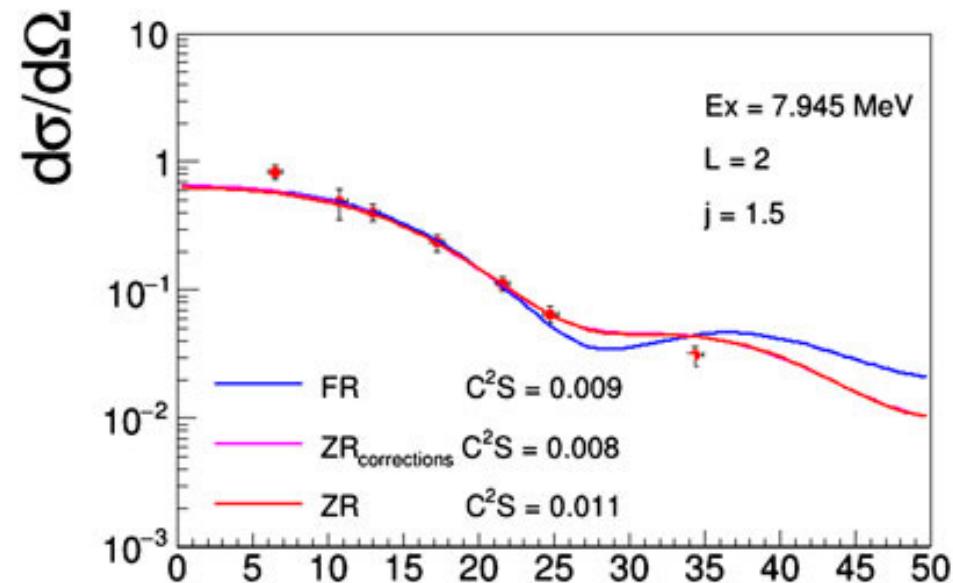
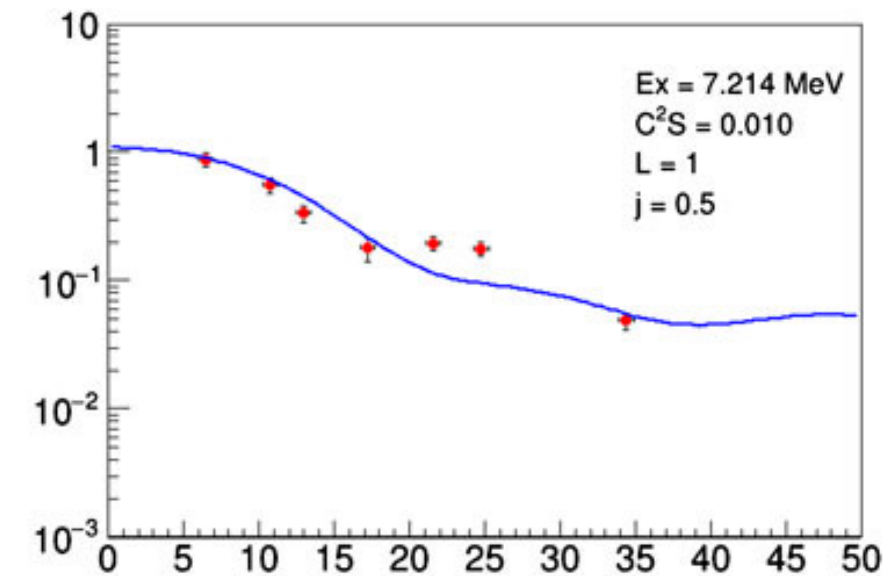
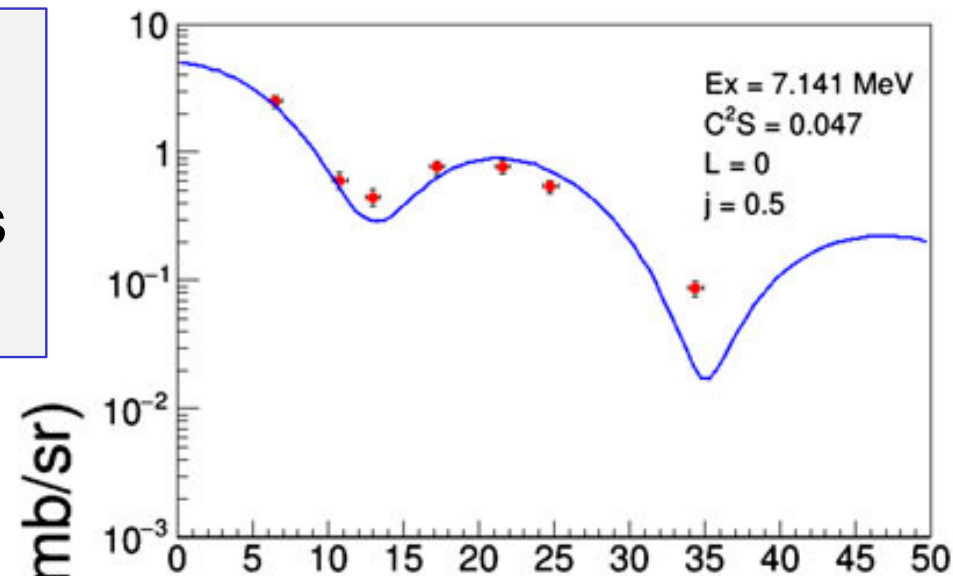
$\chi_{aA}^* \chi_{aB}$ = distorted waves



DWBA

P enhancement & Mg depletion in globular clusters
 Pollution by early generation stars
 ← importance of $^{30}\text{Si}(p,\gamma)^{31}\text{P}$

Low E resonances not accessible due to Coulomb barrier

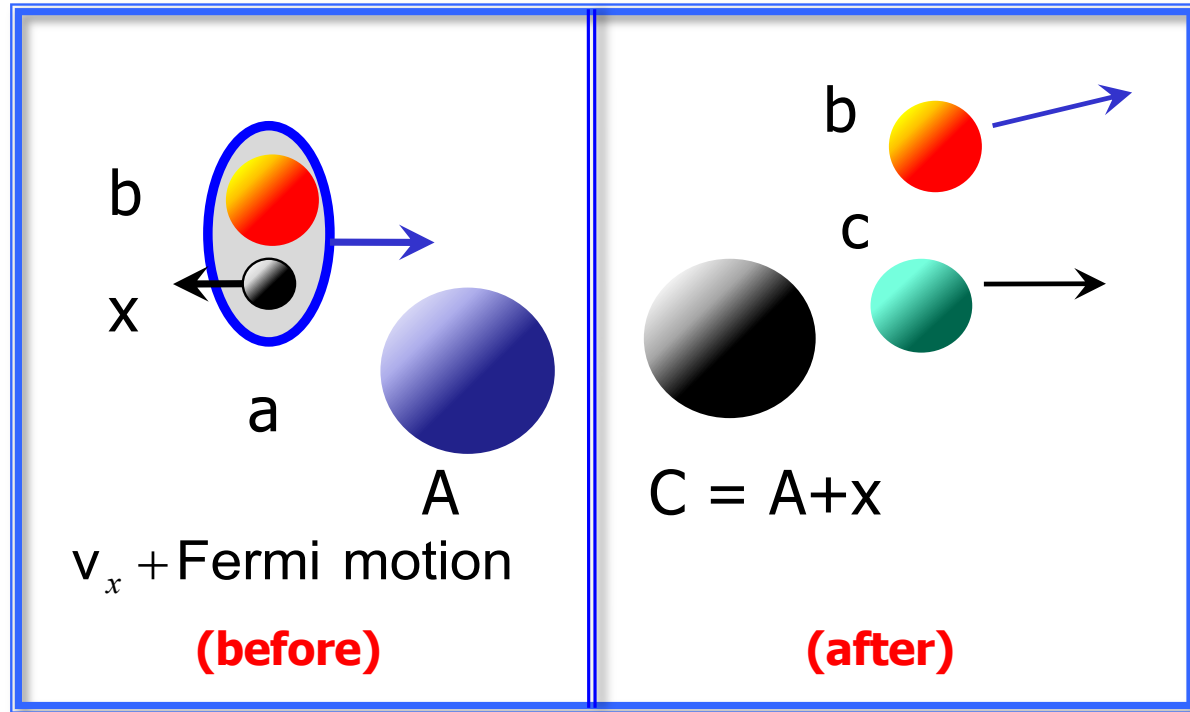


$\theta_{c.m.} (^\circ)$

^{31}P states populated with $^{30}\text{Si}(^3\text{He},d)^{31}\text{P}$

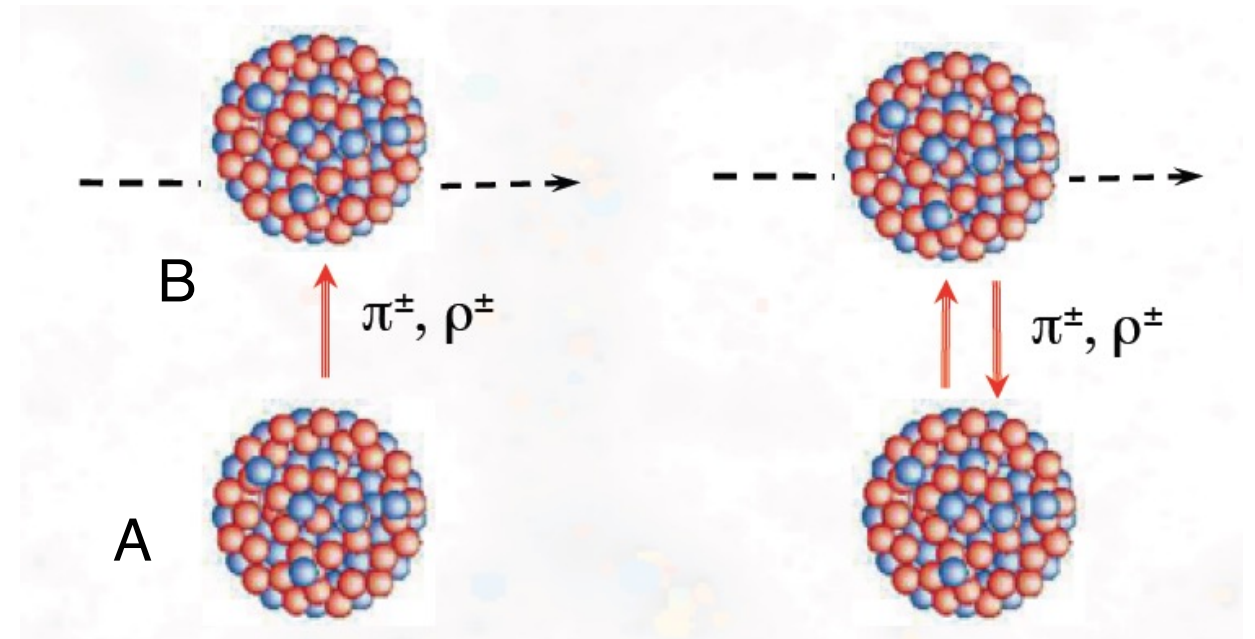
Trojan horse method

+ many other indirect methods



Applications to astrophysical $A + x \rightarrow C + c$ reactions

Charge exchange



One step

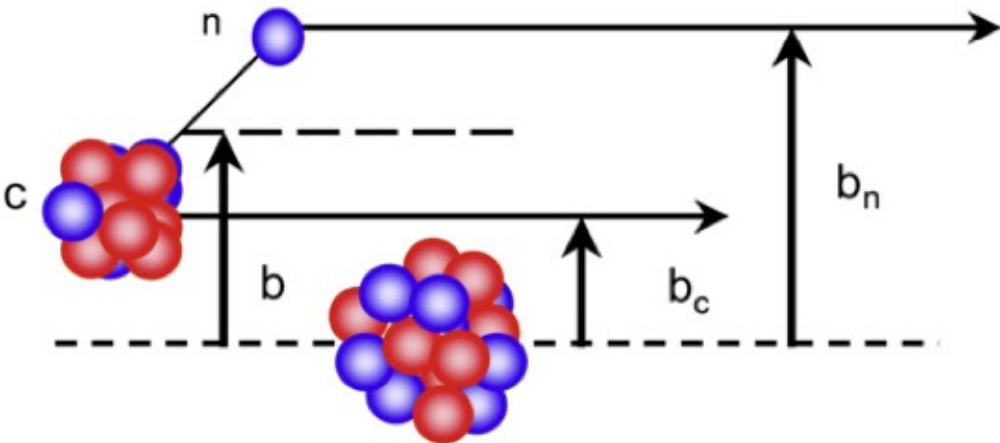
Two step
(meson exchange)

Applications to electron capture and ν induced reactions in stars

(double-beta decay)
NUMEN

Knockout reactions

Distribution of single particle strength in nuclei



Theory for indirect methods for NA

- **Optical potentials:** (a) parameter quantification analysis, (b) microscopic theory
- **Off-shellness:** On-shell energy/momentum of extracted information not well established for most reactions. I.e., extracted NA cross sections not the same as with free particles
- **Relativistic corrections**, 100 MeV/nucleon \sim 10% nucleon mass: (a) kinematics easy, (b) dynamics difficult because of retardation, simultaneity. Problem worsens at large E_{lab}
- **Multinucleon collisions** not well assessed in knockout, (p,2p) or CE reactions
- **Factorization** into structure and reaction parts not consistent (e.g., different interactions, eigen and scattering states obtained with different Hamiltonians)
- **Medium effects**, nuclear polarizabilities, coupled channels, too simplified
- **No statistical theory** exists for nuclear reactions in the nucleus-nucleus continuum